

SOME ASPECTS OF BASIC GEOCHEMISTRY IN COAL SCIENCE

Dalway J. Swaine
CSIRO Division of Coal and Energy Technology
P.O. Box 136, North Ryde NSW, 2113
Australia

Keywords: coal, geochemistry, trace elements

ABSTRACT

Several instances of the use of basic geochemistry in coal science are given, using Australian bituminous coals as examples. The mode of occurrence of manganese is related to associations with siderite and calcite, the reason being cation replacement. High concentrations of boron, arsenic, phosphorus and other elements in deposits found in some boilers were due to the presence of boron phosphate and boron arsenate, two compounds that have not been found in nature. The proportions of soil/rock and flyash particles in atmospheric particulates deposited near a power station have been estimated by using the marked differences in germanium concentrations.

INTRODUCTION

In his pioneering geochemical research, V.M. Goldschmidt studied trace elements in coal. Several elements were discovered and determined in coal by Goldschmidt and coworkers in Gottingen during the 1930s (1). The basic principles enunciated by Goldschmidt are applicable to coal geochemistry. Much of the early trace-element studies depended on the development of sensitive analytical methods, mainly in optical emission spectroscopy. Some examples of the applications of Goldschmidt's work will be outlined based on experimental work on Australian coal carried out at the CSIRO, North Ryde.

MANGANESE IN BITUMINOUS COAL

As with other trace elements in coal, manganese can be found associated with the organic and with the inorganic matter. In most bituminous coals manganese occurs predominantly in the mineral matter fraction. In Australian bituminous coals from the Sydney Basin, New South Wales and from the Bowen Basin, Queensland, it was found that there was a marked concentration of manganese in siderite and in calcite (Table 1). On the basis of ionic radii (1) Mn^{2+} is expected to be able to substitute for some of the Fe^{2+} in siderite. Although the difference in ionic radius between Mn^{2+} and Ca^{2+} is greater than that for Mn^{2+} and Fe^{2+} , substitution can still occur in calcite. These results were used initially to propose that manganese occurs in Australian bituminous coals mainly in siderite and calcite components of the mineral matter. Direct evidence for the replacement of some Ca^{2+} ions by Mn^{2+} ions in calcite from a Pittsburgh coal was found by an electron paramagnetic resonance method (2). There is indirect evidence for the close association of manganese and 'carbonate' iron (that is, total iron less pyritic iron) from data for 56 samples of coal from the Lithgow seam, New South Wales (Figure 1, correlation coefficient $r = 0.89$). Samples of coal containing dolomite had relatively low concentrations of manganese, namely 10-150 ppm Mn (3).

TRACE ELEMENTS IN PHOSPHATIC BOILER DEPOSITS

When bituminous coal is fired in boilers using spreader stokers or chain grates, deposits were found in some parts of the boiler system. These deposits often had very high concentrations of phosphorus and many trace elements, including arsenic, boron, germanium, lead and zinc (Table 2). Indeed, bismuth, indium and thallium were found in some boiler deposits before they had been detected in Australian coals (4). Results in Table 2 show some of the concentrations in deposits from the burning of Australian bituminous coals which are relatively low in trace elements. The highest concentrations were found in specific locations in the boiler system, for example in the vertical riser tubes of the spreader stoker-fired boiler. The deposit on the superheater tubes of the chain grate stoker-fired boiler was in two distinct layers, namely a 2 mm thick inner layer with an outer layer superimposed on it. The high elemental concentrations were confined to the inner layer. On the basis of laboratory work by Schulze (5) who prepared boron phosphate (BPO_4) and boron arsenate ($BAsO_4$) and determined their crystal structures, Goldschmidt (1) stated that these two compounds are isostructural with β -cristobalite. Since these compounds have never been found in nature they were sought in the two deposits highest in arsenic, boron and phosphorus, and boron phosphate was identified. Later a further study established that $BAsO_4$ was present in solid solution in BPO_4 (6).

A possible mechanism for the formation of BPO_4 involves a reaction between calcium phosphate and silica to give phosphorus pentoxide, which could then react with boron trioxide formed from the decomposition of organically-combined boron in coal, to give boron phosphate (4). A similar mechanism has been proposed for the formation of boron arsenate (6). It is interesting to note that there are some high concentrations of germanium in the boiler deposits, probably the highest found in coal-derived material. Such deposits have not been used for the production of germanium, but other coal-derived materials have been processed in several countries to yield small quantities of germanium for the manufacture of semi-conductors.

GERMANIUM AS AN INDICATOR OF FLYASH IN ATMOSPHERIC PARTICULATES

Power stations emit trace elements to the atmosphere, mostly associated with fine flyash particles. There is an on-going interest in the composition of atmospheric particulates, especially in the concentrations of trace elements of environmental significance. Samples of material deposited in areas near power stations, say up to about 20 km away, contain predominantly soil/rock and flyash particles in proportions that are not easily measured. A study of the trace-element contents of flyash from an Australian power station showed that there was a distinct enrichment of some elements in the fine particles (less than about 3 μm diameter) which predominate in the stack emissions. Comparisons of the compositions of flyash with those for rocks and soils, using available geochemical data show that germanium has the highest ratio for flyash to soil/rock material (Table 3). The mean values for germanium in fine flyash and soils in the area around the Australian power station were 75 and 1.5 ppm respectively. Applying this to samples of deposition enabled the proportions of flyash to be calculated from results for 12 three-monthly samples (Table 4). As expected the proportions of flyash decreased with distance from the power station. The variations in the ranges of values at any location are caused by changes in meteorological conditions, especially wind direction. It is surprising to find some very low proportions, for example 4 and 7%, in samples collected near the power station, but this was in keeping with seasonal changes in wind direction. Another geochemical interpretation of these results was carried out by comparing them with the amounts of trace elements released by rock weathering (7).

CONCLUSIONS

The examples discussed here indicate how basic geochemistry, mostly emanating from Goldschmidt's work, can be used to elucidate some aspects of the trace-element geochemistry of coal and coal usage.

REFERENCES

1. Goldschmidt, V.M. 'Geochemistry', Clarendon Press: Oxford, 1954, 730 pp.
2. Malhotra, V.M.; Graham, W.R.M. 'Origin of the Mn^{2+} e.p.r. spectrum in Pittsburgh No.8 bituminous coal', *Fuel* 1985, 64, 270-272.
3. Brown, H.R.; Swaine, D.J. 'Inorganic constituents of Australian coals', *J. Inst. Fuel* 1964, 37, 422-440.
5. Schulze, G.E.R. 'The crystal structure of BPO_4 and $BAsO_4$ ', *Z. Physik. Chem.* 1934, B24, 215-240.
6. Swaine, D.J.; Taylor, G.F. 'Arsenic in phosphatic boiler deposits'. *J. Inst. Fuel* 1970, 43, 261.
7. Swaine, D.J.; Goodbeer, W.C.; Morgan, N.C. 'The deposition of trace elements from the atmosphere', In *Trace Elements in New Zealand: Environmental, Human and Animal* (Eds. R.G. McLaren, R.J. Haynes, G.P. Savage) 1989 pp. 1-10.

Table 1. Manganese in carbonate minerals found in Australian bituminous coals

Mineral and location	Mn (ppm)
Siderite, Tongarra seam, Sydney Basin	3000
Siderite, Benley seam, Queensland	10000
Calcite, Wallarah seam, Sydney Basin	10000
Calcite, Blackwater, Queensland	19000
Calcite from fissure in seam, Queensland	2240

Table 2. Contents of trace elements in boiler deposits; based on (4)

Type of boiler and coal	Content of trace element (as%)					
	As	B	Ge	P	Pb	Zn
Spreader stoker:						
superheater tubes	0.08	0.05	0.1	11.0	1.0	1.0
vertical riser tubes	0.8	3.0	0.1	15.0	0.3	0.6
economiser outlet dust	0.1	0.15	0.01	1.5	0.04	0.2
coal (ppm)	1	6	8	400	10	50
Chain grate stoker:						
superheater tubes						
inner layer	1.0	5.0	1.0	25	1.0	1.0
outer layer	0.0001	0.015	0.002	1.2	0.004	<0.03
coal (ppm)	1	15	9	580	10	50

Table 3. Contents of germanium

Earth's crust	1.5 ppm Ge	Soil	
Sandstone	0.8	- range	1-2.5 ppm Ge
Limestone	0.2	- mean	1.5
Shale	1.6	Fine flyash	
		- range	50-100
		- mean	75

Table 4. Flyash in deposition at different locations

Distance of location from power station (km)	Flyash range (%)	Flyash mean (%)
1.8	7-80	40
1.5	4-33	11
3.9	0.5-10	5
5.3	<1-5	2.5
27.4	0.1-2.5	0.7

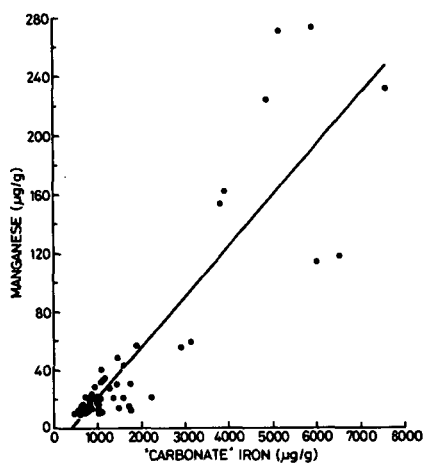


Figure 1. Plot of concentrations of manganese against 'carbonate' iron

A COMPARATIVE STUDY OF THE TRACE ELEMENT GEOCHEMISTRY IN COALS FROM ALBERTA, CANADA

Thomas Gentzis
Alberta Research Council
Devon, Alberta T0C 1E0 CANADA

Fariborz Goodarzi
Geological Survey of Canada
Calgary, Alberta T2L 2A7 CANADA

Keywords: Trace Elements, Geochemistry, Coal

INTRODUCTION

Alberta contains vast reserves (approximately 2185 megatonnes) of subbituminous and high-volatile bituminous coals, with an additional 1345 Mt considered as "indicated" and 3890 Mt as "inferred" (Smith, 1989). Virtually all of Canada's subbituminous coal resources, which are suitable for mine-mouth power generation, are found in the Interior Plains of Alberta. In addition, low sulphur (< 1.0%), high-volatile bituminous, exportable thermal coals occur in the Outer Foothills region of the province. Almost 90% of Alberta's power originates from six coal-fired generating stations. These are: (1) the 1987 MW Sundance station; (2) the 766 MW Keephills station; (3) the 570 MW Wabamun Lake station; (4) the 400 MW Genesee station; (5) the 735 MW Battle River station; and (6) the 760 MW Sheerness station (Figure 1a). The first four stations are located approximately 70-100 kms to the west and southwest of Edmonton, the fifth 180 kms east of Edmonton and the sixth 160 kms northeast of Calgary.

Coal contains almost every element in the periodic table and many of the elements are released, on particles or in vapour phase, to the environment, during coal combustion. In 1991, the Alberta Research Council, along with the Geological Survey of Canada, initiated a major program, financed by the power utility companies and the Alberta Government, on the "impact of coal quality on the utilization potential of Alberta subbituminous coals". Before examining the mobilization of elements during coal combustion and their emissions to the atmosphere, it is very important to study the concentration, mode of occurrence, lateral, and vertical variation of elements in the coal seams currently mined or those to be mined, within the boundaries of the minesite. As a result, this study deals with the elemental concentration and variation in coals from the Highvale mine (feedstock for the Sundance and Keephills plants), Whitewood mine (Wabamun plant), Vesta mine (Battle River plant) and Obed Mountain coal deposit (exported to Ontario as thermal coal) (Figure 1b).

The main focus of the paper is on the concentration of selected trace elements with known toxic responses to humans and the biological system, when emitted by coal-fired power stations, such as As, Hg, Mn, Se, and V, to name but a few. The elements in coals from the above mines will be classified according to the mode of their occurrence, with particular emphasis on the geological and geochemical factors influencing their distribution in the coal-bearing succession. Elemental concentrations will be compared and contrasted on a mine-by-mine basis rather than a seam-by-seam basis.

RESULTS AND DISCUSSION

Highvale Mine

Some of the elements of great concern because of their environmental effects are mercury (Hg) and cadmium (Cd). Mercury is volatile and is found either in gaseous form or enriched on the surfaces of fine particles following coal combustion (Clarke and Sloss, 1992). It is readily available for plant uptake and could be responsible for neural, renal and cardiovascular diseases in humans (US DOE, 1989). The Highvale coals contain Hg in the 100 to 400 ppb range (Gentzis, 1993, unpublished data), values which are slightly higher than Australian coals (100 ppb; Swaine, 1990) and lower than US coals (180 ppb; Finkelman, 1980). Low-sulphur coals, such as the Highvale coals (total S < 0.5%), are generally low in Hg and the element is believed to have an inorganic association. Cadmium tends to bioaccumulate in the food chain (Neme, 1991) and is a possible carcinogen to humans and animals (US DOE, 1989). The Highvale coals have Cd content less than 0.2 ppm, values similar to Australian coals (0.01-0.02 ppm) (Swaine, 1990) and lower than US coals (1.3 ppm) (Finkelman, 1980).

Mean elemental concentrations in the Highvale coals are: As (3.82 ppm), Br (286.4 ppm), Cl (72.3 ppm), Cr (11.5 ppm), Cu (20.6 ppm), Se (1.65 ppm), U (2.57 ppm), Th (5.6 ppm), and V (17.1 ppm) (Gentzis *et al.*, 1993). The high concentration of Br in some coal samples is attributed to drilling mud contamination, a phenomenon also observed by Finkelman (*pers. commun.*, 1993) in coals from Pakistan. Sodium content averages 2500 ppm, approximately three times higher than the nearby (12 Kms) Whitewood mine coals. This element has an inorganic association in the Highvale coals, and any detrimental effect of Na may be compensated by Ca in the coals. Other elements with an inorganic association include As, Ba, Cs, Fe, K, Mg, Mo, U, and V; Sr and Ce show an intermediate association, while Br, Cl, B, Co, Dy, and Mn show an organic association. The elements Al, As, Sc, Th and all rare earth elements (REEs) tend to decrease from roof to floor of the coal seams and their concentration often shows a cyclical pattern within the coal-bearing strata, indicative of periods of inundation of the coal-forming environment by clastic sediments.

Crowley *et al.*, (1989) have explained a mobilization pattern when a volcanoclastic layer (tonstein) is located above coal beds using cluster analysis. According to Van der Flier-Keller (1993), the light rare earth elements (LREEs) are associated with clay minerals and the heavy rare earth elements (HREEs) with detrital heavy minerals. All REEs in the Highvale mine subbituminous coal closely follow the Al trend, a behaviour which is expected since the REEs are associated with the inorganic constituents in coals. The high concentration of REEs in the thin coal seam 3 in drillhole HV84-901, which is located underneath a Sr and Ba-rich tonstein band (Figure 2), is believed to be due to migration of the elements by groundwater and subsequent concentration in the coal. The coal seam contains more HREEs than the volcanoclastic layer above because the HREEs were preferentially hydrolyzed or bound to organic complexes and allowed to migrate from the tonstein. The LREEs, being mobile, when liberated during the breakdown of the parent volcanic ash caused by weathering, were preferentially accommodated in clay minerals. The REE pattern in the Highvale coal is thought to be controlled by source lithology (volcanic versus sedimentary partings), by weathering, and other geochemical patterns during and after coal formation.

Ashing of two suites of samples of Highvale coal at 120°C resulted in an enrichment of all elements by a factor of x1.5 to x6.5 in one suite and by x5 to x11 in the other. In the 400°C ashed sample, enrichment factors ranged from x1.5 to x6.5 in the first suite and by x1.5 to 9.5 in the second. The elements Br, Cl, and Se were, surprisingly, enriched by x2 to x6, pointing to the formation of salts (i.e. bromide salts), which occurs as a result of reactions of anions with cations during ashing. At 800°C, Br and Cl were completely volatilized, as expected. Relative enrichment factors (REF), calculated using two methods of the ratio of elemental concentration versus Al concentration in air/crust (method A) and in ash/coal (method B) show method B to give higher and more consistent values.

Generally, there is little information on the variation of elements in coal seams laterally over a long distance, mainly due to variations in basement conditions and other geological factors (folding and faulting). The concept of "variance ratio" (the ratio of maximum to minimum value of an element) was first introduced by Headlee and Hunter in 1953 and subsequently used by Zubovic (1960) and Swaine *et al.*, (1984). The lateral variation of selected elements in pits 3 and 5 of the mine for seams 1 and 2 (the thickest) and corresponding variance ratios show that elements with inorganic association in the Highvale coal (i.e. As, Na, U, Se and Th) have narrow lateral variations in the pits and low variance ratios, whereas elements with organic association (i.e. Br, Cl) have wider lateral variation and higher variance ratio.

Whitewood Mine

The following seams are present in this mine: 1U, 1L, 2, 3, 4, 5, and 6, of which seam 1U is not presently mined and seam 1L is stratigraphically correlatable to seam 1 in the nearby Highvale mine. The mean concentrations of elements are: As (4.7 ppm), Br (15.1 ppm), Cl (21.5 ppm), Co (3.3 ppm), Cr (7.0 ppm), Mo (4.8 ppm), Na (710 ppm), Mn (110 ppm), U (2.5 ppm), Th (6.0 ppm), and V (19.3 ppm) (Gentzis, 1993, unpublished data). Compared to the Highvale coals, these coals are slightly enriched in As and V, depleted in the halides Br and Cl, also in Ba, Cr, Na, Se, and have similar concentration of Co, Mn and U. By world standards (see Clarke and Sloss, 1992, Table 8, p. 26), the Whitewood mine coals are "clean" and suitable for utilization. The ash analysis shows the mean SiO₂ value for all seams to be between 50 and 70 wt.%, Al₂O₃ ranges from 12-27 wt.%, Fe₂O₃ ranges from 1.5-6 wt.%, TiO₂ ranges from 0.4-0.75 wt.%, and CaO is in the 6-15 wt.% range. In addition, MgO varies from 0.6-2.1 wt.%, K₂O from 0.15-0.55 wt.%, Na₂O from 0.4-0.8 wt.% (except for seams 3 and 6) and

SO₃ from 2-6 wt.% (TransAlta Utilities, 1993, unpublished data). The coal ash is depleted in Na₂O and enriched in SO₃ and CaO (lime) compared to the coal ash quality requirements for power generation, outlined by Skorupska (1993). The ash content of the coal is 12-25%, with the exception of seam 1U (37%). A coal containing 20% ash provides an uncontrolled dust loading of 30 g/m², therefore, a collection efficiency of 99.7% is required to meet acceptable emission standards (Skorupska, 1993). In the Wabamun Lake power station, electrostatic precipitators (ESPs) are used to achieve this objective. One problem related to ESP performance in the Wabamun plant is opacity, which results in a decrease in precipitator efficiency. Because the Na₂O content in the ash is lower than the standard requirements dictate, the fly ash resistivity increases resulting in a decrease of the corona current flow.

Vesta Mine

One of the most obvious differences in trace elements between coal from this mine and coal from the other three mines is its high boron (B) content (> 200 ppm) (Gentzis, 1993, unpublished data). Boron in coal is interesting from a geochemical point of view because it can differentiate whether freshwater, mildly brackish, or brackish water conditions prevailed during the early stages of coal formation (Swaine, 1971; Goodarzi and Van der Flier-Keller, 1989; Banerjee and Goodarzi, 1990). Boron is very sensitive to changes in water salinity and remains constant laterally within a minesite. Furthermore, B values usually fall nicely within the limits designated for each generalized depositional setting (< 50 ppm for freshwater, 50-110 ppm for mildly brackish and >110 ppm for brackish) unless there is a secondary B enrichment (Goodarzi and Swaine, 1992). The B content of the Vesta mine coal indicates that the peat interacted with brackish waters, which may have invaded the fluvio-deltaic depositional setting during a marine transgression. Boron in the Vesta mine coal is associated with the organic matter and is depleted (25 ppm) only in one, inertinite-rich sample. The petrological composition of the sample indicates exposure of the peat surface to fire or oxidation and higher temperatures. Depletion of B has been observed in oxidation and combustion zones of naturally heat-affected coal seams (Goodarzi and Swaine, 1993) and is attributed to possible volatilization of the element. During combustion of this coal, B will most likely be redistributed in the bottom ash, the flyash retained by ESPs and fine flyash, which will eventually reach the atmosphere with the stack gases. However, B is not considered to be toxic and may have little detrimental effect in the close environs of the Battle River power station. The Vesta coals are very low in As (<1.0 ppm), Br (<2.3 ppm), V (<3 ppm), U (<1.4 ppm), Mn (<30 ppm), Mo (<2.5 ppm), but are extremely high in Na (range is 4200-4900 ppm) (Gentzis, 1993, unpublished data).

Obed Mountain Mine

The B content of the coal ranges from 27 to 100 ppm, but generally it is < 50 ppm, indicating freshwater to possibly slightly brackish water depositional environment. The element is depleted in the sedimentary partings (12-27 ppm) and enriched in the coal intervals immediately underneath. This behaviour points to downward mobilization of B from parting to coal of soluble to groundwater B, a phenomenon believed to be enhanced by increased oxidation leading to formation of leachates containing enough soluble B to affect groundwater (Goodarzi and Swaine, 1993). The range in elemental concentration in the two thickest seams are as follows: As 2-7.6 ppm; Br 5.9-10.1 ppm; Cl 76.4-87.2 ppm; Cr 3.4-11.2 ppm; Co 1.2-2.9 ppm; Mn 21.5-39.3 ppm; Mo 2.1-5.5 ppm; Se 1-1.2 ppm; U 1-2 ppm; Th 1.2-2.8 ppm (Gentzis, 1993, unpublished data); the lack of Na (mean is 117 ppm) could lead to potential problems in ESP performance.

Most elements increase in concentration with ash content, thus are inorganically associated in the coal. The vertical variation of certain elements is very similar, such as Th and U; also Zn, Rb, Cs, and K; Br and Cl; Na, Mg, Ti, As, and Fe. It was observed that U, Se, Sb, and Mo were concentrated preferentially in the upper part of the seams, while Br and Cl were enriched in the middle part. The elemental pairs: Mn and Sc, Co and Cu, Se and U, Rb and Cs, and the HREE are concentrated in coal intervals immediately underneath roof sediments or major partings. The Obed Mountain coals are depleted in most elements compared to coals formed under freshwater conditions, such as Highvale and Whitewood, except for Cl.

CONCLUSION

The elemental concentrations in the subbituminous coals from Alberta are related to the environment of coal deposition, the presence of volcanoclastic layers (tonsteins), the action of groundwater, the degree of weathering, and the nature of country rocks. The coal seams studied contain low concentrations of environmentally or industrially-sensitive elements, such as As, B (except for the Vesta coal), Cl, Mo, Se, Na, Ca, U,

and S, both vertically and laterally. The coals are "clean" and suitable for utilization. Elements associated with the mineral matter in coal are concentrated in the 800°C ashed coal, when compared to the fresh coal. There is also a progressive concentration of Br from the fresh to the 120°C and the 400°C ashed samples, pointing to the formation of salts.

REFERENCES

- 1) Banerjee, I. and Goodarzi, F., 1990 Paleoenvironmental and sulphur-boron contents of the Mannville (Lower Cretaceous) coals of southern Alberta, Canada, *Sedimentary Geology*, vol. 67, p. 297-310.
- 2) Clarke, L.B. and Sloss, L.L., 1992 Trace Elements-emissions from coal combustion and gasification, *International Energy Agency Report CR/49*, London, 111 pp.
- 3) Crowley, S.S., Stanton, R.W. and Ryer, T.A., 1989 The effect of volcanic ash on maceral and chemical composition of the C coal bed, Emery coalfield, Utah, *Organic Geochemistry*, vol. 14, p. 315-331.
- 4) Finkelman, R.B., 1980 Mode of occurrence of trace elements in coal, Ph.D. thesis, University of Maryland, College Park, MD, 301 pp.
- 5) Gentzis, T., Goodarzi, F. and Hickinbotham, A., 1993 Impact of coal quality on the utilization potential of coals from the Highvale Mine, Alberta, *Conference Proceedings, 7th International Conference on Coal Science*, Banff, Alberta, September 12-17, vol. 1, p. 93-97.
- 6) Goodarzi, F. and Van der Flier-Keller, E., 1989 Organic petrology and geochemistry of intermontane coals from British Columbia 3. The Blakeburn open cast mine near Tulameen, British Columbia, Canada, *Chemical Geology*, vol. 75, p. 227-247.
- 7) Goodarzi, F. and Swaine, D.J., 1992 Geochemistry of Boron in Australian and Canadian coals, *Proceedings of the Canadian Coal and Coalbed Methane Geoscience Forum*, Parksville, British Columbia, p. 319-332.
- 8) Goodarzi, F. and Swaine, D.J., 1993 Behaviour of Boron in coal during natural and industrial combustion processes, *Energy Sources*, vol. 15, p. 609-622.
- 9) Headlee, A.J.W. and Hunter, R.G., 1953 Elements in coal ash and their industrial significance, *Industrial Engineering Chemistry*, vol. 45, p. 548-551.
- 10) Neme, C., 1991 *Electric Utilities and Long-Range Transport of Mercury and Other Toxic Air Pollutants*, Centre for Clean Air Policy, Washington, DC, USA, 125 pp.
- 11) Skorupska, N.M., 1993 Coal specifications-impact on power station performance, *International Energy Agency Report CR/52*, London, 120 pp.
- 12) Smith, G.G., 1989 *Coal Resources of Canada*, Geological Survey of Canada Paper 89-4, 146 pp.
- 13) Swaine, D.J., 1971 Boron in coals of the Bowen Basin as an environmental indicator, *Proceedings of the Second Bowen Basin Symposium*, Geological Survey of Queensland, Report No. 62, p. 41-48.
- 14) Swaine, D.J., Godbeer, W.C and Morgan, N.C., 1984 Variations in contents of trace elements in coal from one seam, Report NERDDP, No. EG84/339, 103 pp.
- 15) Swaine, D.J., 1990 *Trace Elements in Coal*, Butterworths, London, 278 pp.
- 16) US DOE-United States Department of Energy, 1989 *Clean coal technology demonstration program, final programmatic environmental impact statement*, DOE/EIS-0146, US Department of Energy, Washington, DC, USA.
- 17) Van der Flier-Keller, E., 1993 Rare earth elements in Western Canadian coals, *Energy Sources*, vol. 15, p. 623-638.
- 18) Zubovic, P., 1960 Minor element content of coal from Illinois Beds 5 and 6 and their correlatives in Indiana and Western Kentucky, *United States Geological Survey Open File Report*, No. 537, 79 pp.

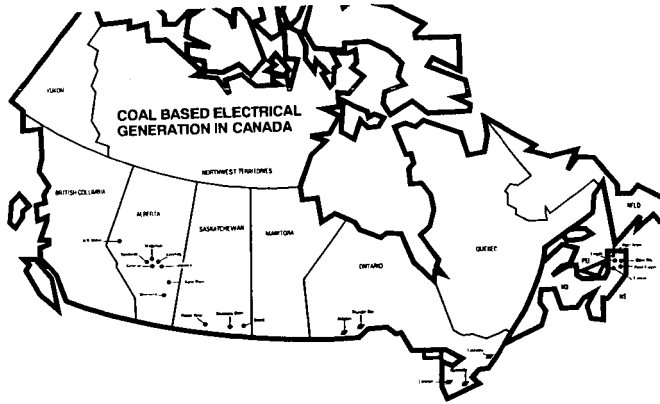


Figure 1a. Map of Canada showing location of power stations in Alberta (after Canadian Coal Association Directory, 1993).

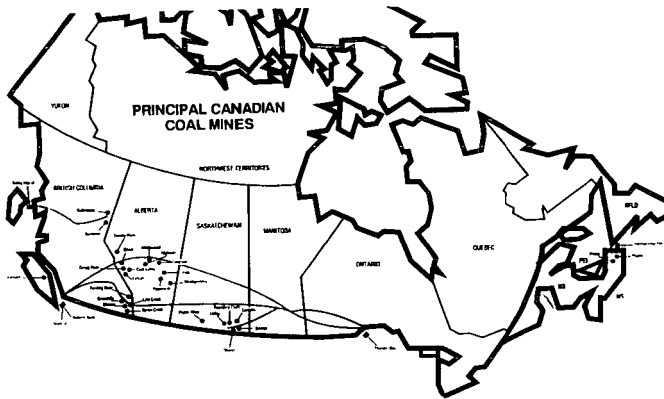


Figure 1b. Map of Canada showing location of coal mines in Alberta (after Canadian Coal Association Directory, 1993).

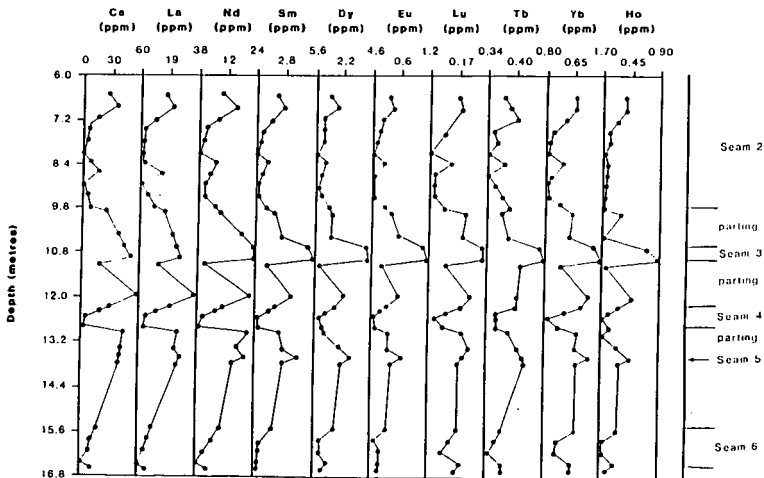


Figure 2 Vertical variation of REEs in drillhole HV84-901, Highvale mine.

PETROGRAPHIC AND GEOCHEMICAL ANATOMY OF LITHOTYPES FROM THE BLUE GEM COAL BED, SOUTHEASTERN KENTUCKY

James C. Hower¹, Darrell N. Taulbee¹, Susan M. Rimmer², and Liria G. Morrell¹
¹University of Kentucky Center for Applied Energy Research, Lexington, KY 40511
²University of Kentucky, Department of Geological Sciences, Lexington, KY 40506

Keywords: coal geochemistry, macerals, Kentucky

INTRODUCTION

The nature of the association of major, minor, and trace elements with coal has been the subject of intensive research by coal scientists (Swaine¹; and references cited therein). Density gradient centrifugation (DGC) offers a technique with which ultrafine coal particles can be partitioned into a density spectrum, portions of which represent nearly pure monomaceral concentrates. DGC has been typically conducted on demineralized coals² assuring, particularly at lower specific gravities, that the resulting DGC fractions would have very low ash contents.

In order to determine trends in elemental composition, particularly with a view towards maceral vs. mineral association, it is necessary to avoid demineralization. To this end the low-ash, low-sulfur Blue Gem coal bed (Middle Pennsylvanian Breathitt Formation) from Knox County, Kentucky, was selected for study. The objective of this study was to determine the petrography and chemistry, with particular emphasis on the ash geochemistry, of DGC separates of lithotypes of the Blue Gem coal bed.

EXPERIMENTAL

SAMPLE PREPARATION AND CHARACTERIZATION

Samples were obtained from the Blue Gem coal bed from a mine site in the Barbourville 7½ minute quadrangle, Knox County, Kentucky. The coal bed, 70 cm thick, was sampled in a series of five benches. Sample KCER-5447 represents the 10.0 cm basal bench of the coal bed. KCER-5445 represents an 11.6 cm lithotype from the middle of the coal bed.

Bench samples were crushed and split following procedures recommended by ASTM standard D2013.³

Proximate, ultimate, and sulfur analyses were determined for each bench sample according to standard ASTM techniques.³

Subsplits of the -20 mesh coals were mixed with epoxy resin and prepared into pellets for petrographic analysis and polished according to standard procedures.⁴

DENSITY GRADIENT CENTRIFUGATION SEPARATION

Maceral separation was based on the DGC method developed by Dyrkacz and co-workers⁵⁻⁶ with certain modifications.² Additional modifications included omission of the demineralization step, crushing the feed coal to -325 mesh, and adding Brij-35 surfactant to the separation media (due to the smaller particle size) to suppress particle agglomeration.

PIXE ASH GEOCHEMISTRY

The major and minor element geochemistry of the high temperature ashes of all of the lithotypes, the whole coal samples of the three lithotypes subjected to DGC separation, and the "whole coal" DGC density fractions was determined using Proton Induced X-ray Emission (PIXE). Procedures for PIXE analysis can be found in Savage.⁷

X-ray fluorescence analysis of the lithotype high temperature ashes was conducted at the CAER using techniques described by Hower and Bland.⁸

RESULTS

PETROGRAPHIC ANALYSIS OF BENCH AND DGC SAMPLES

Petrographically, the bench samples have relatively high vitrinite contents, with samples containing between 77.6 and 87.3% vitrinite (Table 1). Coal rank is high volatile A bituminous (0.88% R_{max}). Petrography of the KCER-5445 DGC separates is given on Figure 1.

In the DGC fractions recovered between 1.25-1.30 g/mL, vitrinite content is over 90%. The partitioning of macerals into relatively pure fractions with little association of

mineral matter was therefore encouraging for the interpretations to be made in the accompanying geochemical studies.

In each study sample, there is an abrupt transition from vitrinite-dominated to semifusinite-dominated DGC fractions at about 1.30-1.31 g/mL and a similar, though less abrupt, transition from semifusinite- to fusinite-dominated fractions at about 1.33-1.34 g/mL. Mixed maceral fractions dominate the lower density range.

GEOCHEMICAL CHARACTERIZATION OF BENCH SAMPLES

Aside from the top bench of the coal bed, KCER-5443, which has an ash content of 9.15% and a total sulfur content of 2.32%, the coal is very low in ash (0.40 - 1.47%) and sulfur (less than 0.8%). Elemental analyses suggest the presence of clays (Si and Al), carbonates (Fe and Ca), and, in the upper bench, possibly pyrite (Fe and S). This is supported by previous observations on the mineralogy of this coal bed.⁹ Several trace elements are enriched in the center of the coal bed (Ba, Cu, Mo, and Sr); other elements (Cr, Co, Mn, V, Ti, and Zr) increase towards the base of the coal.

GEOCHEMISTRY OF DGC SAMPLES

Based on analysis of the whole-coal and lithotype (non-DGC) ashes, Cs in the DGC-derived samples appears to be solely from the CsCl salt solutions used to prepare the DGC gradient. The PIXE geochemistry on the whole-coal basis was calculated on a Cs-free basis. The Cl content on the whole-coal basis was also adjusted stoichiometrically for Cs remaining from the DGC processing.

Cl and Br, both of which are best evaluated on the whole-coal basis, maximize in the vitrinite-rich separates.

In very-low ash samples such as these, organic sulfur is the most prevalent element other than C, H, N, and O. S and Cl trends for KCER-5445 are shown on Figure 2. On the whole-coal basis (pre-DGC), the sulfur content of KCER-5445 exceeds the ash content.

Ash-basis geochemistry is based on several assumptions: 1/ the "ash" percentage is 100% minus the "carbon" reported in the PIXE analysis ("carbon" includes all elements lighter than Na); 2/ most of the sulfur is organic and not part of the ash although organic sulfur can be fixed as sulfate in the low-temperature ashing process; and 3/ Cl and Br are volatilized, perhaps as HCl and HBr, in the ashing process.

Among the major elements, only P and Mg exhibit 10^2 order-of-magnitude ranges in concentration. In the case of Mg, the concentration peaks in the KCER-5445 >1.40 g/mL fractions. Ca and Mn are also relatively concentrated through this range, suggesting that the fusinite may be associated with a dolomite or magnesite with Mn substitution. Ca is also high in 5445 and 5447 1.22-1.30 g/mL fractions, but drops in the semifusinite-rich fractions. Fe is higher in 5445, peaking in the fractions above 1.31 g/mL. Siderite (FeCO_3), generally dispersed in vitrinite, is an important mineral phase in the Blue Gem.¹⁰ The Ca-Fe-Mg trends could be indicative of a shift in the dominant carbonate phase.

Si has a high concentration in the 5445 <1.12 g/mL fraction, perhaps representing biogenic silica, and in the pellets (material that exceeds the range of the density gradient) from the DGC runs. The Al variation is high in 5445 but somewhat muted in 5447 where DGC fraction 1 was not analyzed. K and the K/Al ratio minimizes in the vitrinite-rich fractions. K is also higher in 5447 than in 5445. Rb, which can substitute for K, only appears in the high-ash pellets.

P is exceptionally high in the 5445 1.18-1.22 g/mL fractions. The 1.20-1.22 g/mL fraction was analyzed for the other two coals but P was not significantly higher than in the other fractions.

On the ash basis, Ti maximizes in the high vitrinite fractions with 5447 having higher Ti concentration than 5445. Zr generally follows the Ti trends, peaking in the 5447 1.29-1.30 g/mL fraction at 6.5% (ash basis).

V maximizes in the high-vitrinite fractions, with 5447 having much higher concentrations, up to 14% in the 5447 1.29-1.30 g/mL fraction. In part, Cr follows the V trend, maximizing in the same fraction. Cr also has a high concentration in the 5445 1.12-1.15 g/mL fraction, corresponding to high concentrations of Ni, Cu, Mn, Zn, and Pb.

Ga, Ge, and Y peak in the lighter fractions and in the vitrinite-rich fractions and are higher in 5447 than in 5445. As and Se have greater concentrations in 5445 and peak in the lighter fractions and in the vitrinite-rich fractions. The highest concentration of As was found in the whole-lithotype ash of KCER-5443, a lithotype not processed by DGC. The As may be associated with pyrite in that high-sulfur lithotype.

Sr peaks in the vitrinite-rich fractions with similar trends and concentrations in each lithotype.

The elemental associations, or at least coincidences, noted are: Mg-Ca, Fe-Ca, and Mn-Ca; Ti-Zr; V-Cr; Cr-Ni-Cu-Mn-Zn-Pb (in a low-density split), Co-Ni, and Cu-Zn; Ga-Ge-Y; and As-Se. Of additional interest is the consistency of association of an element with a particular density split. Fraction 21, the high density "pellet" recovered from the rotor outer wall should contain minerals and associated elements not otherwise associated with macerals. Not surprisingly, elements clearly associated with mineral phases, such as Si and Al in clays, exhibit much higher concentrations in the pellet than in the lighter fractions. Many elements have somewhat mixed trends but Cl and Br are clearly higher in the organic-rich fractions than in the pellet. As, with Se showing an indeterminate trend, and Ga, with Ge showing an indeterminate trend, are higher in the organic-rich fractions. As noted above, Sr is one element which is consistently higher in the highest vitrinite fractions. Ca is also high through the vitrinite range although its peak is broader than the Sr peak. It is possible that Sr is closely associated with the carbonate phase of the vitrinite-rich fractions. Ga and Ge also tend to peak in the vitrinite-rich fractions.

REFERENCES

1. Swaine, D.J., 1990, Trace elements in coal. London, Butterworths, 278 p.
2. Taulbee, D.N., Poe, S.H., Robl, T.L., and Keogh, R., 1989, Density gradient centrifugation separation and characterization of macerals groups from a mixed maceral bituminous coal. *Energy & Fuels*, 3, 662-670.
3. American Society for Testing Materials (ASTM), 1989, Annual book of ASTM Standards: Coal and Coke. ASTM, Philadelphia.
4. Stach E., Mackowsky, M-Th., Teichmüller, M., Taylor, G.H., Chandra, D, and Teichmüller, R., 1982, Stach's Textbook of Coal Petrology, Third Edition, Gebrüder Borntraeger, Berlin, 535 pp.
5. Dyrkacz, G.R., Bloomquist, C.A.A., and Horwitz, E.P., 1981, Laboratory scale separation of coal macerals. *Separation Science and Technology*, 16, 1571-1588.
6. Dyrkacz, G. R., and Horwitz, E.P., 1982, Separation of coal macerals. *Fuel*, 61, 3-12.
7. Savage, J.M., Wong, A.S., and Robertson, J.D., 1992, Thick-target PIXE/PIGE analysis of complex matrices. *Jour. Trace and Microprobe Techniques*, 10, 151-168.
8. Hower, J.C., and Bland, A.E., 1989, Geochemistry of the Pond Creek coal bed, Eastern Kentucky coalfield. *International Journal of Coal Geology*, 11, 205-226.
9. Rimmer, S.M., Hower, J.C., Esterle, J.S., and Moore, T.A., in preparation, Petrology of the Blue Gem coal bed. To be submitted to the *International Journal of Coal Geology*.
10. Hower, J.C., Rimmer, S.M., and Bland, A.E., 1991, Ash geochemistry of the Blue Gem coal bed. *International Journal of Coal Geology*.

Table 1. Proximate analysis and maceral content of samples used in study.

KCER #	Ash (dry)	S _T (dry)	VM (dry)	Vit	Fus	Sfus	Mic	Ex	Res
5445	0.40	0.63	39.13	78.5	6.0	2.8	2.5	10.1	0.1
5447	1.47	0.61	37.03	77.6	7.2	3.6	2.7	8.7	0.2

Figure 1. Group maceral content of KCER-5445 vs. DGC fraction.

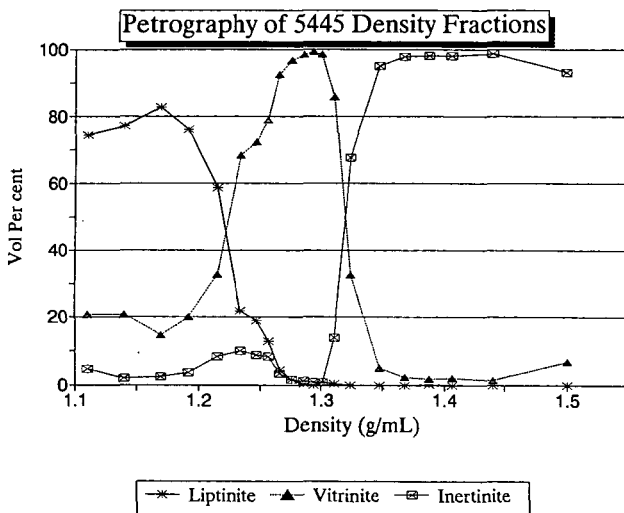
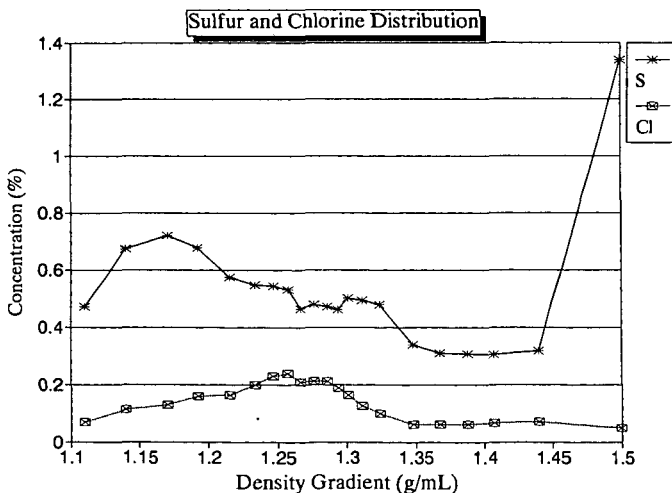


Figure 2. S_T and Cl of KCER-5445 vs. DGC fraction.



THE DISTRIBUTION OF TEN TRACE ELEMENTS AND MINERALS IN THREE LIGNITE SEAMS FROM THE MAE MOH MINE, THAILAND

Hart, Brian, Powell M.P., Fyfe, W.S. Department of Earth Sciences University of Western Ontario, London, Canada; Ratanasthien, B. Department of Geology, University of Chiang Mai, Chiang Mai, Thailand.

Keywords: Lignite, mineralogy, trace elements.

Introduction

Understanding the association of major, minor and trace elements in lignites and their accompanying strata is important from a number of perspectives (1) which include: potential health problems from environmental pollutants, rehabilitation after mining, combustion for power etc. The material which follows represents some preliminary observations on the mineralogy and distribution of 10 trace elements in lignites and accompanying sediments from the Mae Moh mine, Thailand.

Samples collected from freshly exposed mine faces were air dried and analyzed for moisture and ash. Trace element concentrations were determined on "whole" coals and sediments by NAA and XRF. All chemical analyses are expressed as a fraction of the total dry sediment. Mineralogy of both LTA and sediments was determined by XRD. The chemistry and morphology of individual particles were examined by the Electron microprobe. The analyses are used to make some conclusions about the spatial occurrence of these elements within the seam and their partitioning between organic and inorganic phases.

Mineralogy: XRD Analysis

In samples with >50% ash the mineralogy was determined on untreated material. In samples with <50% ash the mineralogy was determined on oxygen plasma low temperature ash. The minerals identified by XRD analysis include quartz, kaolinite, pyrite/marcasite, calcite, gypsum, illite, smectite (mixed-layer clay), jarosite, bassanite, spinel, anhydrite and ferroxahydrate.

Mineralogy Discussion

For the most part, the greater than 50% ash samples represent the mineralogy of the sediments (overburden, underclays and interseam partings) associated with the coals. In both the Q and K seams as well as the lower portion of J seam calcite dominates the mineralogy. In a previous study (2) a similar distribution for calcite was identified where it was suggested that the calcite might be both biogenic and derived from weathered limestone bedrock. Both origins are possible as the underlying Triassic sequence is marine and fresh water gastropods have been identified in many interseam sediments (3). Pyrite was identified in all but 4 sediment samples. While preliminary SEM work has indicated that much of the pyrite within the sediment and coal samples is framboidal, it also occurs as nodules and fracture fillings. The occurrences suggest both a syngenetic and epigenetic formation for the sulphide. Based on SEM analysis the quartz identified in all but 2 samples appears to be mostly detrital. Siliceous zones in which some of the quartz is extremely fine grained, may be due in part to an authigenic or biogenic origin. Preliminary SEM work has shown the clay minerals to be very fine grained. Detailed clay mineralogy on selected samples indicates that the proportion of kaolinite is slightly higher than illite and the occurrence of expandable clays increases down the section. The illite is likely detrital, and the poor crystallinity of the kaolinite suggests a similar origin.

Within samples of LTA calcite, as in the sediments, appears to be more common in the Q and K seams while quartz is identified throughout the section. Pyrite is present, mostly a major constituent, in all but the upper 2 LTA samples from J seam. As in the sediments, the proportion of kaolinite is greater than illite in the LTA samples. Minerals not identified in the sediments; bassanite (except in 2 samples), anhydrite and ferroxahydrite, are artifacts created during the ashing procedure. Anhydrite and bassanite are both dehydration products from gypsum. Bassanite can also form by the combination of organically associated Ca and sulphur released during the ashing procedure. Ferroxahydrite forms from similar mobile components in the coal as they are released during the ashing (4).

Vertical element variations

The NAA and XRF analysis for 10 elements in samples collected from the three seams is given in table 1.

J seam. For the elements reported, except U, the concentration decreases from the top to the bottom of the seam (Fig 1a;Cr as an example). The consistently high concentration of ash in samples from the upper portion of the seam is coupled with higher concentrations of trace elements. The elements Mo and Sb (Fig 1a;Sb) also showed increased concentrations in samples from the lower portion of the seam, while the concentration of U (Fig 1b;U) is variable.

K seam. The elements As, Co, Cr, Mo and U show higher concentrations in the samples closer to the seam margins (Fig 1b;U). Antimony, and to some degree Pb, are concentrated in the upper portion of the seam only (Fig1b:Pb). The distribution of Se down the seam is variable. The lowest concentration of all elements is found in the mid portion of the seam where the ash content of the samples is also low.

Q seam. Within the Q seam all elements except As and Se show a marked overall concentration increase from top to the bottom of the seam (Fig 1c;Co). Selenium is concentrated in the middle of the seam (Fig 1c;Se) while As is enriched in the upper 2 samples as well as the lower portion of the seam (Fig 1c;As).

Interpretation of element distribution

The relationship between ash content and element concentration in a coal can be used as a guide to determine whether an element is preferentially associated with the organic or inorganic fraction of the coal (5). Pearson correlation coefficients were calculated for 10 elements versus ash in each of the 3 seams. Based on these correlations only 2 types of element associations were recognized; those elements which are inorganically associated and those elements which show a mixed inorganic-organic association.

Correlation coefficients in the J seam reveal that only Pb and Th are inorganically associated. The remainder of the elements had correlation coefficients indicative of mixed organic-inorganic associations. In a more restricted group of samples, representing only mine designated lignite seams, an inorganic affinity was indicated for all elements except Mo, Sb and U. Correlation coefficients for the latter 3 elements indicates a mixed organic-inorganic association. Correlation coefficients for elements in K seam indicate that Mo, Ni, Pb, Sb, and U are most likely to be inorganically associated, whereas As, Co, Cr, Se, and Th show a mixed organic-inorganic

association. In the Q seam Cr, Mo, Pb, Th and U show a strong inorganic affinity while a mixed association is indicated for As, Co, Ni, Sb and Se.

Except for those elements which are consistently inorganically associated, for example Pb, there appears to be no reasonable agreement between correlation coefficients of elements with ash and their vertical distribution. The concentration for most elements in this study group, expressed as a fraction of the total dry sediment, appears to be linked to the inorganic content of the lignite seam. For example the upper samples in J seam are both high in ash and high in trace elements. Furthermore the samples from K seam which are low in ash are consistently low in trace elements. These observations are not necessarily indicated by the correlation coefficients.

Inconsistencies in correlation coefficients exhibited by many of the trace elements can be related to their wide range in concentration. A single sample can easily skew the distribution thereby changing the elements apparent association from one group to another. A good example of this is Co in Q seam where, apart from one, sample Q4A (Fig1c), the concentration clearly parallels the ash content.

The interpretation therefore is that most of the elements are associated with inorganic grains and occur either bound within minerals, as oxide films surrounding mineral particles or as ions adsorbed onto the surface of a mineral such as kaolinite. This interpretation works well for those elements which show distinct enrichment in sediment samples; for example, Q seam where Cr and Th are concentrated in both the mid-seam parting and the underclay.

Since the ash content of lignites reflects both the actual mineral particles and exchangeable ions held in the organic material, the possibility exists that a number of trace elements could be held in organic combination. Fractionation experiments (6) have shown that Cr, V and Ni were at least partially, or in the case of Cu and Zn wholly, complexed with the organic matter. Although no fractionation studies were performed on these coals an organic association is indicated for at least some of the Se, particularly in samples where high concentrations are not coupled with high ash content. The element As shows a similar relationship to ash in some samples and may also be partially organically complexed. However isomorphic substitution of As for Fe in pyrite may give rise to high As concentrations even in those low ash lignite samples which contain pyrite.

References

1. Swaine, D.J. "Trace Elements in Coal"; Butterworths and Co.: London, 1990; p.278
2. Ward, C.R., *International Journal of Coal Geology*, 1991, 17, 96-93.
3. Watanasak, M. "Proc. Int. Symp. on Intermontane Basins: Geology and Resources" T.Thanasuthipitak and P. Ounchanum, Eds. ; Chaing Mai University 1989, 327-335.
4. Morgan, M., E.; Jenkins, R.G.; Walker, P. L. *Fuel* 1981, 60, 189-193.
5. Karner, F.R.; Benson, S.A.; Schobert, H.H.; Roaldson, R.G. "The Chemistry of Low Rank Coals", H.H. Schobert Eds.; Amer. Chem. Symp. Series 264; Amer. Chem. Soc. Washington, DC, 1984, 175-193.
6. Miller, R.N.; Given, P. H. *Geochem. Cosmochem. Acta*, 51, 1311-1322.

TABLE 1 TRACE ELEMENT CONCENTRATION FOR 10 ELEMENTS IN 3 SEAMS FROM THE MAE MOH MINE

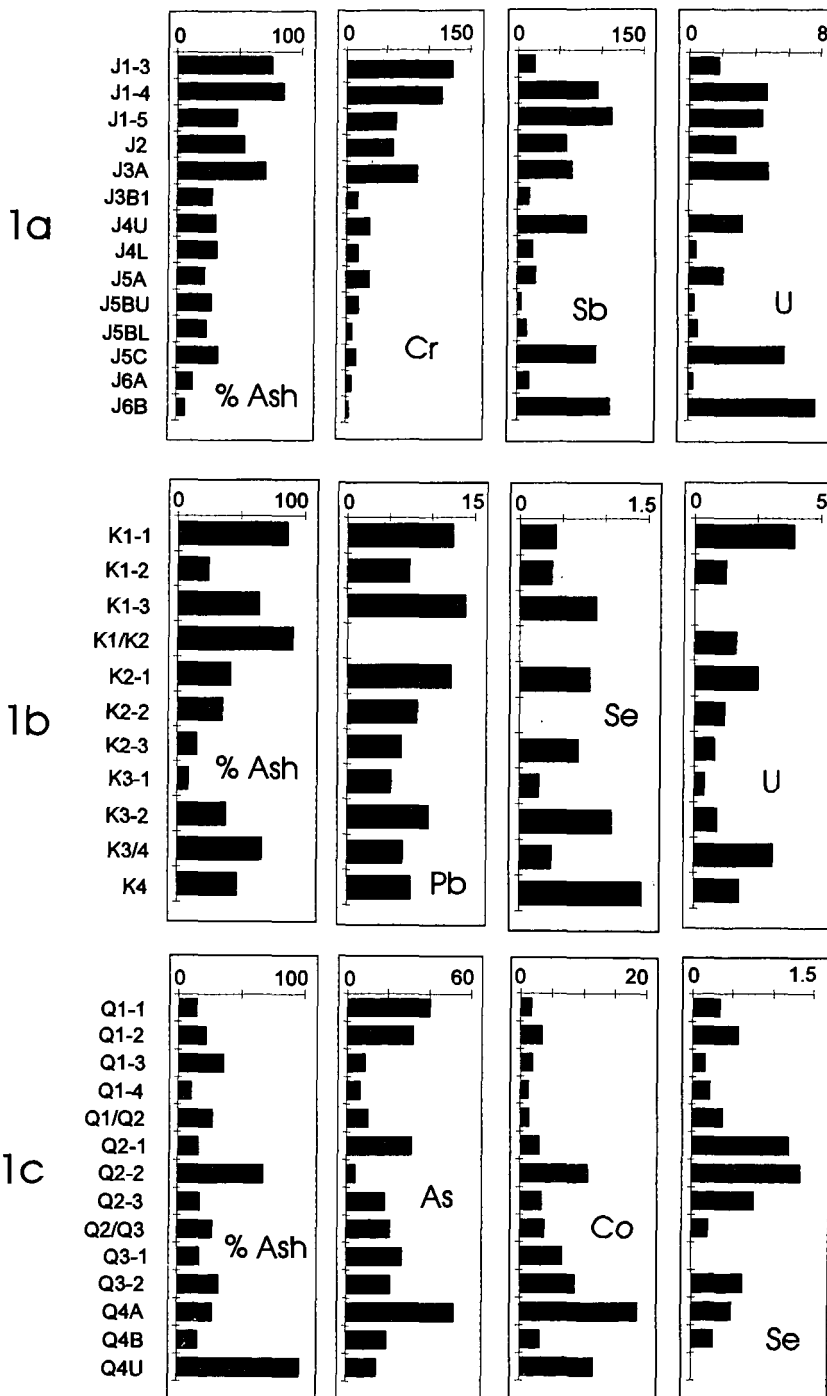
SAMPLE #	% Ash	As	Co	Cr	Mo	Ni	Pb	Sb	Se	Th	U
J1-1,2	91.82	28.80	6.95	122.95	6.63	57.97	30.67	3.28	0.88	25.12	2.31
J1-3	78.07	71.11	13.19	127.88	5.35	60.19	21.35	2.09	2.07	17.03	1.83
J1-4	85.65	269.43	37.38	114.91	28.60	249.86	18.84	9.58	1.18	16.33	4.74
J1-5	48.31	180.29	16.23	60.52	16.30	32.53	10.58	11.22	1.48	6.62	4.45
J2	54.40	65.94	10.33	58.94	8.88	30.56	14.35	5.80	1.60	9.16	2.88
J3A/J2	93.27	350.74	11.16	97.11	4.80	46.17	17.07	4.05	1.09	21.82	1.98
J3A	71.00	93.91	21.81	85.75	9.74	57.31	9.57	6.60	1.12	12.94	4.80
J3A/J3B1	92.75	15.92	11.20	98.70	1.94	39.51	23.68	0.78		19.03	0.22
J3B1	29.78	26.88	8.16	14.27	5.62		5.7	1.49	0.38	1.87	
J3/J4	90.59	71.32	7.04	32.54	6.74		7.07	3.01		5.58	2.01
J4U	31.48	117.35	16.98	28.88	12.02	44.42	4.62	8.21	1.19	2.54	3.28
J4U/J4L	62.41	68.58	9.46	69.88	2.82	21.91	15.65	2.69		14.88	1.48
J4L	32.42	79.18	14.47	14.82	4.01	22.52	4.72	1.92	1.28	2.16	0.44
J4/J5	98.07	41.52	6.76	25.39	8.07	18.82	7.13	3.60		4.98	4.01
J5A	22.63	95.11	3.98	29.31	5.14	22.09	4.81	2.28	0.79	0.85	2.10
J5A/J5B	85.68	68.14	7.90	28.73	2.82		10.05	2.63		4.95	1.70
J5B U	28.38	37.85	7.88	15.78	3.34	23.72	4.04	0.59	0.84	1.71	0.37
J5BU/J5BL	89.48	23.69	3.08	8.64		8.39		0.83	0.42	2.01	0.45
J5BL	24.21	54.62	5.78	7.38	2.40	7.82	3.8	1.23	0.49	0.92	0.55
J5B/J5C	67.00	109.47	8.40	29.17	8.50		9.8	3.43	0.89	8.69	1.80
J5C	34.07	105.04	7.57	12.78	24.38	13.89	8.83	9.54		9.78	5.83
J5/J8	94.41	3.07	8.23	32.30	3.89	22.84	8.93	0.48	0.62	7.22	2.33
J8A	13.40	61.41	1.85	7.15	4.55	0.00	4.73	1.58	0.48	0.15	0.31
J8A/J8B	85.20	8.49	5.73	19.13	1.78	12.61	7.38	0.68	0.62	4.81	0.58
J8B	7.07	35.10	2.03	3.80	13.08		3.48	11.08	0.39	0.71	7.70
J8B-1	88.74	85.30	2.93	5.47	4.15	10.09		2.47	0.50	1.08	0.60

Sample #	% Ash	As	Co	Cr	Mo	Ni	Pb	Sb	Se	Th	U
K1-1	89.32	31.57	8.59	25.46	8.17		12.43	6.38	0.42	4.98	3.18
K1-2	24.34	40.65	3.38	14.56	3.31		7.34	1.15	0.38	3.07	1.00
K1-3	64.35	ND	8.96	32.44	ND	27.87	13.85	ND	0.80	8.85	ND
K1/K2	91.06	38.94	0.39	4.18	3.71			2.12		0.15	1.33
K2-1	41.98	21.79	8.76	29.11	5.31	14.67	12.28	2.90	0.82	8.26	2.02
K2-2	35.61	11.68	3.48	11.48			8.32	1.65		2.80	0.68
K2-3	15.42	13.08	2.05	7.58	1.77	13.35	8.48	1.28	0.69	2.00	0.64
K3-1	9.13	9.41	1.83	3.78	1.68	10.95	5.27	1.05	0.23	0.59	0.34
K3-2	38.78	58.28	9.88	18.32	3.55	19.17	9.69	2.00	1.08	3.11	0.73
K3/K4	88.70	28.02	7.88	15.04	8.83		8.68	2.50	0.38	2.68	2.50
K4	47.45	75.02	14.58	26.64	4.88	19.75	7.55	1.98	1.43	4.60	1.48

Sample #	% Ash	As	Co	Cr	Mo	Ni	Pb	Sb	Se	Th	U
Q1-1	15.38	40.17	1.78	2.66			4.32	0.21	0.34	0.21	
Q1-2	22.50	32.16	3.57	2.21	1.48	10.61	3.12	0.36	0.57	0.23	0.22
Q1-3	38.30	8.72	2.00	2.50			4.7	0.48	0.18	0.27	
Q1-4	11.33	6.84	1.39	2.98		5.44	4.22	0.33	0.22	0.28	
Q1/Q2	27.90	10.39	1.50	1.77			5.97	0.38	0.39	0.23	
Q2-1	18.55	31.42	3.08	9.58	2.97			0.95	1.20	2.06	0.58
Q2-2	87.68	4.58	10.82	35.31		28.78	11.88	0.40	1.35	8.70	
Q2-3	17.62	18.61	3.55	12.50	3.46	15.97	4.4	1.08	0.77	2.80	0.58
Q2/Q3	27.50	21.24	3.98	8.22	3.00	11.94	4	0.74	0.21	1.02	
Q3-1	17.44	27.05	6.73	17.75	6.60	24.07	9.13	1.64		4.33	1.85
Q3-2	32.87	21.24	6.73	23.68	3.46	22.85	11.17	0.72	0.63	5.98	0.49
Q4A	27.89	52.44	18.78	24.31	7.92	45.73	11.25	2.74	0.50	5.11	2.37
Q4B	18.30	19.65	3.22	9.18	2.70	14.80	4.87	1.01	0.27	0.46	
Q4	96.64	14.80	11.71	38.82	6.88	30.34	11.03	2.08		9.55	4.49

All trace element data reported as ppm.
 Blank spaces in the table indicate the concentration was below detection limits
 ND = no data

FIGURE 1. VERTICAL DISTRIBUTION OF 10 ELEMENTS IN THE 3 LIGNITE SEAMS FROM MAE MOH, THAILAND FOR J SEAM, ONLY THOSE SEAMS DESIGNATED AS LIGNITE ARE INCLUDED



FLUORINE IN COAL AND COAL BY-PRODUCTS

J.D. Robertson,^{1,2} A.S. Wong^{1,2} and J.C. Hower²
Department of Chemistry¹ and Center for Applied Energy Research²
University of Kentucky
Lexington, KY 40506-0055

Keywords: Fluorine, PIGE, Coal

INTRODUCTION

Fluorine occurs in trace amounts in most coals. It is typically associated with minerals of the apatite group, principally fluorapatite and clays, and with fluorite, tourmaline, topaz, amphiboles and micas¹. The average fluorine content of US coal is, according to the tabulation of Swanson *et al.*², 74 $\mu\text{g/g}$. In the United States, the lowest average fluorine concentration of 30 $\mu\text{g/g}$ is found in coals from Eastern Kentucky and the highest average value of 160 $\mu\text{g/g}$ is found in coals from Wyoming and New Mexico.³ The concentration range of fluorine in European coals is similar to that found in the US while the average fluorine content of Australian coals ranges from 15 to 500 $\mu\text{g/g}$.⁴

Fluorine is released into the atmosphere during the combustion of coal. According to a National Academy of Sciences report, coal combustion accounts for a significant fraction (10%) of the total atmospheric emissions of fluorine in the United States.⁵ Because of its effect upon environmental quality and health, fluorine has been classified as an element of moderate concern in the development of the coal resource.⁶ With the increased utilization of this energy resource, it is important to be able to reliably determine the fluorine content of coals and coal by-products.

The amount of fluorine in coals and geological materials is generally determined using an ion selective electrode or, more recently, ion chromatography to measure the concentration of fluoride ions in a solution prepared from the sample. The most common chemical pretreatment techniques include alkali fusion,^{7,8} oxygen bomb digestion,^{1,7} and pyrohydrolysis.^{1,7,9,10,11} The ASTM standard method (D3761-79) is based on the oxygen bomb procedure; a simple and convenient sample preparation technique. The validity of the oxygen bomb and alkali fusion methods has, however, been called into question as these two procedures consistently yield lower results than those obtained by pyrohydrolysis.^{7,9,12} This is most likely due to the incomplete dissolution of fluorine from the sample by these two procedures. The end result of this discrepancy is a wide range of fluorine values in the literature and the lack of certified fluorine values for coal and fly ash standards.

In order to aid the certification process, we have determined the fluorine content of several coal and fly ash standards by an alternate method; proton-induced gamma-ray emission (PIGE) analysis. PIGE is a rapid, non-destructive analysis technique that is based upon the detection of the prompt gamma rays that are emitted following a charged-particle-induced nuclear reaction. The energy of the gamma ray is indicative of the isotope present, and the intensity of the gamma ray is a measure of the concentration of the isotope. This ion beam technique is mainly used in the analysis of light elements. It has been used to determine the fluorine content of various geological materials^{13,14} and of the NIST 1632a and 1633a coal and fly ash standards.^{10,15} We have, using the method of standard additions, determined the fluorine content in NIST bituminous coal SRM 1632b, subbituminous coal SRM 1635, coal fly ash SRM 1633a, USGS Lower Bakerstown coal CLB-1, CANMET BCR 40 and SARM 20.

EXPERIMENTAL PROCEDURE

The PIGE measurements were performed at the University of Kentucky 7.5 MV Van de Graaff accelerator.¹⁶ The nuclear reactions utilized in these PIGE measurements are $^{19}\text{F}(p,p_1)^{19}\text{F}$, $E_\gamma = 110$ keV and $^{19}\text{F}(p,p_2)^{19}\text{F}$, $E_\gamma = 197$ keV. The samples were irradiated with an external 2.5 MeV proton beam in 1 atm. of He. The γ rays were detected with an ORTEC HPGe detector, 20% relative efficiency, with a FWHM resolution of 2.40 keV at 1274 keV. The beam, normal to the target surface, was rastered over the sample at 1 Hz irradiating a spot of 5 mm by 7 mm. The proton beam current, on the extraction foil, ranged from 100 to 150 nA, and the collected charge ranged from 90 to 140 μC . The irradiation times were adjusted to obtain an uncertainty in the counting statistics of less than 5% (except for SRM 1635, where the uncertainty was less than 10% after 20 minutes of counting time) in the areas of the 110- and 197-keV γ -ray peaks. The irradiation time per sample ranged from 15 to 20 minutes. Rather than adjust the beam current to maintain a constant count rate, a pulser was used to correct for the dead time in the γ -ray spectra. Typically, the dead time in the measurements was less than 3%.

For the standard addition measurements, one blank and four spiked samples were prepared for each coal standard. The spiked samples were prepared by adding appropriate amounts (from 5 to 25 μL) of the NIST SRM 3183 fluoride ion chromatographic solution ($[\text{F}^-] = 1000$ $\mu\text{g/g}$) to

approximately 250 mg of coal. The concentration of fluorine spikes ranged from 25 to 90 $\mu\text{g/g}$. After addition of the fluorine solution, the spiked samples were oven dried for 24 hours at 50°C. The dried samples were then mixed in a polystyrene vial with a methacrylate ball for 30 minutes. The blank and spiked samples were then pelletized in a 13-mm stainless steel die at 90 Mpa. High purity graphite powder (Johnson Mathey, Ultra 'F' spectroscopic grade) was mixed with the NIST 1633a fly ash SRM in order to obtain a stable pellet. The blank and spiked samples of NIST 1633a were prepared from this mixture. Two sets of standard addition samples were prepared and analyzed for each standard. Figures I and II show the typical fluorine standard addition curves obtained.

RESULTS AND DISCUSSION:

The results obtained from the standard addition method for each standard are listed in Table I. The fluorine values, which are reported on a dry weight basis, are the weighted average of the concentration values obtained from the 110- and 197-keV standard addition curves on two series of standard addition samples. The limits of detection (LOD) for the measurements (Table I) are based on a minimum observable peak area of 3**v**bkg where bkg is the background over 1 FWHM about the gamma-ray (197 keV) peak's centroid. The LOD for fluorine in coal ranged from 2 to 8 $\mu\text{g/g}$, depending upon the ash content in the coal. The relative standard deviation for a single measurement, based upon counting statistics, ranged from 0.9 % to 10 %.

In order to determine if the concentration of the fluorine changed during the proton irradiation, a single pellet of NIST SRM 1632a sample was subjected to four consecutive 15-minute irradiations at 150 nA. No significant variations were observed in the normalized 110- and 197-keV gamma-ray yields in the multiple bombardments. The average normalized yield was $133 \pm 2 \text{ } \gamma\text{/s}/\mu\text{C}$ for the 110-keV gamma-ray peak, and $145 \pm 1 \text{ } \gamma\text{/s}/\mu\text{C}$ for the 197-keV gamma-ray peak. The overall average of the normalized yield for SRM 1632a during four days of consecutive measurements (10 irradiations) was $126 \pm 6 \text{ } \gamma\text{/s}/\mu\text{C}$ for the 110-keV gamma-ray peak, and $141 \pm 6 \text{ } \gamma\text{/s}/\mu\text{C}$ for the 197-keV gamma-ray peak.

As can be seen from the comparison presented in Table II, the fluorine concentration values obtained in this work for the NIST, SARM and BCR standards agree well with the values obtained by pyrohydrolysis. The fluorine values obtained by oxygen bomb digestion are, on the other hand, consistently lower than the PIGE and pyrohydrolysis values. As noted above, this is most likely due to the incomplete dissolution of fluorine from the sample by this sample preparation procedure.

We are currently using PIGE as a rapid, instrumental technique to investigate how fluorine partitions in wet and dry FGD equipped coal combustion systems. Results from this study will be presented.

ACKNOWLEDGEMENTS

This work was supported in part by the Department of Energy and the Kentucky EPSCoR program. We are indebted to Ms. Jean Kane and Mr. Robert Dureau for the standards used in this work.

REFERENCES

1. W.G. Godbeer and D.J. Swaine, *Fuel* 66, 794 (1987).
2. V.E. Swanson, J.H. Medlin, J.R. Hatch, S.L. Coleman, G.H. Wood, S.D. Woodruff and R.T. Hilderbrand, *Collection, chemical analysis and evaluation of coal samples in 1975*, US Dept. of Interior, Geological Survey, Report No. 76-468, 1976.
3. A.J. Dvorak, US Nuclear Regulatory Commission Report No. NUREG-0252, 1977.
4. D.J. Swaine in *Combustion of Pulverized Coal-The Effect of Mineral Matter*, I.M. Stewart and T.F. Wall, Eds., University of Newcastle, NSW, 1979, pp 14-18.
5. M. Fleischer, R.M. Forbes, R.C. Harriss, L. Krook and J. Kubota in *Geochemistry and the Environment Vol. 1*, Nat. Acad. Sci., 1974.
6. U.S. National Research Council, *Trace Element Geochemistry of Coal Resource Development Related to Environmental Quality and Health*, National Academy Press, Washington, D.C., 1980.
7. K.J. Doolan, *Anal. Chim. Acta* 202, 61 (1987).
8. M.W. Doughten and J.R. Gillison, *Energy and Fuels* 4, 426 (1990).
9. T.D. Rice, *Talanta* 35(3), 173 (1988).
10. V.B. Conrad and W.D. Brownlee, *Anal. Chem.* 60, 365 (1988).

11. E.L. Obermiller, Consolidation Coal Co., Library, PA, Personal Communication (1991).
12. A. Savidou and T. Paradellis, *J. of Coal Quality* 9 (2), 44 (1990).
13. I. Roelands, G. Robaye, G. Weber and J.M. Delbrouck-Habaru, *Chem. Geol.* 54, 35 (1986).
14. J.R. Bird and E. Clayton, *Nucl. Instr. Meth.* 218, 525 (1983).
15. E. Clayton and L.S. Dale, *Anal. Lett.* 18(A12), 1533 (1985).
16. J. M. Savage, A. S. Wong, and J. D. Robertson, Thick-Target PIXE/PIGE Analysis of Complex Matrices, *J. of Trace and Microprobe Tech.*, 10 (2-3) (1992) 151-168.

TABLE I

Fluorine Concentrations* ($\mu\text{g/g}$) of NIST, SARM, CLB and BCR Coal and Fly Ash Standards Determined by Standard Addition PIGE Measurements.

Sample ID	Fluorine ($\mu\text{g/g}$)	Ash (wt%)	LOD ($\mu\text{g/g}$)
NIST 1635	28 ± 1	4.7	6.2
NIST 1632b	48 ± 2	6.8	3.9
SRM 1633a	93 ± 10	100	15
CLB-1	68 ± 7	-	2.0
BCR 40	114 ± 6	-	5.9
SARM 20	148 ± 13	35.3	4.6

* Dry weight.

TABLE II

Fluorine Concentrations for NIST, SARM and BCR Standards Obtained by PIGE, Pyrohydrolysis, and Oxygen Bomb Digestion.

Sample ID	PIGE	Pyrohydrolysis	Oxygen Bomb
NIST 1635	28 ± 1	$39^7, 42^{10}, 34, 35^{11}$	$18, 12^{11}$
NIST 1632b	48 ± 2	$46^7, 58^{10}$	
NIST 1633a	93 ± 10	$82^7, 73^9, 81^{10}, 89^{11}$	$25, 22^{11}$
BCR 40	114 ± 6	$128^{10}, 122, 119^{11}$	107^{11}
SARM 20	148 ± 13	$148^1, 152^7, 141^{10}, 130^{11}$	$86^1, 107, 110^{11}$

FIGURE I
Fluorine Standard Addition Curve of NIST 1635 Coal Standard

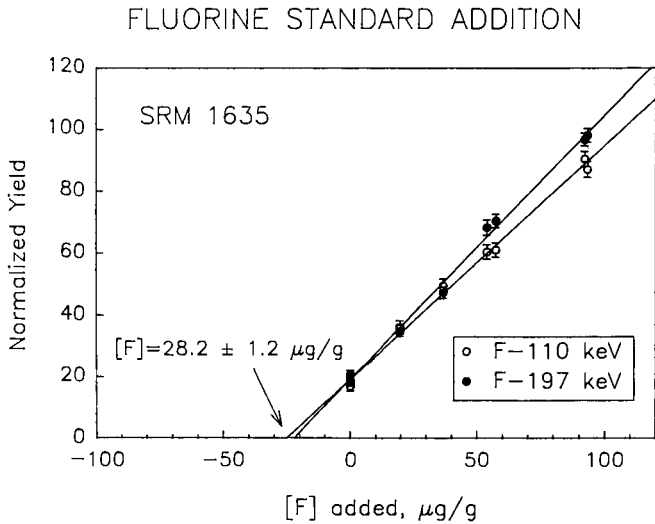
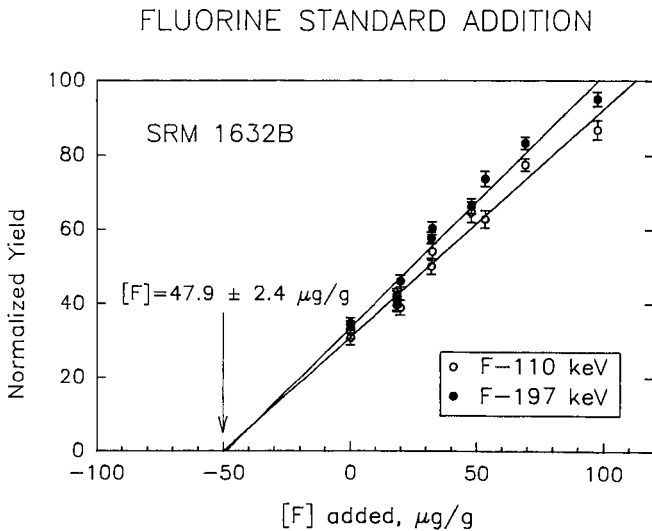


FIGURE II
Fluorine Standard Addition Curve of NIST 1632b Coal Standard



MODES OF OCCURRENCE OF TRACE ELEMENTS IN COAL FROM XAFS SPECTROSCOPY

Frank E. Huggins, J. Zhao, N. Shah, G.P. Huffman
233 Mining and Mineral Resources Building
University of Kentucky
Lexington, KY 40506

Keywords: XAFS spectroscopy, mode of occurrence, trace elements.

INTRODUCTION

It is well known that elements exist in coal in a variety of different modes of occurrence [1,2]. Such modes can vary from the element being totally dispersed in the macerals (e.g. organic sulfur, carboxyl-bound Ca in lignite) to discrete mineral occurrences (e.g. pyrite, FeS₂, quartz, SiO₂, etc.). Recently, we showed that X-ray absorption fine structure (XAFS) spectroscopy is capable of recording spectra from elements present in coal at concentration levels as low as 5 ppm [3]. Such information, obtained directly with a minimum of sample preparation, is proving to be invaluable for the elucidation of a trace element's mode of occurrence. In the previous work, we used XAFS spectroscopy to identify the principal modes of occurrence of arsenic and chromium in various coals. Here, we present more recent XAFS spectroscopic observations on these and other trace elements in coal and take the opportunity to discuss the ramifications of such XAFS studies for geochemical investigation of trace elements in coal.

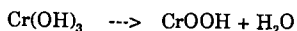
EXPERIMENTAL

XAFS spectra of trace elements in coal were obtained at one or other of the two major U.S. synchrotron sources: the Stanford Synchrotron Research Laboratory (SSRL), at Stanford University, CA, and the National Synchrotron Light Source (NSLS), at Brookhaven National Laboratory, NY. Procedures for obtaining XAFS spectra of trace elements are described in detail elsewhere [3]. Spectra were recorded, usually in multiple scans, by means of a 13-element germanium detector specifically designed for trace element studies [4]. Coal samples were suspended in the X-ray beam in thin (6 μm) polypropylene bags. Analysis of the XAFS spectra was performed at the University of Kentucky on a MicroVAX II computer. As is usually done, the XAFS spectrum was subdivided into the X-ray absorption near-edge structure (XANES) and the extended X-ray absorption fine structure (EXAFS) regions. All XANES spectra shown here are calibrated with respect to a reference material containing the element of interest. The zero energy points in the Cr, Mn, As, and Br XANES spectra are defined as the first maximum in the derivative of the spectrum of Cr in stainless steel (5.989 keV), the spectrum of metallic Mn (6.539 keV), the spectrum of As₂O₃ (11.867 keV), and the spectrum of KBr (13.474 keV), respectively.

XAFS RESULTS

(a) Chromium:

The XANES spectra of chromium in most U.S. bituminous coals vary little from coal to coal, indicating that there is probably just one major chromium mode of occurrence [3]. Furthermore, the XANES spectra clearly demonstrate that chromium is present in coal exclusively in the trivalent state, Cr³⁺. Previously, chromium has been postulated to occur in coals in association with clay minerals, or as chromite (FeCr₂O₄) [1,2], and possibly as an organic complex in low-rank coals [5,6]. However, comparison of the XANES spectra of a wide variety of Cr³⁺ compounds and minerals with the common XANES spectrum of Cr in coal eliminated all of the previously postulated chromium-bearing mineral forms as the Cr XANES spectra of coals showed little resemblance to either Cr³⁺-bearing silicates or to chromium oxide minerals, including chromite. Finally, based on some published spectra of other Cr³⁺ phases [7], it was decided to investigate the chromium hydroxides and oxyhydroxides, although based on the rarity of such phases in nature [8,9], it appeared to be unlikely. Cr(OH)₃ was prepared by precipitation from a solution of chromium nitrate at 25°C using ammonium hydroxide. The blue-green precipitate was filtered, washed, and then dried in air. The XANES spectrum of Cr hydroxide closely resembled that published elsewhere [7], but, although there were superficial similarities to the Cr XANES of coal, it was not a compelling match. The chromium hydroxide was then heated overnight (18 hours) at 140°C. A weight loss of about 19% was recorded that corresponded well to the elimination of one water molecule from the unit formula of chromium hydroxide and the formation of CrOOH:



X-ray diffraction of the CrOOH phase formed this way showed that it was an amorphous phase, closely related to ferrihydrite [10], rather than one of the very rare crystalline chromium oxyhydroxide minerals that have been found only in unique localities in Guyana and Finland [8]. More importantly, the Cr XANES of this material did closely resemble (Figure 1) the Cr XANES of coal and it now appears that the Cr XANES of coal arises from Cr in an oxyhydroxide form. However, it still remains to be demonstrated whether Cr exists as CrOOH in one of its own mineral forms, or whether it is in a complex oxyhydroxide solid solution with other trivalent ions. As has been demonstrated synthetically [10], substitution of Cr in goethite, FeOOH, can occur up to at least 10% of the Fe, and hence, Cr-substituted goethite might be considered a possible mode of occurrence for Cr. However, such an occurrence would only be possible if goethite were a primary occurrence of iron in coal. There is little or no evidence for such a supposition, and much against.

Once the primary occurrence of Cr in coal was established, some Cr XANES spectra that were not fully compatible with just CrOOH as the only Cr-bearing phase were re-examined. To assess the presence of a second Cr phase in addition to CrOOH in these spectra, spectral addition and subtraction procedures were attempted. Figure 2 shows the simulation of the Cr XANES spectrum of a lignite from Indonesia, in which personnel at the U.S. Geological Survey had observed chromite microscopically (R. B. Finkelman and L. F. Ruppert, pers. comm. 1992). A reasonably good simulation of this spectrum can be made from the weighted addition of the spectra of CrOOH (60%) and FeCr_2O_4 (40%). The sensitivity of this spectral simulation method of XANES analysis is about $\pm 10\%$.

(b) Arsenic:

As demonstrated elsewhere [3], it is possible to use As XANES spectroscopy to discriminate between arsenical pyrite, in which arsenic substitutes for sulfur in the pyrite structure, and arsenopyrite (FeAsS), in which it is an essential element. Of the coals examined to date, only one, a Pittsburgh seam coal, has been found to contain significant arsenopyrite. More recently, we have examined coals of relatively low As content (<5 ppm) from low-rank coals from western U.S. coal-fields. Despite the poor signal-noise ratio of these spectra (Figure 3), it is possible to conclude that the As XANES spectra of such coals are similar to each other and different from those of the bituminous coals of higher arsenic content (>10 ppm) reported earlier. From the position of the main peak, it would appear that the oxidation state of the arsenic is As^{3+} ; however, better quality data are needed to identify whether arsenic is enclosed in a sulfur or oxygen nearest neighbor environment.

(c) Manganese

As reviewed by Swaine [1], manganese has been postulated to occur in a variety of geochemical environments in coal, including carbonates, clays, pyrite, porphyrins, and, in lower-rank coals, in organic association. Owing to a similar ionic size and electronic structure, the geochemistry of Mn^{2+} tends to be similar to that of calcium, except that Mn has much a higher chalcophilic nature and can form sulfide minerals more readily.

Some preliminary XAFS data have been obtained on manganese in U.S. coals. A progression of Mn XANES spectra with rank are shown in Figure 4. The lowest rank coal (Beulah) exhibits a Mn XANES spectrum that is closely similar to that exhibited by calcium in carboxyl form in low-rank coals, whereas the Mn XANES spectrum of the Pocahontas #3 coal of highest rank, exhibits an asymmetric split main peak similar to that found for Mn in carbonates. The intermediate spectra, with the exception of the Wyodak coal, can not be simulated by additions of the two extreme spectra. Hence, there is at least one more Mn form of occurrence that contributes significantly to the Mn XANES spectra of the Pittsburgh and Upper Freeport coals. This form has yet to be identified.

(d) Bromine

XAFS spectroscopy has proven very useful for investigating the mode of occurrence of chlorine in coal [11]. XAFS spectroscopy clearly shows that chlorine is neither present as an organochlorine functionality nor as an inorganic chloride; rather, chlorine exists in coal as chloride anions in the moisture associated with the macerals, most probably held at the maceral surface by ionic attraction to polar organic functional groups. On geochemical grounds, it would be expected that the trace halogens (bromine and iodine) should have a similar mode of occurrence to that of chlorine. Some preliminary XAFS experiments on bromine in coal confirm this expectation. Bromine K-edge XANES spectra of KBr, KBr in aqueous solution, and of two coals are shown in Figure 5. The profiles of all four of these spectra are very

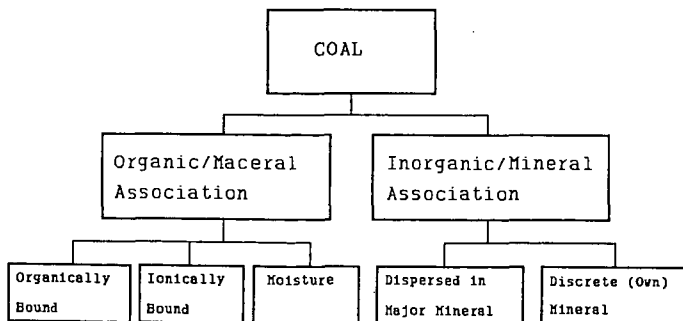
similar to the corresponding chlorine K-edge XANES spectra [11], indicating that the bromine mode of occurrence in coal is similar to that of chlorine.

DISCUSSION:

The unanticipated observation of Cr in oxyhydroxide form in coal by XAFS spectroscopy begs the question of whether other elements might also be present in coal in similar oxyhydroxide form or even hydroxide form. Presumably, such species would have to be sufficiently lithophilic not to react with sulfur, but incompatible with aluminosilicate (clay) structures. A number of elements that are typically trivalent in geochemical behavior would appear to fit such requirements; these include Sc, V, Y, and the rare-earth elements. All of these species have been reported to form an oxyhydroxide or hydroxide phase with stability fields compatible with geological conditions of coal formation [12]. Hence, it is possible, by analogy to chromium, that these elements may be found in coal as oxyhydroxide or hydroxide minerals. However, the larger trivalent cations (Y, REE) are also candidates for reaction with phosphate anions that may also be present during coal formation.

For two of the elements discussed here, arsenic and manganese, the mode of occurrence has been demonstrated to be quite different between low-rank coals (lignites and subbituminous coals) from the western U.S. and higher-rank coals (bituminous) from the eastern U.S. In previous work [13], the occurrence of calcium has also been shown to be distinctly different between such groups of coals. Many more elements are postulated [1,5] to be in organic association in low-rank coals than in higher-rank coals because of carboxyl groups present in the former. Clearly, this "decarboxylation" transition from low-rank coal to high rank coal is a key factor in the mobilization and mineralization of many elements during coalification and needs to be investigated in detail.

The terminology applied to elemental modes of occurrence is currently relatively imprecise because previous methods used to infer such information have not been sufficiently discriminating. For example, float/sink testing can be used to categorize elements by their "organic affinity", but such a concept does not impart any information as to how the element is actually bound to the coal macerals. Similarly, X-ray mapping in the electron microscope or microprobe can demonstrate that certain elements are associated with the organic matter, but do not provide information as to how the element is bound. However, in principle, such information can now be obtained from XAFS spectroscopy and a more expanded classification for elemental forms-of-occurrence is required. Such a proposed classification scheme with precise definitions for modes of occurrence is shown below. This scheme would appear to be sufficient for all the methods, both direct and indirect, that are currently used to infer elemental modes of occurrence in coal.



Organic/Maceral Association:

Organically bound: Involves direct covalent -M-C- or similar bond

Ionically bound: Involves an ionic bond with polar organic group

Moisture: Soluble anionic or cationic species in maceral pore moisture

Inorganic/Mineral Association:

Dispersed mineral: substitution of minor element for major element

Discrete mineral: element is essential to mineral's existence.

CONCLUSIONS:

The potpourri of data on trace element modes of occurrence in coal presented in this paper demonstrate the value of XAFS spectroscopy in trace element geochemistry. All measurements are made directly on the coal with a minimum of preparation and,

hence, with minimal chance of alteration or contamination of the mode of occurrence. Furthermore, XAFS is equally capable of determining dispersed elements (e.g. carboxyl bound Mn in Beulah lignite; Br in moisture), as well as the discrete mineralogical occurrences (Mn in carbonates, CrOOH , etc.). Such direct measurements afford the opportunity to provide much new information about trace elements in coal and put to rest various misconceptions about trace element occurrences in coal that have accumulated over the years.

ACKNOWLEDGEMENTS

We are grateful to Feng Zhen (University of Kentucky) for assistance with the preparation of $\text{Cr}(\text{OH})_3$, and to R. B. Finkelman and L. F. Ruppert (U.S. Geological Survey, Reston, VA) for donation of coal samples for this study. This work was supported by the Office of Exploratory Research, Electric Power Research Institute, Palo Alto, CA, and by the U.S. Department of Energy, Pittsburgh, PA. We also acknowledge the U.S. DOE for its support of the synchrotron facilities in the U.S.

REFERENCES

1. Swaine, D.J., Trace Elements in Coal, Butterworths, London, 1990.
2. Finkelman, R.B., In: Atomic and Nuclear Methods in Fossil Energy Research, (Eds. Filby, R.H., et al.); Plenum Press, New York, 1982, pp. 141-149.
3. Huggins, F.E., Shah, N., Zhao, J., Lu, F., and Huffman, G.P., Energy & Fuels, 7, 482-489, 1993.
4. Cramer, S.P., Tench, O., Yocum, N., and George, G.N., Nucl. Instrum. Meth., A266, 586-591, 1988.
5. Miller, R.N., and Given, P.H., Geochim. Cosmochim. Acta, 50, 2033-2043, 1986.
6. Miller, R.N., and Given, P.H., Geochim. Cosmochim. Acta, 51, 1311-1322, 1987.
7. Manceau, A., Charlet, L., J. Coll. Interf. Sci., 148, 425-435, 1992.
8. Milton, C., et. al., U.S. Geological Survey, Prof. Paper, 887, 1976, 29pp.
9. Burns, V.M., and Burns, R.G., Geochim. Cosmochim. Acta, 39, 903-910, 1975.
10. Schwertmann, U., and Cornell, R.M., Iron Oxides in the Laboratory, VCH, Weinham, 1991.
11. Huggins, F.E., and Huffman, G.P., submitted to Fuel, 1994.
12. Levin, E.M., Robbins, C.R., and McMurdie, H.F., Phase Diagrams for Ceramists, Vol. 1, American Ceramic Society, Columbus, OH, 1964.
13. Huffman, G.P., and Huggins, F.E., In: Chemistry of Low-Rank Coals, (Ed. Schobert, H.H.), ACS Symposium Series, Vol. 264, American Chemical Society, Washington, DC, 1984, pp. 159-174.

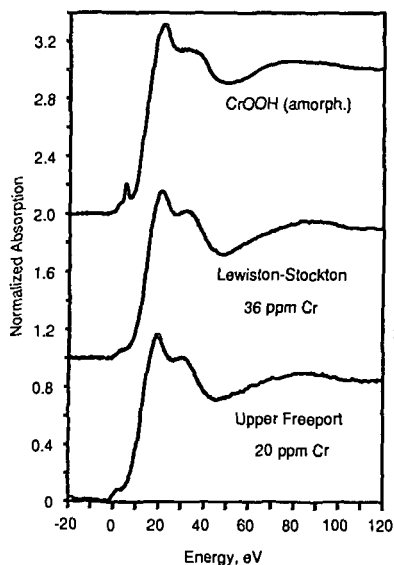


Figure 1: Comparison of Cr XANES spectrum of CrOOH with those for two bituminous coals.

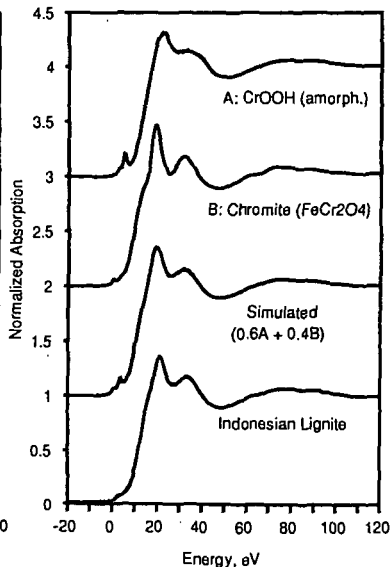


Figure 2: Simulation of Cr XANES for a coal by addition of Cr standard spectra.

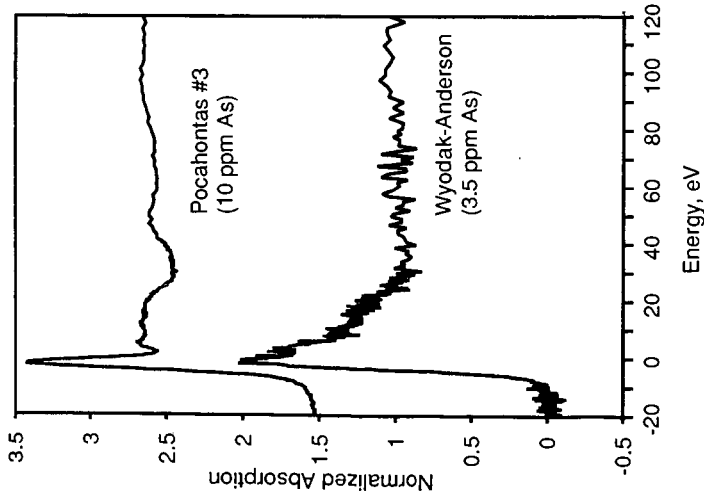


Figure 3: Comparison of As XANES spectra of bituminous and subbituminous coals.

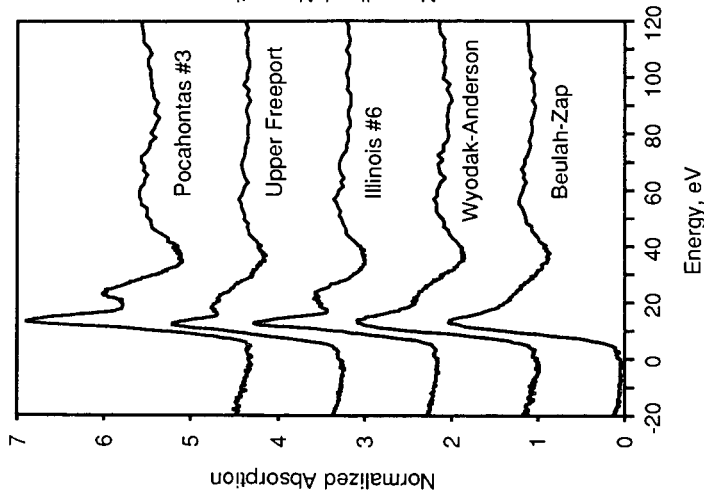


Figure 4: Mn XANES spectra of five Argonne premium sample coals

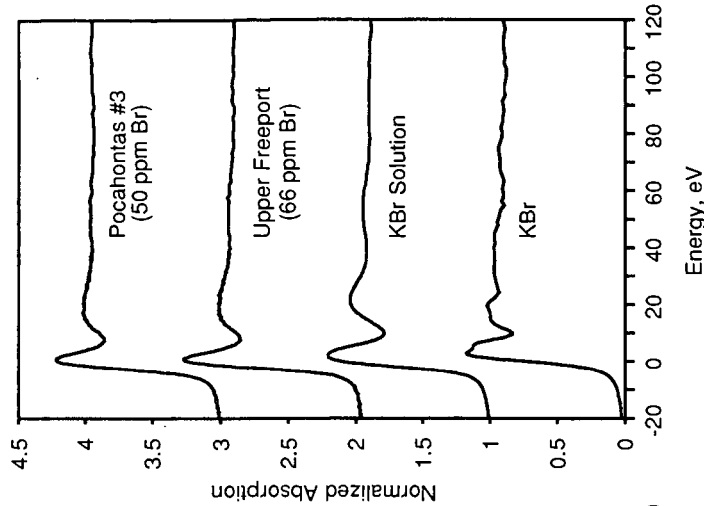


Figure 5: Br XANES spectra of two coals, KBr, and KBr in aqueous solution.

ELEMENTAL CHARACTERIZATION OF COAL ASH LEACHATES

by

John F. Cerbus

Department of Civil Engineering, University of Illinois,
205 North Mathews Ave., 3230 Newmark Laboratory

Sheldon Landsberger

Department of Nuclear Engineering, University of Illinois,
103 South Goodwin Ave., 214 Nuclear Engineering Laboratory

Susan Larson

Department of Civil Engineering, University of Illinois,
205 North Mathews Ave., 3230 Newmark Laboratory

Urbana, Illinois 61801

Keywords: Heavy metals in coal ash leachates, Use of multi-elemental techniques in coal ash analysis.

INTRODUCTION

Over 50 million tons of coal ash are produced annually in North America [Warren and Dudas, 1989]. Technological improvements in air pollution control have decreased stack emissions but have also increased contaminant concentrations in the ash of coal-fired boiler applications. The leaching of heavy metals and other elements during regulatory tests may cause coal ash to be classified as hazardous waste, complicating land disposal. The hazardous nature of coal ash remains unclear because current toxicity tests fail to characterize effectively the elemental distribution and chemical solubility of trace metals in the landfill environment. Leaching characteristics of ash samples can be investigated with various laboratory extraction procedures in association with multi-elemental techniques (e.g. Neutron Activation Analysis and Inductively Coupled Plasma Atomic Emission Spectroscopy). Such methods provide a more thorough analysis of coal ash leaching dynamics than the regulatory assessments can demonstrate. Experimental results may assist operators of coal-fired boiler industries in selecting coal types and operating conditions to minimize the leaching of environmentally key elements.

RESEARCH OBJECTIVES

Recent state environmental agency concern about the classification of coal-fired boiler technology wastes may result in substantial cost increases for waste disposal. The objective of this research study is to investigate the hazardous potential of industrial coal-fired boiler technology wastes. A laboratory leaching procedure known as a water-batch extraction was performed on fly ash samples. Additionally, through the use of multi-elemental analytical techniques, the fly ash and corresponding coal samples were characterized. In this way, the elemental leaching dynamics and relationships of elemental levels between coal, ash, and leachates have been examined.

COAL ASH CHARACTERISTICS

Certain physical and chemical properties undoubtedly play key roles in ash-water interactions. Coal fly ash is the partially combusted solid waste particulates of small enough diameter to be entrained in flue gas. One study determined 63% of the examined fly ash particles were in the range of 2-50 μm in diameter [El-Mogazi et al., 1988]. Forms of potentially toxic metals are selectively deposited on the outer surface of coal ash particles [Hopke, 1983]. Such surface components are not bound to the internal silicate matrix and therefore are readily leachable [Hopke, 1983]. Three major matrices compose fly ash, silicate glass, mullite quartz, and magnetic spinel [El-Mogazi et al., 1988]. Investigations have found the magnetic matrix to be particularly important in the release of toxic elements [El-Mogazi et al., 1988].

SAMPLE DESCRIPTION

The coal, and fly ash samples for this study were provided by the United States Army Construction Engineering Research Lab (USACERL). The samples originated from Abbott Power Plant (Champaign, Illinois), Chanute Air Force Base (Rantoul, Illinois), and the Rock Island Arsenal (Rock Island, Illinois).

REGULATORY CONSIDERATIONS

The current regulatory benchmark test designed to identify wastes likely to leach hazardous concentrations of toxins is the toxicity characteristic leaching procedure (TCLP). If extract concentrations of certain elements or organic compounds exceed regulatory limits the waste is classified as hazardous. The eight regulated elements are As, Ba, Cd, Cr, Hg, Pb, Se, and Ag. The TCLP replaced the existing extraction-procedure (EP) toxicity test standard in 1990, which was inadequate for organic compounds [Bishop, 1990]. With the implementation of the TCLP, the regulatory focus is now on

environmental impact, behavior, and leachability of contaminants instead of on contaminant levels in waste [Bishop, 1990]. The TCLP uses acetic acid as the extractant and is run for 18 hours in a closed vessel. Acetic acid is a common product of the anaerobic degradation processes found in municipal solid waste landfills. The test, however, fails to effectively characterize the elemental distribution and chemical solubility of coal ash in an ash monofill.

Waste stabilization may be used to reduce leaching in conjunction with land disposal. Such processes attempt to immobilize a waste within an inert matrix. Examples include using Portland Cement, specialized polymers, and plastics as binding agents but such processes are often cost prohibitive [Wentz, 1989]. The TCLP may be implemented following stabilization to gauge the success of the such processes [Biedry, 1990].

LEACHING TECHNIQUES

Previous workers have employed a variety of methods to examine coal ash leaching. Techniques have ranged from laboratory scale extractions to monitoring large outdoor test plots of ash. Some researchers used aggressive, 'worst-case' approaches trying to leach as much from the ash as possible. Such methods most likely involve leaching conditions which would never be encountered naturally.

The preferred strategy is to construct a leaching scheme which accelerates the natural behavior of ash buried in a landfill [Buchholz, 1993]. The EP and TCLP regulatory leaching tests were not specifically designed to measure the behavior and toxicity of coal ash in an ash monofill. The use of acetic acid as an extractant in the above tests may not be representative of the leaching conditions found in an ash monofill.

For this study, the long term washing of coal ash in an ash monofill was simulated in the laboratory using a water (deionized) batch extraction technique. The deionized water used was a simulated acid-rain solution with low levels of nitric and sulfuric acid added. The resulting pH was a mildly aggressive 5.2. The liquid-to-solid (LS) ratios were slowly increased, using short intervals initially to better characterize the first stages. Samples for each LS ratio were prepared over consecutive days with orbital agitation periods of approximately 24 hours in between.

ELEMENTAL ANALYSIS

Thorough analysis of trace elements present in coal, ash and leachate samples usually involves the use of atomic emission spectroscopy. Multi-elemental techniques in which many elements can be analyzed simultaneously are desirable. Elemental concentrations in the coal and ash samples were determined using Neutron Activation Analysis (NAA). Furthermore, the leachates produced by the laboratory extraction methods were characterized with Inductively Coupled Plasma Atomic Emission Spectroscopy (ICP-AES). Quality assurance and quality control were maintained through the use of standard reference materials, procedure blanks and appropriate trace metal laboratory procedures such selecting ultra-pure reagents.

ELEMENTAL COMPOSITION OF COAL AND FLY ASH SAMPLES

Figures 1 and 2 depict the levels of the TCLP elements in the coal and fly ash samples, respectively. Cadmium and levels were not determined for the coal and ash samples but were examined in the leachate analysis. Levels of Hg and Ag are below detection limits for all three varieties of coal and ash. Ba and Cr are the most dominant TCLP elements in the coal and ash samples. Concentrations are elevated in the fly ash compared to the coal as expected, most likely due to the high surface area to volume ratio differences.

ELEMENTAL COMPOSITION OF LEACHATES

Levels of Ag (MDL = 8 ppb), As (MDL = 280 ppb), Cd (MDL = 24 ppb), Cr (MDL = 18 ppb), Hg (MDL = 40 ppb), Pb (MDL = 51 ppb) and Se (MDL = 490 ppb) were below method detection limits (MDL) for all LS ratios. Be, Cu, Fe, Sb, Sn, Ti, and Tl levels were also below detection limits for all samples. The MDL is defined as the minimum concentration of a substance that can be identified, measured, and reported with a 99% confidence of a greater-than-zero concentration. Therefore, of the TCLP elements, only Ba was found at significant levels. Figure 3 depicts the Barium leaching pattern. The detectable elements with the highest levels in the leachates included, in descending order, S, Ca, Na, K, B, Si, Mg, Al, Sr, Mo, Li, Ba, V, Cr, Zn, Mn, Co, Ni, and P. Figure 4, depicts the leaching pattern for boron which is somewhat common for elements susceptible to quick initial leaching with decreasing levels thereafter. In contrast, the Ba pattern for the Abbott ash (Figure 3) shows increasing levels after reaching an apparent minimum. This may be explained by the outer layers of the ash matrices having been washed off thereby exposing more barium to the leaching solution.

DISCUSSION AND CONCLUSIONS

Bowen (1966) reported average boron levels in soil to be approximately 10 ppm. Elevated levels of boron in leachates may be of environmental interest. El Mogazi et al. (1988) described a coal ash which leached boron levels toxic to plants. It should be stressed that slightly elevated levels of naturally occurring elements may not result in readily apparent effects, but such levels may be toxic to soil microbial communities and surface vegetation.

The coal fly ash varieties examined in this study apparently are not likely to leach high concentrations of TCLP elements when disposed of in an ash monofill. High levels of sulfur would be expected to leach quite readily. Space limitations in this preprint prohibit the discussion of other, possibly environmentally significant leaching patterns of elements such as Al, V, Co and Ni.

CONTINUING RESEARCH AND ACKNOWLEDGMENTS

The research presented above is a small part of a larger project involving 40-element characterizations of three coal varieties, 40-element characterizations of corresponding fly and bottom ash samples, and 32-element characterizations of water batch and selective-reagent sequential extractions of the fly and bottom ash. The sequential technique employed was developed by Tessier et al. (1979). Selective reagents were used to partition trace elements into chemical forms likely to be released under various environmental conditions. A rough idea of the chemical speciation of trace metals can be inferred from the analysis. The chemical partitions are readily exchangeable, bound to carbonates or surface oxides, bound to iron and manganese oxides, and bound to organic matter. [Tessier, et al., 1979]. The use of sequential techniques provides the researcher with a significant improvement in characterization over the regulatory extraction tests.

This work was funded by the United States Army Construction Engineering Research Laboratory (USACERL). The required inductively-coupled plasma analysis was performed at the Illinois State Water Survey located in Champaign, Illinois.

LITERATURE CITED

- Biedry, J., Managing Waste to Meet Federal Land Ban Rules, *Pollution Engineering*, October, (1990).
- Bishop, J., Range of Options Shrinks for Disposing RCRA Wastes; Enforcement Tightens, *Hazmat World*, November, (1990).
- Bowen, H. J. M., *Trace Elements in Biochemistry*, Academic Press, New York, (1966).
- Buchholz, Bruce Alan, Elemental Characterization of Municipal Solid Waste Incinerator Ash and its Leachates Using Neutron Activation Analysis and Inductively Coupled Plasma Atomic Emission Spectroscopy, Ph.D. Thesis, University of Illinois at Urbana-Champaign, Department of Nuclear Engineering, (1993).
- El-Mogazi, D., D. J. Lisk and L. H. Weinstein, A Review of Physical, Chemical and Biological Properties of Fly Ash and Effects on Agricultural Ecosystems, *Science of the Total Environment*, 74 (1988) 1-37.
- Hopke, Phillip K., *Analytical Aspects of Environmental Chemistry*, Chemical Analysis Series, Vol. 64, John Wiley and Sons, New York, (1983).
- Tessier, A., P. G. C. Campbell and S. Bisson, Sequential Extraction Procedure for the Speciation of Particulate Trace Metals, *Analytical Chemistry*, 51 (1979) 844-850.
- Warren, C. J. and M. J. Dudas, Leachability and Partitioning of Elements in Ferromagnetic Fly Ash Particles, *Science of the Total Environment*, 83 (1989) 99-111.
- Wentz, Charles A., *Hazardous waste management*, Chemical Engineering Series, McGraw-Hill, New York, (1989).

Figure 1
TCLP ELEMENTS IN COAL SAMPLES

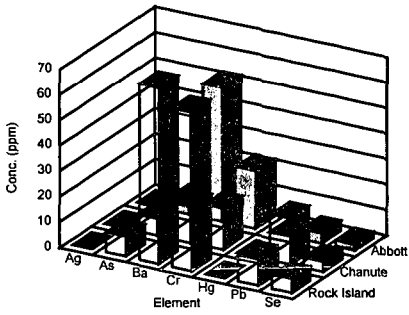


Figure 2
TCLP ELEMENTS IN FLY ASH SAMPLES

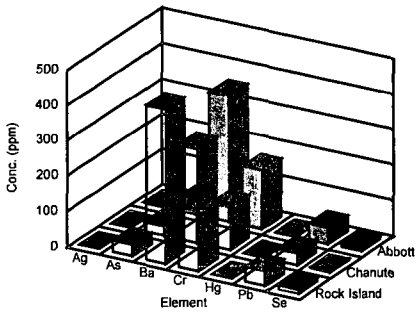


Figure 3 Barium (Ba) MDL = 0.002 ppm
Water Batch Extraction - Fly Ash

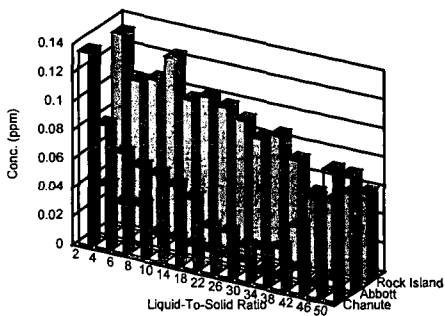


Figure 4 Boron (B) MDL = 0.030 ppm
Water Batch Extraction - Fly Ash

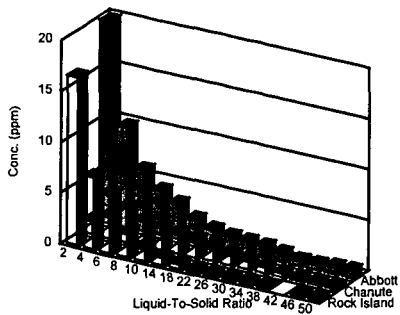
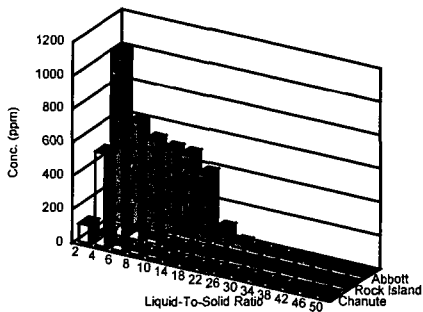


Figure 5 Sulfur (S) MDL = 0.090 ppm
Water Batch Extraction - Fly Ash



RELIABILITY AND REPRODUCIBILITY OF LEACHING PROCEDURES TO ESTIMATE THE MODES OF OCCURRENCE OF TRACE ELEMENTS IN COAL

Curtis A. Palmer, Marta R. Krasnow, Robert B. Finkelman and William M. d'Angelo;
U.S. Geological Survey, National Center, MS 956, Reston, VA 22092

Key words: Solvent leaching of coal, trace elements, reproducibility and reliability

INTRODUCTION

The 1990 amendments to the Clean Air Act have renewed interest in chemical forms or modes of occurrence of trace elements for potentially toxic trace elements in coal. Selective solvent leaching has been useful in estimating these modes of occurrence^{1,2,3,4,5}. This technique is much faster than previous attempts to determine the modes of occurrence of trace elements in coal, such as scanning electron microscopy⁶, analysis of density separates of coal^{7,8} and low-temperature ash⁹. However, relatively little has been published about the reproducibility and reliability of the solvent leaching procedure. For this paper, three previously analyzed coal samples were leached individually and (or) sequentially with 1N CH₃COONH₄, 2N HCl, 48% HF, and 2N HNO₃ using procedures described previously^{4,5}. The concentrations of 45 elements were determined by analyzing the leachate by inductively coupled argon plasma-atomic emission spectroscopy (ICAP-AES) and (or) the residue by instrumental neutron activation analysis (INAA).

RESULTS

The percent determined by both INAA and ICAP-AES of each element sequentially leached by each solvent in the Illinois #6 coal is given in Table 1. The method of determining the percent leached is different for each technique. The percent leached by ICAP-AES is calculated by:

$$(C_s V_s / W_s) / C_{wc} \times 100 \quad (1)$$

where C_s is the concentration of the element in solution V_s is the volume of the solution, W_s is the weight of the fraction prior to leaching (starting weight); and C_{wc} is the concentration of the element in the original whole coal sample given in Table 2. The percent leached in each fraction determined by INAA was calculated by

$$P_L - (C_{wc}W_s - C_fW_f / C_{wc}W_s) \times 100 \quad (2)$$

where P_L is the total percent leached by all fractions previously leached (P_L is zero for the CH₃COONH₄ fraction); C_f is the concentration of the element in the residue after leaching and W_f is the weight of the fraction after leaching (final weight). The errors calculated are based on counting statistics¹⁰ and are propagated through the calculations for the elements determined by INAA. Although the errors of concentrations determined by INAA are generally relatively low (1-10%), errors in the final calculation are much greater due to the subtractions and division in equation 2. Errors on individual elemental concentrations were not available for ICAP-AES. The data indicates that errors in these concentrations are generally higher than INAA errors, because more elements are near the detection limits of the ICAP-AES technique¹¹. Because equation 1 does not have subtraction terms, the overall errors may be comparable. In cases where the error was greater than the percent leached value, this value was converted to an upper limit and denoted by a * in the tables. In a few cases, equation 2 led to a negative number. If that number was less than the calculated error, then the value was reported as an upper limit with a * as above; but when the value exceeded the error value, no value could be calculated and a ? was reported in a manner similar to Finkelman et al⁴ in 1990.

Considering the errors, there is generally good agreement between INAA and ICAP-AES results. The INAA results can also be evaluated against the data reported in the 1990 study included in Table 1. The comparison to previous data is generally good, but there are some exceptions. The 1:7 HNO₃ solution used in this study was more effective than 1:9 HNO₃. The differences in nitric acid leaching between this study and the 1990 study have been attributed to oxidation of the coal matrix by the stronger solution⁵.

Results for the Buelah-Zap lignite sample and the Lower Bakerstown coal sample (Tables 3-6) are similar to the results found for the Illinois #6 coal sample. The leaching study on the Lower Bakerstown coal was done in duplicate to further assist in evaluate reproducibility. Results from individual leaching experiments some in duplicate or triplicate can be found on Table 7. Many of these experiments were done in duplicate or triplicate. Hot (80° C) and room temperature (RT) HCl and HNO₃ acid were used to determine if differences in temperature were important. Generally, differences in temperature were not as significant as were differences in concentration.

(1) Miller, R.N.; Given, P.H., A Geochemical Study of the Inorganic Constituents in Some Low Rank Coals, DOE, Final Report FE-2494-TR-1, 1986 314 pages.

(2) Hurley, J.P.; Steadman, E.N.; Kleesattel, D.R. Distribution of Inorganics, DOE, Final Report for Period Ending March 31, 1986.1986, 320 pages.

(3) Baxter, L.L.; Hardesty, D.R. Fate of Mineral Matter. In Hardesty, D.R. ed. Coal Combustion Science Quarterly Progress Report January-March 1992., Sandia Report SAND92-8210, 1992 p. 3-1-3-47.

(4) Finkelman, R.B.; Palmer, C.A.; Krasnow, M.R.; Aruscavage, P.J.; Sellers, G.A.; Dulong, F.T. *Energy and Fuels*, 1990, 4 (6) 755-766.

(5) Palmer, C.A.; Krasnow, M.R.; Finkelman, R.B.; d'Angelo, W.M. Submitted to J. Coal Quality. (4) (6) Finkelman, R.B., Modes of occurrence of trace elements in coal, *US Geol. Surv.* 1981, OFR 81-99. 301 pages.

(7) Zubovic, P.; Standnichenko, T.; Sheffey, B. The Association of Minor Elements with Organic and Inorganic Phases of Coal, *US Geol. Surv.* 1980, Professional Paper No.400-B, p B84-B87.

(8) Gluskoter, H.J.; Ruch, R.R.; Miller, W.G.; Cahill, R.A.; Dreher, G.B.; Kuhn, J.K., Trace elements in Coal: Occurrence and Distribution, *IL Geol. Surv.* 1977, Circular 499. 154 pages.

(9) Palmer, C.A.; Filby, R.H. *Fuel*, 1984, 63, 318-326.

(10) Palmer, C.A. *Energy and Fuels*, 1990, 4(5), 436-439

(11) Doughten, M.W.; Gillison, J.R. *Energy and Fuels*, 1990, 4(5), 426-430

Table 1. Percent of selected elements sequentially leached from the Illinois #6 coal by different solvents. The concentrations of elements used to calculate the percent leached were determined by instrumental neutron activation analysis (INAA) on residue of the leached coal. The concentrations of the elements used to calculate the percent leached were determined directly by inductively coupled argon plasma atomic emission spectrometry (ICAP-AES) on the leached solutions. * = number converted to an upper limit due to high errors in calculations; ND = not determined, ? No value could be determined from data, 1990 refers to data previously reported by Finkelman et al.⁴

Element-method	CH ₃ COONH ₄		HCl		HF		HNO ₃	
	Run1	1990	Run1	1990	Run1	1990	Run1	1990
B-ICAP-AES	1	ND	32	ND	45	ND	<18	ND
Na-INAA	73±4	65	10±5	0	15±6	0	6±0.4	15
Na-ICAP-AES	70	ND	12	ND	<2	ND	<3	ND
Mg-ICAP-AES	8	ND	7	ND	57	ND	142	ND
Al-ICAP-AES	17	ND	36	ND	42	ND	47	ND
Si-ICAP-AES	0	ND	1	ND	ND	ND	2	ND
P-ICAP-AES	<44	ND	<50	ND	<58	ND	<100	ND
K-INAA	9±7	13	<12*	0	<91	78	<10*	>7
K-ICAP-AES	<21	ND	<24	ND	81	ND	<57	ND
Ca-ICAP-AES	71	ND	21	ND	2	ND	3	ND
Sc-INAA	<10*	0	<23*	15	64±14	32	20±16	4
Ti-ICAP-AES	<2	ND	3	ND	81	ND	9	ND
V-ICAP-AES	<20	ND	30	ND	219	ND	124	ND
Cr-INAA	<1*	0	?	22	53±4	9	33±8	24
Cr-ICAP-AES	<3	ND	22	ND	71	ND	52	ND
Mn-ICAP-AES	71	ND	21	ND	8	ND	<8	ND
Fe-INAA	9±1	0	9±1	0	4±1	0	75±6	48
Fe-ICAP-AES	0.5	ND	4	ND	10	ND	122	ND
Co-INAA	10±1	19	47±2	39	15±3	0	23±4	7
Co-ICAP-AES	<24	ND	43	ND	<31	ND	<64	ND
Ni-INAA	27±16	35	<30*	32	39±20	0	41±23	0
Ni-ICAP-AES	17	ND	36	ND	42	ND	47	ND
Cu-ICAP-AES	<10	ND	<11	ND	<13	ND	78	ND
Zn-INAA	8±6	ND	21±9	ND	58±9	ND	12±10	ND
Zn-ICAP-AES	<1	ND	26	ND	58	ND	18	ND
As-INAA	10±7	0	19±10	17	<18*	0	60±11	0
Se-INAA	21±4	0	<7*	0	<7*	0	65±5	0
Br-INAA	40±9	53	?	?	?	?	?	?
Rb-INAA	<26*	ND	<27*	ND	67±21	ND	<38*	ND
Sr-INAA	<49*	30	<100*	0	<40*	5	<20*	ND
Sr-ICAP-AES	36	ND	10	ND	19	ND	22	ND
Y-ICAP-AES	<25	ND	<29	ND	<33	ND	<69	ND
Zr-ICAP-AES	<5	ND	<5	ND	46	ND	<12	ND
Ag-ICAP-AES	<100	ND	<100	ND	<100	ND	<100	ND
Sb-INAA	<16*	0	<16*	13	22±11	0	60±13	6
Cs-INAA	<2*	0	15±7	0	71±8	0	20±8	88
Ba-INAA	28±13	11	22±19	25	31±20	9	20±15	8
Ba-ICAP-AES	32	ND	18	ND	35	ND	28	ND
La-INAA	<3*	0	38±3	37	11±2	4	43±1	29
Ce-INAA	<10*	8	45±15	38	<25*	0	40±17	24
Ce-ICAP-AES	<17	ND	34	ND	<22	ND	<46	ND
Nd-INAA	20±12	ND	<100*	ND	?	ND	58±20	ND
Sm-INAA	13±10	0	40±15	44	<20*	0	37±17	13
Eu-INAA	17±10	0	29±14	40	<20*	0	38±16	7
Tb-INAA	21±16	0	<40*	28	<40*	0	39±26	12
Yb-INAA	<15*	0	<22*	0	25±16	18	53±16	0
Lu-INAA	<18*	ND	<38*	ND	<40*	ND	55±28	ND
Hf-INAA	?	0	<2*	8	62±11	23	<12	9
Ta-INAA	<16*	0	<18*	0	48±17	0	36±19	0
W-INAA	?	0	?	0	?	0	?	0
Pb-ICAP-AES	<24	ND	30	ND	12	ND	50	ND
Th-INAA	<2*	0	24±14	30	<28*	0	51±16	14
U-INAA	<19*	0	<22*	16	24±15	0	40±16	0

Table 2. Concentrations of trace elements in the original Illinois #6 coal sample in parts per million except as noted.

<u>B</u>	<u>Na</u>	<u>Mg</u>	<u>Al (%)</u>	<u>Si (%)</u>	<u>P</u>	<u>K (%)</u>	<u>Ca (%)</u>	<u>Sc</u>	<u>Ti</u>	<u>V</u>	<u>Cr</u>	<u>Mn</u>
160	1020	750	1.25	3.0	47	0.2	0.93	2.3	700	34.5	35.8	76
<u>Fe (%)</u>	<u>Co</u>	<u>Ni</u>	<u>Cu</u>	<u>Zn</u>	<u>As</u>	<u>Se</u>	<u>Br</u>	<u>Rb</u>	<u>Sr</u>	<u>Y</u>	<u>Zr</u>	<u>Ag</u>
2.7	4.4	30	10.1	201	4.7	4.2	5.72	16	32.2	4.1	22.8	0.62
<u>Sb</u>	<u>Cs</u>	<u>Ba</u>	<u>La</u>	<u>Ce</u>	<u>Nd</u>	<u>Sm</u>	<u>Eu</u>	<u>Tb</u>	<u>Yb</u>	<u>Lu</u>	<u>Hf</u>	<u>Ta</u>
0.84	0.94	86	5.99	10.2	6.5	1.03	0.226	0.134	0.47	0.06	0.435	0.176
<u>W</u>	<u>Pb</u>	<u>Th</u>	<u>U</u>									
1.51	8.6	1.85	4.27									

Table 3. Percent of selected elements sequentially leached from the Buelah-Zap lignite by different solvents. The concentrations of elements used to calculate the percent leached were determined by instrumental neutron activation analysis (INAA) on residue of the leached coal. The concentrations of the elements used to calculate the percent leached were determined directly by inductively coupled argon plasma atomic emission spectrometry (ICAP-AES) on the leached solutions. * = number converted to an upper limit due to high errors in calculations; ND = not determined, ? No value could be determined from data, 1990 refers to data previously reported by Finkelman et al.⁴

Element-method	CH ₃ COONH ₃		HCl		HF		HNO ₃	
	Run1	1990	Run1	1990	Run1	1990	Run1	1990
B-ICAP-AES	<17	ND	40	ND	<26	ND	<40	ND
Na-INAA	54±4	95	26±5	0	18±5	0	19±1	0
Na-ICAP-AES	<100	ND	<100	ND	<100	ND	<100	ND
Mg-ICAP-AES	101	ND	11	ND	17	ND	42	ND
Al-ICAP-AES	1	ND	28	ND	66	ND	1	ND
Si-ICAP-AES	<1	ND	10	ND	ND	ND	3	ND
P-ICAP-AES	<22	ND	100	ND	<34	ND	<66	ND
K-INAA	41±21	?	<32*	0	<100	>85	<100	ND
K-ICAP-AES	<100	ND	<100	ND	<100	ND	<100	ND
Ca-ICAP-AES	82	ND	23	ND	1	ND	0	ND
Sc-INAA	?	0	50±6	15	45±11	32	<13*	4
Ti-ICAP-AES	<7	ND	23	ND	66	ND	<21	ND
V-ICAP-AES	167	ND	<86	ND	<100	ND	<100	ND
Cr-INAA	?	14	?	70	?	0	22±6	0
Cr-ICAP-AES	371	ND	<66	ND	203	ND	<100	ND
Mn-ICAP-AES	46	ND	42	ND	<5	ND	<10	ND
Fe-INAA	<10*	15	37±14	0	<28*	0	50±22	0
Fe-ICAP-AES	<1	ND	34	ND	9	ND	30	ND
Co-INAA	?	5	75±5	58	13±7	0	<12*	0
Co-ICAP-AES	<100	ND	<100	ND	<100	ND	<100	ND
Ni-INAA	<17*	0	32±14	0	<44*	0	<30*	0
Ni-ICAP-AES	<27	ND	69	ND	<100	ND	<100	ND
Cu-ICAP-AES	76	ND	<32	ND	<41	ND	<79	ND
Zn-INAA	3±1	0	<73*	76	<23*	16	<1*	0
Zn-ICAP-AES	<27	ND	82	ND	67	ND	<79	ND
As-INAA	<6*	16	22±8	4	19±1	0	44±1	11
Se-INAA	<17*	0	9±6	0	?	0	58±12	0
Br-INAA	1±0.1	0	?	?	?	?	?	?
Rb-INAA	16±8	ND	<23*	ND	>23	ND	>34*	ND
Sr-INAA	64±1	45	>32*	54	?	0	?	0
Sr-ICAP-AES	76	ND	26	ND	1	ND	<1*	ND
Y-ICAP-AES	<67	ND	<100	ND	<100	ND	<100	ND
Zr-ICAP-AES	<11	ND	<13	ND	61	ND	<33	ND
Ag-ICAP-AES	<100	ND	<100	ND	<100	ND	<100	ND
Sb-INAA	<13*	0	<19*	0	68±30	14	<40*	30
Cs-INAA	<10*	0	<46*	0	>68	82	?	?
Ba-INAA	<13*	23	71±13	73	29±15	?	<1	?
Ba-ICAP-AES	18	ND	87	ND	16	ND	1	ND
La-INAA	?	0	75±9	83	13±10	0	<18*	7
Ce-INAA	?	14	69±13	70	18±13	0	14±8	7
Ce-ICAP-AES	<61	ND	92	ND	<91	ND	<100	ND
Nd-INAA	33±25	ND	>47	ND	0	ND	>16	ND
Sm-INAA	<5*	0	73±8	81	18±14	0	<21*	7
Eu-INAA	<19*	0	71±30	79	>50	0	<40*	7
Tb-INAA	<11*	0	70±15	84	17±15	0	<20*	3
Yb-INAA	<20*	0	87±31	72	<40*	0	<45*	7
Lu-INAA	<22*	ND	64±18	ND	<38*	ND	<28*	ND
Hf-INAA	?	0	<10*	0	81±10	55	<10*	0
Ta-INAA	?	0	<13*	0	94±13	37	14±11	0
W-INAA	?	0	?	0	?	0	?	0
Pb-ICAP-AES	<100	ND	172	ND	<100	ND	<100	ND
Th-INAA	?	0	39±8	60	60±8	0	21±9	29
U-INAA	<18*	0	54±27	60	34±31	27	<40*	0

*Includes amount leached by HF

Table 4. Concentrations of trace elements in the original Buelah-Zap lignite sample in parts per million except as noted.

<u>B</u>	<u>Na</u>	<u>Mg</u>	<u>Al</u>	<u>Si</u>	<u>P</u>	<u>K</u>	<u>Ca (%)</u>	<u>Sc</u>	<u>Ti</u>	<u>V</u>	<u>Cr</u>	<u>Mn</u>
79	4960	3740	4000	6700	120	250	1.48	0.76	190	3.7	2.4	81
<u>Fe</u>	<u>Co</u>	<u>Ni</u>	<u>Cu</u>	<u>Zn</u>	<u>As</u>	<u>Se</u>	<u>Br</u>	<u>Rb</u>	<u>Sr</u>	<u>Y</u>	<u>Zr</u>	<u>Aq</u>
4800	0.82	5	5	5.23	2.63	0.59	1	0.93	530	2	12	0.14
<u>Sb</u>	<u>Cs</u>	<u>Ba</u>	<u>La</u>	<u>Ce</u>	<u>Nd</u>	<u>Sm</u>	<u>Eu</u>	<u>Tb</u>	<u>Yb</u>	<u>Lu</u>	<u>Hf</u>	<u>Ta</u>
0.173	0.5	610	2.67	3.92	2.3	0.4	0.081	0.52	0.26	0.036	0.293	0.92
<u>W</u>	<u>Pb</u>	<u>Th</u>	<u>U</u>									
0.38	1.5	0.9	0.41									

Table 5. Percent of selected elements sequentially leached from the Lower Bakerstown coal by different solvents. The concentrations of elements used to calculate the percent leached were determined by instrumental neutron activation analysis (INAA) on residue of the leached coal. The concentrations of the elements used to calculate the percent leached were determined directly by inductively coupled argon plasma atomic emission spectrometry (ICAP-AES) on the leached solutions. * = number converted to an upper limit due to high errors in calculations; ND = not determined, ? No value could be determined from data, 1990 refers to data previously reported by Finkelman et al.⁴

Element-method	CH ₃ COONH ₄			HCl			HF			HNO ₃		
	Run1	Run2	1990	Run1	Run2	1990	Run1	Run2	1990	Run1	Run2	1990
B-ICAP-AES	<100	<100	ND	<100	<100	ND	<100	<100	ND	<100	<100	ND
Na-INAA	10±4	10±4	0	<7*	<10*	0	75±5	75±5	65	<8*	<9*	0
Na-ICAP-AES	19	13	ND	8	<9	ND	61	72	ND	<13	<16	ND
Mg-ICAP-AES	10	12	ND	6	7	ND	41	48	ND	5	5	ND
Al-ICAP-AES	59	45	ND	11	16	ND	36	24	ND	38	<18	ND
Si-ICAP-AES	<0.2	<0.3	ND	0.3	0.5	ND	ND	ND	ND	4	<1	ND
P-ICAP-AES	12	<9	ND	54	78	ND	14	17	ND	<13	19	ND
K-INAA	<13*	<13*	0	<22*	<18*	0	>89	>85	>79	>2	>1	ND
K-ICAP-AES	<58	<88	ND	<64	<88	ND	84	<100	ND	<100	<100	ND
Ca-ICAP-AES	75	66	ND	21	22	ND	18	18	ND	9	8	ND
Sc-INAA	<3*	<3*	8	14±3	16±3	63	33±3	31±3	23	<3*	6±3	0
Th-ICAP-AES	<4	<3	ND	<3	<4	ND	49	53	ND	21	11	ND
V-ICAP-AES	<20	<30	ND	<22	<30	ND	49	52	ND	<44	<53	ND
Cr-INAA	<4*	<4*	0	?	?	0	?	?	12	?	?	11
Cr-ICAP-AES	<12	<17	ND	<12	<18	ND	104	109	ND	77	73	ND
Mn-ICAP-AES	65	60	ND	<23	<32	ND	<26	<39	ND	<48	<57	ND
Fe-INAA	<12*	<11*	15	29±7	42±7	26	29±7	23±7	8	40±8	33±8	4
Fe-ICAP-AES	17	<0.2	ND	40	61	ND	8	8	ND	35	49	ND
Co-INAA	60±3	60±3	59	11±3	12±3	8	<7*	<6*	0	8±3	8±3	0
Co-ICAP-AES	79	67	ND	<17	<23	ND	<19	<28	ND	<33	<40	ND
Ni-INAA	39±14	39±14	55	<38*	<19*	0	<19*	<19*	0	22±18	34±18	0
Ni-ICAP-AES	59	45	ND	10	15	ND	36	24	ND	39	<16	ND
Cu-ICAP-AES	46	<15	ND	21	24	ND	21	30	ND	<22	<26	ND
Zn-INAA	53±6	53±6	64	31±8	19±8	21	<9*	<13*	0	<11*	<11*	0
Zn-ICAP-AES	72	64	ND	18	43	ND	9	9	ND	<5	39	ND
As-INAA	<5*	6±4	0	57±5	46±5	41	15±6	16±6	6	30±5	30±5	6
Se-INAA	<10*	<11*	0	<18*	<23*	0	<14*	<25*	0	74±14	70±14	0
Br-INAA	<4*	<4*	0	7±4	17±4	19	9±4	<4*	15	<40*	<40*	0
Rb-INAA	<24*	<24*	ND	<22*	<23*	ND	>91	>90	ND	>7	>3	0
Sr-INAA	<25*	<25*	16	<24*	<33*	0	58±24	63±24	9	<28*	<30*	11
Sr-ICAP-AES	19	17	ND	7	9	ND	41	44	ND	8	8	ND
Y-ICAP-AES	<31	<47	ND	<34	<47	ND	<39	<59	ND	<69	<83	ND
Zr-ICAP-AES	<6	<10	ND	<7	<10	ND	30	36	ND	14	<17	ND
Ag-ICAP-AES	<100	<100	ND	<100	<100	ND	<100	<100	ND	<100	<100	ND
Sb-INAA	<6*	<6*	10	37±4	38±5	33	20±4	21±4	21	22±4	30±4	0
Cs-INAA	<17*	<17*	12	<17*	<18*	?	84±19	85±20	37	>21*	<21*	14
Ba-INAA	<17*	<17*	23	<19*	<19*	?	75±19	79±18	?	17±15	23±18	>23
Ba-ICAP-AES	22	11	ND	67	12	ND	27	19	ND	10	<8	ND
Lb-INAA	<4*	<4*	0	10±5	11±5	0	13±5	16±5	5	25±4	34±4	22
Ce-INAA	<4*	<4*	0	14±4	14±4	3	12±5	14±4	0	22±5	34±3	22
Ce-ICAP-AES	<20	<30	ND	<22	<30	ND	<25	<37	ND	<44	<53	ND
Nd-INAA	<19*	<19*	ND	22±17	30±17	ND	17±1	16±3	ND	26±17	32±17	ND
Sm-INAA	<3*	<3*	0	22±5	19±4	9	10±4	12±4	0	15±4	24±4	17
Eu-INAA	<5*	<5*	0	28±7	23±6	14	<14*	9±7	7	12±7	22±7	16
Tb-INAA	<7*	<7*	0	23±10	20±10	15	<16*	<10*	0	12±10	23±10	16
Yb-INAA	<12*	<12*	20	<18*	16±9	?	13±8	<15*	?	<15*	17±8	9
Lu-INAA	<8*	<8*	ND	<16*	<23*	ND	<17*	11±8	ND	11±9	15±8	ND
Hf-INAA	<10*	<10*	0	<8*	<10*	0	41±8	40±8	21	<9*	10±8	7
Ta-INAA	<9*	<9*	0	<20*	<13*	0	19±13	17±12	0	19±12	34±12	0
W-INAA	?	?	0	<25*	<23*	0	42±24	40±21	15	<30*	26±19	0
Au-INAA	>31	>28	ND	?	?	ND	?	<32*	ND	?	<33*	ND
Pb-ICAP-AES	35	<53	ND	62	101	ND	5	<7	ND	<79	<94	ND
Th-INAA	<4*	<4*	0	9±5	13±4	0	9±4	9±4	6	15±4	16±4	10
U-INAA	15±13	<20*	0	<18*	<18*	0	37±17	24±17	22	<24*	19±17	9

Table 6. Concentrations of trace elements in the original Lower Bakerstown coal sample in parts per million except as noted.

B	Na	Mg	Al (%)	Si (%)	P	K	Ca (%)	Sc	Ti	V	Cr	Mn
2.86	170	330	0.74	1.07	360	700	1.4	2	430	10.4	9.1	9.7
Fe (%)	Co	Ni	Cu	Zn	As	Se	Br	Rb	Sr	Y	Zr	Ag
0.86	6.92	17.9	10.6	47.9	2.63	0.59	34.1	4.85	82	3.33	16	0.41
Sb	Cs	Ba	La	Ce	Nd	Sm	Eu	Tb	Yb	Lu	Hf	Ta
1.5	0.29	34	6.08	10.4	3.65	1.20	0.23	0.14	0.54	0.67	0.38	0.11
W	Au	Pb	Th	U								
0.65	0.001	5.84	1.32	0.53								

Table 7. Percent of selected elements leached from the Lower Bakerstown coal by different solvents. Individual experiments were conducted using room temperature solvents (RT) and 80°C solvents (hot). The numbers after RT and hot indicate run numbers. The concentrations of elements used to calculate the percent leached were determined by instrumental neutron activation analysis (INAA) on residue of the leached coal. The concentrations of the elements used to calculate the percent leached were determined directly by inductively coupled argon plasma atomic emission spectrometry (ICAP-AES) on the leached solutions. * = number converted to an upper limit due to high errors in calculations; ND = not determined, ? No value could be determined from data.

Element- method	CH ₃ COONH ₄		HCl				HF		HNO ₃			
	RT1	RT1	RT2	RT3	Hot1	Hot2	RT1	RT1	RT2	RT3	Hot1	Hot2
B-ICAP-AES	<100	<100	<100	<100	<100	<100	<100	<100	<100	<100	<100	<100
Nb-INAA	9±4	17±3	15±3	19±3	31±4	30±4	86±4	35±4	25±4	19±4	18±4	30±4
Nb-ICAP-AES	15	16	<59	<59	<59	<65	124	31	<59	<85	<65	<65
Mg-ICAP-AES	47	57	28	29	57	60	67	30	30	31	40	51
Al-ICAP-AES	59	57	<56	<56	68	67	70	75	66	78	81	80
Si-ICAP-AES	<0.3	1	<2	<2	16	17	ND	3	<2	17	6	7
P-ICAP-AES	<9	69	72	72	88	92	83	73	71	99	80	92
K-INAA	<13*	12±10	13±11	12±11	37±11	39±11	<99*	31±10	15±11	13±11	16±11	22±11
K-ICAP-AES	<86	<9	<100	<100	<100	<100	99	<86	<100	<100	<100	<100
Ca-ICAP-AES	62	77	100	97	121	131	41	108	108	119	117	135
Sc-INAA	<3*	17±2	18±3	19±2	29±2	28±2	47±2	35±2	21±2	20±2	20±2	29±3
Ti-ICAP-AES	<4	<43	<23	<23	<23	<26	54	<4	<23	<25	<23	<26
V-ICAP-AES	<29	<29	<100	<100	<100	<100	57	<29	<100	<100	<100	<100
Cr-INAA	<6*	<4*	<6*	<4*	<4*	9±4	23±4	15±4	<7*	<5*	?	8±6
Cr-ICAP-AES	<17	<17	<100	<100	<100	<100	42	<17	<100	<100	<100	<100
Mn-ICAP-AES	56	43	<100	<100	<100	<100	68	40	<100	<100	<100	<100
Fe-INAA	<4*	49±4	48±4	53±3	54±4	53±4	59±4	97±5	96±5	96±5	96±5	96±5
Fe-ICAP-AES	<0.2	53	53	53	58	60	56	108	104	113	103	116
Co-INAA	80±2	70±2	70±2	72±3	73±3	73±2	72±3	85±2	79±2	80±3	79±3	83±2
Co-ICAP-AES	65	65	<100	<100	<100	<100	65	73	<100	<100	<100	<100
Ni-INAA	33±13	44±13	50±13	51±13	46±13	61±13	59±13	70±13	63±13	65±13	61±13	68±13
Ni-ICAP-AES	47	57	<56	<56	66	67	70	75	68	76	81	80
Cu-ICAP-AES	<14	31	<94	<94	<94	<100	57	87	<84	<100	<100	<100
Zn-INAA	57±8	84±5	84±5	85±5	86±5	85±5	85±5	93±5	87±5	86±5	83±5	90±5
Zn-ICAP-AES	88	100	220	124	128	116	138	150	103	144	125	116
As-INAA	<5*	60±4	59±4	62±4	61±4	60±4	65±4	96±4	84±4	96±4	96±4	95±4
Se-INAA	<10*	<10*	21±9	<15*	11±10	<15*	<15*	86±10	57±10	58±10	49±9	78±10
Br-INAA	<4*	11±3	16±3	16±3	73±3	73±3	29±3	57±3	36±3	23±3	23±3	44±3
Rb-INAA	<14*	<24*	<22*	18±14	48±14	45±14	81±16	38±14	<24*	15±14	<34*	28±14
Sr-INAA	<18*	23±17	<34*	<29*	84±18	73±18	52±17	61±17	40±20	30±17	22±17	49±17
Sr-ICAP-AES	17	22	28	29	83	90	48	48	35	38	68	75
Y-ICAP-AES	<45	<45	<100	<100	<100	<100	<45	<45	<100	<100	<100	<100
Zr-ICAP-AES	<10	<9	<62	<62	<62	<70	81	<10	<62	<69	<70	<69
Ag-ICAP-AES	<100	<100	<100	<100	<100	<100	<100	<100	<100	<100	<100	ND
Sb-INAA	<5*	36±3	44±3	32±3	28±3	25±3	34±3	56±3	21±4	48±3	47±3	54±3
Cs-INAA	<14*	<17*	18±12	22±12	56±13	56±13	78±14	42±12	15±12	27±12	23±12	36±14
Ba-INAA	<22*	<20*	<17*	<15*	45±11	53±12	70±12	47±12	<15*	23±18	>25	19±14
Ba-ICAP-AES	15	12	<30	<30	64	72	141	29	<29	<33	49	54
La-INAA	<5*	13±3	17±3	20±3	58±3	58±3	13±3	52±3	22±3	19±3	19±3	43±3
Ce-INAA	<3*	15±4	21±4	24±3	59±3	59±3	9±3	55±3	25±3	24±3	23±3	47±3
Ce-ICAP-AES	<29	<29	<100	<100	<100	<100	<29	29	<100	<100	<100	<100
Nd-INAA	<13*	14±12	<25*	17±12	40±12	61±12	<16*	57±12	24±11	<15*	31±12	46±12
Sm-INAA	<5*	25±3	29±3	30±3	59±3	58±3	11±3	59±3	36±3	32±3	32±3	50±3
Eu-INAA	<5*	24±5	30±5	32±5	56±5	54±5	10±5	56±5	34±5	35±5	35±5	51±5
Tb-INAA	<7*	17±7	29±7	28±7	40±7	39±7	8±7	43±7	27±7	27±7	24±7	42±7
Yb-INAA	<7*	8±6	<12*	9±6	25±5	21±6	<6*	35±5	14±6	12±6	12±6	18±6
Lu-INAA	<6*	11±6	<13*	13±7	23±5	24±5	8±5	34±5	16±5	13±6	9±6	24±6
Hf-INAA	<6*	<9*	?	<6*	<12*	8±6	40±6	12±6	<6*	<11*	<13*	7±6
Ta-INAA	?	?	?	?	?	?	<13*	<9*	?	?	?	?
W-INAA	?	?	?	?	<14*	?	23±13	<14*	?	?	?	?
Au-INAA	<60*	<44*	33±30	?	59±33	<31*	?	<32*	<42*	<56*	?	?
Pb-ICAP-AES	<52	93	<100	<100	<100	<100	32	98	<100	<100	<100	<100
Th-INAA	<3*	9±3	10±5	13±3	29±3	29±3	8±3	32±3	14±3	17±5	15±3	25±4
U-INAA	<24*	<19*	<24*	34±12	29±11	32±11	21±12	44±11	23±12	28±12	20±12	36±12

TRACE ELEMENTS IN COAL: A USGS PERSPECTIVE OF THE CLEAN AIR ACT

R. B. Finkelman
U.S. Geological Survey, MS 956
Reston, VA 22092

Keywords: coal quality, data base, modes of occurrence.

INTRODUCTION

The provisions of the 1990 Clean Air Act Amendments require the U.S. Environmental Protection Agency (EPA) to evaluate the hazards to public health resulting from emissions by electric utility steam-generating plants. Among the substances listed in the Act as hazardous air pollutants are about a dozen elements found in coal (As, Be, Cd, Co, Cr, Hg, Mn, Ni, Pb, Sb, Se, and U). Coal combustion can be a primary anthropogenic source for some of these elements (especially Be, Co, Hg, Sb, Se).

There is no publicly available data base that contains comprehensive information on the trace element content of coal beds that are used for combustion. Therefore, the EPA has chosen the U.S. Geological Survey (USGS) Coal Quality Data Base to use in their evaluation of the impact of coal switching and to estimate the trace element input load to electric utility steam generating plants.

THE USGS COAL QUALITY DATA BASE

The USGS Coal Quality Data Base is an interactive, computerbased data base. It contains comprehensive analyses of more than 13,000 samples of coal and associated rocks from every major coal-bearing basin and coal bed in the United States and about 1,000 analyses of coal samples from other countries. The data in the Coal Quality Data Base represent analyses of the coal as it exists in the ground. The data commonly are presented on an as-received whole-coal basis.

SAMPLE COLLECTION AND ANALYTICAL PROTOCOL

The recommended procedures for collecting samples for analyses that were included in the data base are described by Stanton (1). Detailed information on the geographic location (State, county, longitude and latitude, mine, etc.) and geologic and stratigraphic information (thickness, depth, geologic age, formation, member, bed, etc.) are recorded for each sample.

Coal and associated rock samples were analyzed for the concentrations of approximately 75 major, minor, and trace elements (2) by the USGS, and for the standard coal characteristics by the U.S. Bureau of Mines and commercial testing laboratories using American Society of Testing and Materials standards (3). The standard coal characteristics include proximate and ultimate analysis, calorific value, forms of sulfur, ash-fusion temperatures, free-swelling index, and air-drying loss. Equilibrium moisture, apparent specific gravity, and Hardgrove Grindability Index are determined on selected samples. A total of 136 parameters are determined for each sample.

NATURE OF THE COAL QUALITY DATA BASE

The samples collected and submitted for analysis and inclusion in the data base consist primarily of full bed core and channel samples. Some of the bed samples were collected in benches or in measured intervals of the bed. The bench or interval analyses can be weighted by thickness and composited to obtain a calculated analysis of the full coal bed. Where possible, clastic rocks (partings, overburden, underburden) associated with the coal bed also were collected and analyzed.

Finkelman and others (4) compiled a bibliography of publications containing element data from the Coal Quality Data Base. This report also contains the number of analyzed samples for each State and the number of those analyses that have been published. Approximately half of the data in the data base has been included in publications.

During the past 5 years an additional 500 analyses have been added to the data base. About 75 percent of the samples were collected and analyzed prior to 1982. In some basins, many of the coal samples were collected from active surface and underground mines. In some of these areas, mining is no longer active. Nevertheless, the data from these areas are still useful for regional projections of coal quality variation.

The addition of coal quality data from the Illinois Geological Survey (approximately 700 analyses) and from the New Mexico Bureau of Mines and Geology (approximately 550 analyses) will enhance the Coal Quality Data Base.

VERTICAL AND LATERAL VARIATIONS OF THE COAL QUALITY DATA

One of the more common uses of the USGS coal quality data is to evaluate vertical and lateral distribution of coal quality parameters. Table 1 contains arithmetic means for the potentially hazardous air pollutants in several coal basins (data for all tables are from reference 5). Several elements exhibit a wide range of concentrations among the coal basins; for example, cadmium ranges from 0.1 ppm in the Appalachian basin to 4.2 ppm in the Interior Coal Province. In contrast, mercury ranges from 0.12 ppm in the Powder River basin to only 0.22 ppm in the Gulf Coast Province.

Table 2 contains arithmetic means of the potentially hazardous air pollutants in six coal beds within the Appalachian basin. Mercury and antimony show a greater range within the coal basin than among coal basins. Table 3 contains arithmetic means for the potential air pollutants in six coal samples from the Pittsburgh coal bed from Ohio, Pennsylvania, and West Virginia. In this sample suite arsenic and beryllium have larger ranges than they do in tables 1 or 2. Finally, at bench scale, the smallest sampling scale in the data base, table 4 shows large trace element ranges, among bench samples from the Pittsburgh coal bed, for arsenic, beryllium, cobalt, chromium, and mercury. These data demonstrate that trace element ranges may be larger within a coal bed than between coal basins (for example see mercury).

STATISTICAL CORRELATIONS

One indirect method of deducing an element's mode of occurrence is to determine its correlation with ash yield, sulfur, or other coal quality parameters. This is often a useful, but potentially misleading, procedure. In a geologic data base, such as the USGS Coal Quality Data Base, correlation coefficients generally reflect a common source rather than a close chemical or physical affinity. For example, Cecil and others (6) found evidence of extensive mobilization of many trace elements in the Upper Freeport coal bed. Because this geochemical system was closed for many elements, the elements retained statistical correlations with ash yield and other parameters, despite these elements having changed chemical form and distribution patterns. Finkelman (7) came to a similar conclusion on the basis of research on the Gulf Coast lignites.

MODES OF OCCURRENCE AND TEXTURAL RELATIONS

The USGS Coal Quality Data Base provides information on the concentration and vertical and lateral distribution of many coal quality parameters including the major, minor, and trace elements. This information is useful, especially for seeking coals with particular coal quality characteristics or for determining regional trends. However, to anticipate the environmental impact, technological behavior, or byproduct potential of an element, information is needed on the modes of occurrence (chemical form) and textural relations of the element. Currently, this information is not included in the data base. The USGS has, however, conducted extensive investigations on the modes of occurrence and textural relations of the elements in coal (8-12).

CONCLUSION

The trace element information contained in the U.S. Geological Survey Coal Quality Data Base may aid EPA in addressing several provisions of the 1990 Clean Air Act Amendments. Information on the modes of occurrence and textural relations of potentially hazardous elements may lead to more efficient mitigation of the environmental impact of these elements found in coal.

LITERATURE CITED

1. Stanton, R. W., 1989, Sampling of coal beds for analysis. In *Methods for sampling and inorganic analysis of coal*, D. W. Golightly and F. O. Simon, editors. U.S. Geological Survey Bulletin 1823, p. 7-13.
2. ASTM (American Society for Testing and Materials), 1993, Annual book of ASTM standards, Volume 05.05 Gaseous fuels: Coal and coke. ASTM, Philadelphia, 526 p.
3. Golightly, D. W., and Simon, F. O., editors, 1989, *Methods for sampling and inorganic analysis of coal: U.S. Geological Survey Bulletin 1823*, 72 p.
4. Finkelman, A. C., Wong, C.-J. J., Cheng, A. C., and Finkelman, R. B., 1991, Bibliography of publications containing major, minor, and trace element data from the National Coal Resources Data System. U.S. Geological Survey Open-File Report 91-123, 19 p.
5. Finkelman, R. B., Oman, C. L., Bragg, L. J., and Tewalt, S. J., in press, The U.S. Geological Survey Coal Quality Data Base. U.S. Geological Survey Open-File Report.
6. Cecil, C. B., Stanton, R. W., Allshouse, S. D., and Finkelman, R. B., 1979, Interbed variation in and geologic controls on element concentrations in the Upper Freeport coal. American Chemical Society, Fuel Chemistry Division, Chemical Congress Abstract no. 48.
7. Finkelman, R. B., 1981, Modes of occurrence of trace elements in coal. U.S. Geological Survey Open-File Report 81-99, 312 p.
8. Zubovic, P., Stadnichenko, T., and Sheffey, N. B., 1960, The association of minor elements with organic and inorganic phases of coal. U.S. Geological Survey Professional Paper 400-B, p. B84-B87.
9. Finkelman, R. B., Palmer, C. A., Krasnow, M. R., Aruscavage, P. S., and Sellers, G. A., 1990, Heating and leaching behavior of elements in the eight Argonne Premium Coal Samples. *Energy and Fuels*, v. 4, no. 6, p. 755-767.
10. Finkelman, R. B., 1993, Trace and minor elements in coal. In *Organic geochemistry: Principles and applications*, M. H. Engel and S. A. Macko, editors. Plenum Publishing Corp., New York, p. 593-607.
11. Finkelman, R. B., in press, Modes of occurrence of hazardous elements in coal: Level of confidence. *Fuel Processing Technology*.
12. Palmer, C. A., and Filby, R. H., 1983, Determination of mode of occurrence of trace elements in the Upper Freeport coal bed using size and density separation procedures. *Proceedings, 1983 International Conference on Coal Science*, International Energy Agency, p. 365-368.

Table 1. Variation of potential air toxics among coal basins. (Values are arithmetic means in parts-per-million on a whole-coal basis; figures in parantheses are number of samples.)

Element	Appalachian basin (4,700)	Interior Province (800)	Gulf Coast lignites (200)	Fort Union lignites (350)	Powder River basin (800)
Antimony	1.4	1.5	1.0	0.69	0.57
Arsenic	35.0	20.0	10.0	11.0	5.6
Beryllium	2.5	2.4	2.4	1.0	0.84
Cadmium	0.1	4.2	0.55	0.16	0.16
Chromium	17.0	19.0	24.0	6.4	8.5
Cobalt	7.2	10.0	7.2	2.4	2.3
Lead	8.4	40.0	21.0	4.8	5.5
Manganese	29.0	78.0	150.0	83.0	63.0
Mercury	0.21	0.15	0.22	0.14	0.12
Nickel	17.0	27.0	13.0	4.1	6.4
Selenium	3.5	3.2	5.7	0.82	1.1
Uranium	1.7	3.1	23.0	1.8	1.6

Table 2. Variation of potential air toxics among coal beds in the Appalachian basin. (Values are arithmetic means in parts-per-million on a whole-coal basis; figures in parentheses are number of samples.)

Element	Meigs Creek coal bed (54)	Redstone coal bed (80)	Pittsburgh coal bed (194)	Lower Freeport coal bed (119)	Lower Kittanning coal bed (219)	Sewell coal bed (73)
Antimony	0.3	0.7	0.6	1.2	0.9	1.1
Arsenic	6.7	29.1	20.4	37.3	25.2	11.1
Beryllium	1.4	1.6	1.4	2.7	2.6	2.2
Cadmium	0.08	0.07	0.11	0.11	0.14	0.10
Chromium	16.4	13.8	14.7	17.4	16.8	11.8
Cobalt	3.2	3.5	4.6	7.6	6.7	8.0
Lead	5.3	4.0	4.9	10.4	10.6	5.5
Manganese	30.8	46.3	31.9	42.8	27.2	18.5
Mercury	0.12	0.22	0.18	0.34	0.24	0.16
Nickel	9.5	9.5	10.7	20.4	20.5	18.9
Selenium	2.9	2.4	1.9	5.0	4.3	2.4
Uranium	1.8	1.7	1.1	1.7	1.8	1.4

Table 3. Lateral distribution of potential air toxics within the Pittsburgh coal bed from Ohio, Pennsylvania, and West Virginia. (Values are arithmetic means in parts-per-million on a whole-coal basis.)

Element	Sample					
	1	2	3	4	5	6
Antimony	0.4	1.4	0.4	0.4	1.4	0.3
Arsenic	13.3	75.1	15.0	9.6	79.8	10.0
Beryllium	1.1	1.2	1.6	1.4	1.0	0.3
Cadmium	0.10	0.07	0.14	0.06	0.09	0.04
Chromium	14.4	9.3	10.1	10.3	9.2	10.2
Cobalt	2.8	3.1	11.8	2.7	4.9	1.7
Lead	3.6	3.7	1.5	3.8	6.9	1.0
Manganese	17.8	19.1	55.1	19.7	25.6	25.3
Mercury	0.10	0.22	0.60	0.16	0.28	0.22
Nickel	7.1	6.3	20.9	9.0	9.5	4.3
Selenium	1.5	3.4	3.0	0.9	1.7	1.0
Uranium	0.8	0.3	2.0	0.9	1.4	2.4

Table 4. Variations of potential air toxics from the top to the bottom of a set of bench samples from the Pittsburgh coal bed in Ohio. (Values are in parts-per-million on a whole coal basis. Total thickness of the bed is 52.5 inches.)

Element	Sample						bottom 7
	top 1	2	3	4	5	6	
Antimony	0.6	0.2	0.2	0.2	0.3	0.3	0.4
Arsenic	10.4	12.6	4.9	6.3	8.2	31.9	12.8
Beryllium	3.0	1.5	0.8	0.7	1.6	1.3	3.4
Cadmium	0.10	0.09	0.03	0.05	0.08	0.08	0.09
Chromium	30.4	7.4	6.9	9.8	32.7	11.8	12.5
Cobalt	9.2	2.2	1.6	2.1	6.6	1.3	3.3
Lead	8.7	1.6	1.3	1.4	5.5	1.5	5.1
Manganese	12.6	10.3	8.8	7.34	24.8	8.4	13.7
Mercury	0.24	0.29	0.10	0.14	0.20	0.19	0.05
Nickel	16.6	5.8	2.9	4.7	21.3	5.9	13.7
Selenium	8.5	3.3	1.1	1.5	2.2	0.9	0.9
Uranium	2.0	0.3	0.3	0.4	1.3	0.3	0.6

COAL CLEANING:
A PRE-COMBUSTION AIR TOXICS CONTROL OPTION

David J. Akers, Robert L. Dospoy, and Clifford E. Raleigh, Jr.
CQ Inc.
One Quality Center
Homer City, PA 15748

Barbara Toole-O'Neil
Electric Power Research Institute
Palo Alto, CA 94303

Keywords: Coal Cleaning; Air Toxics Control; Trace Element Reduction

INTRODUCTION

A number of elements and their compounds commonly found in coal are identified by the Clean Air Act (CAA) of 1990 as among 189 hazardous air pollutants (HAPs). These elements include: antimony, arsenic, beryllium, cadmium, chromium, cobalt, lead, manganese, mercury, nickel, and selenium. In addition to these specific elements, radionuclides are also listed as HAPs; these too are known to occur naturally in some coals. Finally, fluorine, in the form of hydrofluoric acid, is listed. The CAA mandates a study of utility air emissions. This study, to be performed by the United States Environmental Protection Agency (EPA), is expected to be presented to Congress by November 1995. In addition, EPA is required by law to perform a health risk assessment and to recommend new air toxic regulations, if necessary, to protect human health. Furthermore, the legislation requires separate studies of mercury emissions, deposition, and health effects. In order to make estimates of power plant HAP emissions, EPA requires information on the HAP concentrations in as-fired coal (i.e., as burned by utilities).

PUBLIC SOURCES OF COAL TRACE ELEMENT DATA

Starting in 1973 and continuing through the present, the United States Geological Survey (USGS) has collected and analyzed thousands of channel and core samples of coal for various quality parameters. The measurement of trace element content was part of this geochemical study. Channel and core samples are sometimes taken of the entire height of a coal seam, including interbedded rock and minerals (partings). In such cases, they represent in-place coal, which is similar to as-mined coal without the roof or floor rock sometimes extracted along with the coal during mining (out-of-seam dilution). USGS sampling protocol is to treat partings under ten centimeters thick as part of the coal seam, while those greater than ten centimeters thick are sampled separately unless they are normally extracted with the coal during mining. Partings are sometimes removed separately in surface mining, but in underground mining, they are always extracted with the coal. Therefore, USGS samples taken in underground mines normally represent in-place coal, while those taken from surface mines may or may not represent in-place coal.

Currently, no comprehensive trace element database is available to government and industry other than the database developed by the USGS. EPA is constrained by the absence of other comprehensive data sources and may use the USGS database for the emissions estimates necessary to perform the health risk assessments required by the Clean Air Act Amendments even though the available analyses are for in-place coal and not as-fired coal. This is a concern because, as shown in Table 1, about 77 percent of eastern and midwestern as-mined coal is cleaned before it is burned. In some cases, the primary effect of coal cleaning is to remove out-of-seam dilution; however, partings may also be removed during cleaning along with fracture filling mineral matter. Recent studies have demonstrated that coal cleaning can also reduce the concentration of most trace elements (Akers and Dospoy, 1993 and DeVito et al., 1993). Since the coal samples in the USGS represent as-mined or in-place coal, the trace element data in the USGS database on many of the eastern and midwestern coals will be higher than as-fired data because most of these coals are cleaned before combustion. Health risk assessments based on the existing USGS coal database will, therefore, tend to overestimate the risk of burning eastern and midwestern coal.

THE CURRENT PROJECT

CQ Inc., under funding by the Electric Power Research Institute, developed an approach that can be used to make coal samples in the USGS database more representative of as-fired rather than in-place coal. This paper presents a description of this approach, which involved the development of regression equations and algorithms for each of 11 trace elements. These equations and algorithms are used to predict the amount of a trace element in as-fired coal given the trace element analyses of channel and core samples in the USGS database. The

paper also presents discussion of the accuracy of the projections and provides an example of how the algorithms are being used.

The final part of this project, currently in progress, is to select those coals in the USGS database that exceed the typical as-fired ash content for the seam and county in which they were mined. For each USGS sample that exceeds the typical ash content, the appropriate algorithm will be applied to predict the trace element concentration of the core or channel sample assuming the coal had been cleaned to the typical ash content. At the conclusion of the project, a modified version of the USGS database will be available for estimating power plant emissions of HAPs.

MATHEMATICAL MODELING AND REGRESSION ANALYSES

Mathematical equations can often be developed to describe the relationships between input and output parameters of a system. In some cases, equations that are derived from theoretical or generally accepted cause-and-effect relationships can be used for modeling reactions to changes in measurable parameters. This is sometimes referred to as mechanistic or fundamental modeling. However, when theoretical knowledge about the relationships between inputs and outputs of a system is lacking, empirically-derived equations may still be developed to describe variable relations in a system.

A common method of empirical modeling is statistical correlation. Correlation, which involves the development of equations to relate results to system effects, can be used to analyze process data, describe its tendencies, and evaluate the intensity of associations among process parameters. A disadvantage with this modeling method is that the existence of a correlation does not mean that the system outputs are necessarily causally related to the input variables used to build the model. A measure of high correlation indicates only that the random variation of the data can be mathematically explained and that a specific tendency or behavior within the data is identified. However, when used correctly, statistical correlation can be an effective and reliable modeling method.

The primary operation involved in statistical correlation is regression analysis. Regression involves fitting linear or nonlinear mathematical equations to data sets in order to describe changes in dependent variables resulting from changes in independent parameters. In the case of linear regression, this is typically referred to as "least-squares" line fitting. In addition, regression is sometimes completed in stages to eliminate variables that are found to be mathematically and statistically unimportant; this is known as step-wise regression.

In order to develop equations that can predict the content of selected trace elements in clean coal after commercial-scale conventional coal cleaning, regression analyses were performed to relate various raw coal quality parameters and cleaning performance data to the trace element reduction. The data used for this work was collected from several sources: CQ Inc. has a database that includes ten commercial-scale coal cleaning tests; Consolidation Coal Company (CONSOL) has published information on trace element reductions in eight commercial cleaning plants (DeVito et al., 1993); and Bituminous Coal Research (BCR) has published trace element data for six commercial plants (Ford and Price, 1982). Finally, Southern Company Services, Inc. (SCS) gathered data on two commercial-scale cleaning tests during a project funded by DOE and EPRI. The final report for the SCS work has been prepared and supplied to EPA by DOE. Altogether, trace element removal data from 26 commercial-scale cleaning tests using coal mined east of the Mississippi River were located. Sufficient information was located to allow development of equations for the following elements: arsenic, beryllium, cadmium, chromium, cobalt, fluorine, lead, manganese, mercury, nickel, and selenium.

Multi-parameter, backward elimination regression analyses and statistical analysis of variance were conducted to develop equation models for each of 11 trace elements. For each system, trace element reductions from the commercial-scale coal cleaning tests and their respective raw coal quality parameters and coal cleaning performance results were gathered and stored into a database file. Various mathematical transformations (square root, logarithmic, and negative inverse) of the original data were also generated and included within this file. Regression of data transformations provided a means to ensure that both linear and non-linear correlation possibilities were examined. These data sets were then input to Minitab™, a computer software statistics package, for backward elimination regression. Information and output from Minitab includes statistics on summary of fit (the applicability and hardness of the equation to describe the variances in the data), analysis of variance, and parameter estimates. All of the equations developed contained ash reduction as a major predictive parameter. Three of the equations also included a total sulfur reduction predictor, while several equations included one or more raw coal analyses in addition to ash reduction.

DATA SCATTER AND MODELING ACCURACY

The primary method used to evaluate regression equation accuracy was to evaluate the comparative fit of measured trace element reductions versus calculated trace element reductions. An example of this method of accuracy check is shown in the figure. In these types of graphs, the dotted line represents an exact correlation between the measured and predicted reductions. That is, if data appear on this line, the equation produced exactly the same value that was measured for a particular coal cleaning test. Similarly, values that plot away from this line indicate that the equation predicted trace element values greater than or less than the actual measured values. Therefore, equation accuracy can be determined by the distance individual values are away from this line. In this example, the graphic suggests that the equation developed for fluorine is accurate, though some points are a significant distance from the line. Some portion of this data scatter is likely caused by sampling or analytical error, but other explanations must also be considered.

Lack of fit may also be caused by differences in the mode of occurrence of these trace elements in raw coal and differences of response to a variety of coal cleaning operations. The mode of occurrence of an element is the physical form and location in which the element is found within a raw coal. In general, trace elements can be found within either the organic portion of a coal or within the mineral matter that is associated with a raw coal. When trace elements are associated with mineral matter or exist as discrete mineral particles, physical coal cleaning methods can be used to remove much of the mineral matter and trace elements from a raw coal. For example, mercury has been reported to occur in coal in a variety of modes: it can be found in pyrite, in epigenetic pyrite, and in sulfides other than pyrite as well as organically bound within coal (Finkelman, 1980). Any organically-bound mercury that may occur in coal cannot be removed by physical coal cleaning technologies, while epigenetic pyrite is often coarse grained and readily removable. Thus, if mercury is organically-bound, concentrations will increase with cleaning; if it is contained in coarse-grained mineral matter, it will be reduced by cleaning with quantities dependent upon the cleaning devices employed, method of operation, and coal characteristics.

Local geologic environment during and after coal formation can also affect the mode of occurrence of a trace element. As a result, mode of occurrence may vary between coal basins or even within a single basin. Because trace element mode of occurrence may vary with location, it is reasonable to expect such a change to be reflected in the geographic location of the coal samples used. An indication of possible impacts based on geographic location is shown in the fluorine data. The figure shows that for the Pennsylvania coals, measured fluorine reductions are always equal to or lower than their corresponding predicted values. For the Alabama coal samples, this situation is reversed--measured fluorine reductions are always equal to or higher than the predicted values. This indicates that the mode of occurrence of fluorine in Pennsylvania coals may inhibit the effectiveness of coal cleaning to remove this trace element. Conversely, the mode of occurrence of fluorine in Alabama coals may help make its removal easier. Unfortunately, when the data used in this study were grouped by state of origin or by coal basin, the number of commercial-scale tests became too small to allow a statistical assessment of the impact of geographic location.

The level of trace element reduction obtained during coal cleaning can also be affected by the different techniques and technologies utilized to remove ash-forming and sulfur-bearing minerals. However, as with location differences, this could not be adequately addressed in this study because of insufficient data. To illustrate this point, consider that most of the known mineral forms of mercury in coal are sulfides, which are typically dense, finely-sized minerals. When liberated from raw coal by crushing or grinding, sulfides can be easily removed by cleaning devices that depend on the differences in density between coal and mineral matter--this is the most common method of coal cleaning. Examples of density-based cleaning devices, which have a wide range of applicability and varying degrees of coal-mineral matter separation performance, include heavy-media cyclones and baths, jigs, and concentrating spirals. Other devices such as froth flotation or agglomeration units clean coal based on the differences in surface properties between the coal and mineral matter. The surface characteristics of many sulfides and coal are sometimes very similar, though, which makes sulfide removal using surface-based methods difficult at times.

AS-FIRED COAL QUALITY DATA

In order to use the regression equations to adjust the USGS channel or core sample data to an as-fired basis, it is first necessary to estimate the ash and sulfur content of a target clean coal. The quality of clean coal produced from coal cleaning plants is primarily driven by raw coal characteristics and market price and specifications. Because raw coal characteristics vary by region and seam and because utility fuel quality demands can vary from region to region, a wide spectrum of clean coal qualities are produced for the utility market. In order to

develop clean coal quality targets that are applicable to specific samples in the USGS database, both raw coal characteristics and local market specifications must be examined.

Within a very limited geographical area (e.g., a county), the characteristics of an individual coal seam are reasonably uniform. In addition, most of the clean coal that is produced from a particular seam in this limited region is of similar quality, especially if much of the coal produced in the localized region is competing for fuel sales to the same electrical generating station. Thus, clean coal quality targets used in algorithms that adjust USGS as-mined or in-place coal quality data to typical as-fired quality levels must be developed for each individual seam in a given county where active mining is occurring. Several public databases and other published sources can be used in gathering the specific information needed to relate regional coal production and individual coal seam information.

SAMPLE ALGORITHM CALCULATION

To apply the algorithms developed during this project, the following information is necessary:

- Initial sample data (raw coal quality data or USGS channel or core data).
- Target clean coal quality.
- The calculated ash, and in some cases sulfur, reduction between the initial sample and the target quality.
- The results of applying the regression equations.
- The results of the trace element concentration calculation.

The sample calculation presented below illustrates the procedures for determining the expected nickel concentration in the cleaned Sewickley Seam coal from Pennsylvania.

SAMPLE DATA

Raw Ash = 32.9%; Raw Heating Value = 9,804 Btu/lb; Raw Nickel = 23.5 ppm

TARGET CLEAN COAL QUALITY (Assumed)

Typical As-fired Sewickley Seam Coal, Greene County, PA
Ash = 12.0% and Heating Value = 13,300 Btu/lb

REDUCTION CALCULATION

Ash reduction is calculated by the following equation:

$$\text{Ash Reduction} = \frac{\frac{\text{Raw Coal Ash Content}}{\text{Raw Coal Heating Value}} - \frac{\text{Clean Coal Ash Content}}{\text{Clean Coal Heating Value}}}{\frac{\text{Raw Coal Ash Content}}{\text{Raw Coal Heating Value}}} \cdot 100$$

$$\text{Ash Reduction} = \frac{\frac{32.9}{9,804} - \frac{12.0}{13,300}}{\frac{32.9}{9,804}} \cdot 100 = 73.11\%$$

APPLICATION OF THE REGRESSION EQUATIONS

In this example, the equation for nickel reduction is used:

$$\text{Nickel Reduction} = \frac{1}{[-0.0867 + (0.0368 \cdot \text{Log (Ash Reduction)})]} - \frac{1}{[-0.0867 + (0.0368 \cdot \text{Log (73.11)})]} \cdot 55.23\%$$

TRACE ELEMENT CONCENTRATION CALCULATION

Once the calculated nickel reduction is determined, the next step is to determine the clean coal nickel concentration using available raw coal data for heating value and nickel concentration and the target clean coal heating value.

$$\text{Nickel Reduction} = \frac{\frac{\text{Raw Coal Nickel Content}}{\text{Raw Coal Heating Value}} - \frac{\text{Clean Coal Nickel Content}}{\text{Clean Coal Heating Value}}}{\frac{\text{Raw Coal Nickel Content}}{\text{Raw Coal Heating Value}}} \cdot 100$$

$$55.23 = \frac{\frac{23.5}{9,804} - \frac{\text{Clean Coal Nickel Content}}{13,300}}{\frac{23.5}{9,804}} \cdot 100$$

$$\text{Clean Coal Nickel Content} = \left[\left(\frac{55.23}{100} \right) \cdot \frac{23.5}{9,804} \right] + \left(\frac{23.5}{9,804} \right) \cdot 13,300 = 14.27 \text{ ppm}$$

Table 2 shows the results of applying this algorithm to adjust the trace element concentration of raw Sewickley Seam coal to an as-fired quality using each of the equations developed for the 11 trace elements. The table also provides a measure of the accuracy of this approach, with differences in predicted versus actual concentrations averaging about 20 percent.

SUMMARY

In order to make more representative estimates of power plant HAP emissions and to perform the health risk assessments required by the Clean Air Act Amendments, EPA requires information on the HAP concentrations in as-fired coal (i.e., as burned by utilities). Currently, the USGS coal database is the only comprehensive source for information on the trace element concentration of coals that is openly available to EPA. Unfortunately, USGS samples taken from many eastern and midwestern underground and surface mines represent in-place or as-mined coal, but not as-fired coal, which is often cleaned before it is burned. To address this problem, equations and algorithms were developed to convert trace element analyses in the USGS database from an in-place to an as-fired basis. This work has provided one means for modifying the USGS database so that it can be used to estimate power plant emissions of HAPs. The study also provides a tool to estimate the impacts of using conventional or advanced coal cleaning techniques to reduce the concentration of trace elements in coals burned by utilities.

REFERENCES

Akers, D. and Dospooy, R., "An Overview of the Use of Coal Cleaning to Reduce Air Toxics," Minerals and Metallurgical Processing, Published by The Society for Mining, Metallurgy, and Exploration, Littleton, CO, Vol. 10, No. 3, pp 124-127, August 1993.

DeVito, M., L. Rosendale, and V. Conrad, "Comparison of Trace Element Contents of Raw and Clean Commercial Coals," Presented at the DOE Workshop on Trace Elements in Coal-Fired Power Systems," Scottsdale, AZ, April 1993.

Finkelman, R., Modes of Occurrence of Trace Elements in Coal, PhD Dissertation, University of Maryland, Published by University Microfilms International, Ann Arbor, MI, 1980.

Ford, C. and A. Price, "Evaluation of the Effects of Coal Cleaning on Fugitive Elements: Final Report, Phase III," DOE/EV/04427-62, July 1982.

Table 1. Extent of Coal Cleaning by State. Includes metallurgical, steam, and industrial coal.

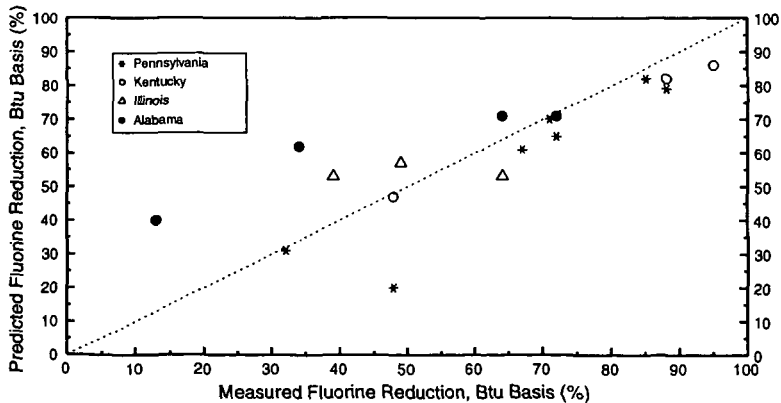
State	Estimated Raw Coal Mined (Million Tons/Year)	Estimated Tonnage Cleaned (Mt %)
Alabama	37.7	77
Illinois	83.7	93
Indiana	49.5	93
Kentucky	215.6	65
Maryland	4.9	92
Ohio	46.7	81
Pennsylvania	90.2	73
Tennessee	7.0	38
Virginia	62.0	81
West Virginia	223.6	81
Total/Average	821.0	77

Source: Coal Preparation and Solids Division, U.S. Department of Energy, Pittsburgh Energy Technology Center, Pittsburgh, PA 15236.

Table 2. Results of an Application of Algorithms on Raw Sewickley Seam Coal

Trace Element	Actual Raw Coal Conc. (ppm)	Actual Clean Coal Conc. (ppm)	Predicted Clean Coal Conc. (ppm)	Absolute % Difference Predicted vs. Actual
As	14.40	9.20	8.43	9.1
Be	1.07	0.98	1.21	19.0
Cd	0.21	0.10	0.12	16.7
Cr	44.00	23.60	29.49	20.0
Co	8.74	4.11	5.66	27.4
F	226.0	97.90	114.42	14.4
Pb	88.80	5.15	45.54	88.7
Mn	206.00	73.00	73.19	0.3
Hg	0.18	0.18	0.16	12.5
Ni	23.50	11.20	15.26	26.6
Se	3.61	2.85	2.81	1.4

Estimation of Algorithm Accuracy. Fluorine.



TRACE ELEMENTS IN ILLINOIS COALS BEFORE AND AFTER CONVENTIONAL COAL PREPARATION

I. Demir¹, R. D. Harvey¹, R. R. Ruch¹, J. D. Steele¹, and K. K. Ho²
¹Illinois State Geological Survey, 615 E. Peabody Drive, Champaign, IL 61820,
²Illinois Clean Coal Institute, Coal Development Park, PO Box 8, Carterville, IL 62918

Keywords: trace elements, Illinois coals, cleaned coal

INTRODUCTION AND BACKGROUND

Responding to recent technological advances and renewed environmental concerns requires improved characterization of Illinois and other US coals. Much of the existing trace element data on Illinois coals are on channel samples; these data need to be supplemented with data on as-shipped coals. Such data will provide a factual basis for the assessment of noxious emissions at coal-fired electric power plants.

The Clean Air Act of 1990 [Public Law 101-549, 1990] identified many trace elements as "Hazardous Air Pollutants" (HAP) (Table 1). A parallel regulation is also underway in Illinois [Illinois Pollution Control Board, 1990]. All of these HAP elements are present in Illinois and other coals [Gluskoter et al., 1977; Harvey et al., 1983] in widely varying amounts. Utilities are presently exempt from having to consider emissions of trace elements; however, this may eventually change after the U.S. EPA completes its risk analyses and establishes emission standards. A database of trace element concentrations in the coals used by utilities is a prerequisite to defining the problem and establishing workable regulations.

Human sources constitute significant portions of the total global input of most trace elements into the atmosphere (Fig. 1). Emissions of trace elements from coal-fired power plants vary widely among countries and regions, reflecting varying trace element concentrations in coals from different sources. Among human sources, energy production (electrical utilities and industrial/domestic sector) is estimated to account for major portions of atmospheric emissions of Hg, Ni, Se, Sn, and V and lesser, but still significant, portions of As, Cd, Cr, Cu, Mn, and Sb. Oil combustion contributes larger portions of Ni, Sn, and V emissions than does coal combustion [Nriagu and Pacyna, 1988; Clarke and Sloss, 1992].

During combustion, trace elements in feed coals are partitioned among gas (flue gas), light particulate (fly ash), and slag/ash phases (Fig. 2). Typically, Hg, Br, Cl, F, and Rn end up in the flue gas; As, Cd, Ga, Ge, Pb, Sb, Sn, Te, Tl, and Zn in fly ash; and Eu, Hf, La, Mn, Rb, Sc, Sm, Th, and Zr in slag/ash deposits. Others show mixed affinities.

Swaine [1989] reviewed the environmental aspects of trace elements in coal. With respect to combustion, modern electrostatic precipitators can trap up to 99% of the fly ash. Swaine concluded that, in general, no trace element posed a significant environmental problem. This assumes that state-of-the-art electrostatic precipitators are used at the power plants and that the coals burned do not have exceptionally high concentrations of noxious elements that would be emitted in a gas phase. Deep physical cleaning of raw coal would reduce the levels of those elements that are associated with minerals [Capes et al., 1974; Gluskoter et al., 1977; Cavallaro et al., 1978; Norton and Markuszewski, 1989].

The purpose of this study was to determine trace element concentrations in as-shipped coals from Illinois mines, and compare the results with data on channel samples that represent coal in place prior to mining. Samples of 34 as-shipped samples were collected and analyzed for trace, minor and major elements, including the 18 HAP elements and others identified to be of greatest environmental concern by the U.S. National Committee for Geochemistry [1980]. Results on 20 of these elements of environmental concern are reported and discussed here. Radioactivity of the as-shipped coal samples was calculated from concentrations of U, Th, and K in the samples. Future work will concentrate on evaluating the further beneficiation of the as-shipped coal samples by fine coal cleaning.

EXPERIMENTAL

Samples and Sample Regions

Cleaned (as-shipped) samples of Illinois coals were collected from each of 33 preparation plants and from a mine that sells its coal after crushing. In most cases, the samples were splits from automatic samplers. Multiple cuts were taken across the coarse output belt over a period of 4 or more hours (commonly 8 to 24 hours) to obtain a representative sample. In some cases, the sample was collected from a stock pile, taking 15 to 20 widely spaced increments with a sampling shovel. All samples were sealed in 5 mil plastic bags or in 5 gallon plastic buckets and transported or mailed to our laboratory within two days. Within a week, the samples were homogenized riffled, crushed, and packaged at our sample preparation laboratory, according to the procedure described in Figure 3.

To maintain confidentiality of the results with respect to individual mines, the Illinois coal field was divided into five multi-county regions (Fig. 4); only the regions from which the samples came from were identified.

Analyses for Trace Elements

Each of the 34 samples was analyzed for trace, minor, and major elements. These elements, their method of analysis, and the precision and accuracy of the methods are shown in Table 2.

RESULTS AND DISCUSSION

Trace Element Database

Our computerized database contains trace element information on 900 samples (Table 3). Figure 5 identifies the 60 elements for which concentrations are

available on many samples in the database. The most useful records are from the 222 channel or equivalent samples which represent coal in-place prior to mining and cleaning. Table 4 and Figure 6 give the averages and variabilities for 20 critical environmental elements for channel samples from Illinois.

Trace Elements and Radioactivity in 34 As-shipped Samples

The concentrations of most of the environmentally critical trace elements in the 34 as-shipped coals (Table 4) vary less widely than those in the channel samples (compare Figs. 6 and 7). Comparison of the data from channel samples and from cleaned coals indicates that conventional coal cleaning can reduce the state-wide mean concentrations of trace elements in channel samples up to 67% (Fig. 8), except for U (12% enrichment). The reduction in elemental concentrations results from the reduction of mineral matter and some leaching by the process water. The enrichment of U in the as-shipped samples relative to channel samples suggests that this element is primarily associated with the organic material. Harvey et al. (1983), who calculated organic affinities from washability tests for Illinois coals, also concluded that U had organic affinity. However, even if U were largely associated with the organic matter, it would likely be located in very fine mineral grains disseminated within the organic matter (Finkelman, 1981; Clarke and Sloss, 1992).

It should be pointed out that, for a given mine, channel samples do not necessarily represent those portions of the seam where feed coals for as-shipped samples were mined. Therefore, the average trends of trace element reductions observed in Figure 8 may not hold for individual mines, as Figure 9 indicates. Zinc enrichment shown in Figure 9 suggests that the channel samples had been preferentially taken from low-Zn parts of the seam in a mine from the NW coal region. Zinc is concentrated in structurally disturbed zones of the seam which are mined but were not channel-sampled.

Because the channel samples were analyzed for fluorine (F) by an old technique, which tends to underestimate F in many coal samples [Wong et al., 1992], the F data from the channel samples and from as-shipped coals cannot be compared to evaluate the fate of F during coal preparation. At present, F analysis is carried out according to Australian hydroxylytic procedure standard AS1038.10.4-1989.

The natural radioactivity of coal, which is derived from the decay of Th-232, U-238 and U-235, and K-40, can be calculated from the observed masses (weights) of U, Th, and K [Cahill, ISGS, personal communication]. The calculated radioactivity data for coals agree with observed radioactive measurements [Coles et al., 1978]. Table 5 shows that for cleaned Illinois coals, the contribution to radioactivity from U and Th is relatively small compared to that from K, which contributes to background radioactivity not only in coal but in all natural environments.

SUMMARY AND CONCLUSIONS

A database on trace elements in channel samples of Illinois coals was used to show the degree of reduction of key environmental elements in 34 as-shipped coals from Illinois mines collected and analyzed for this study. The results indicate that the state-wide mean concentrations of all tested trace elements, except U, are reduced in the cleaned coals relative to those in the channel samples that represent coal in place prior to mining. Because elemental concentrations in coal vary widely from place to place and coal to coal, only mean concentrations from a large number of channel and as-shipped samples should be compared. Better yet, washability studies on individual samples should be done to assess the degree and limit of the removal of trace elements from coal during coal preparation.

ACKNOWLEDGEMENTS

We thank Illinois coal companies for their cooperation in obtaining samples of their as-shipped coals. We also thank H. H. Damberger and W. T. Frankie for their help in the collection of the samples. This research was funded in part by the Illinois Department of Energy and Natural Resources through its Coal Development Board and Illinois Clean Coal Institute and by the U.S. Department of Energy. However, any opinions, findings, conclusions, or recommendations expressed herein are those of the authors and do not necessarily reflect the views of IDENR, ICCI, and US DOE.

REFERENCES

- Capes, C.E., McElhinney, A.E., Russell, D.S., and Sirianni, A.F., *Environmental Science & Technology*, 8 (1), 35 (1974).
- Cavallaro, J.A., Deurbrouck, A.W., Schultz, H., Gibbon, G.A., and Hattman, E.A., *A Washability and Analytical Evaluation of Potential Pollution From Trace Elements in Coal*. US EPA, EPA-600/7-78-038, Washington, D.C (1978).
- Clarke, L.B. and Sloss, L.L., *Trace Elements - emission from coal combustion and gasification*. IEA Coal Research, IEACR/49, London (1992).
- Coles, D.G., Ragaini, R.C., and Ondov, J.M., *Environmental Science and Technology*, 12, 442 (1978).
- Finkelman, R.B., *Modes of Occurrence of Trace Elements in Coal*. US Geological Survey, Open File Report, OPR-81-99 (1981).
- Gluskoter, H.J., Ruch, R.R., Miller, W.G., Cahill, R.A., Dreher, G.B., and Kuhn, J.K., *Illinois State Geological Survey, Circular 499* (1977).
- Harvey, R.D., Cahill, R.A., Chou, C.-L., and Steele, J.D., *Mineral Matter and Trace Elements in the Herrin and Springfield Coals, Illinois Basin Coal Field: Illinois State Geological Survey Contract/Grant Report: 1983-4* (1983).
- Illinois Pollution Control Board, *Toxic Air Contaminants List, Title 35 Illinois Administrative Code, Part 232* (1990).
- Norton, G.A. and Markuszewski, R., *Coal Preparation*, 7, 55 (1989).
- Nriagu, J.O., *Environment*, 32, 7 (1990).
- Nriagu, J.O. and Pacyna, J.M., *Nature*, 333, 134 (1988).
- Public Law 101-549, *Clean Air Act Amendments, Title 3, 104 Stat 2531-2535* (1990).
- Swaine, D.J., *J. Coal Quality*, 8, 67 (1989).
- U.S. National Committee for Geochemistry, *Trace Element Geochemistry of Coal Resource Development Related to Environmental Quality and Health: National*

Table 1. Elements analyzed in project samples

Elements regulated* and analyzed	Other elements analyzed
Antimony	Aluminum
Arsenic	Boron
Beryllium	Calcium
Cadmium	Carbon
Chlorine	Copper
Chromium	Hydrogen
Cobalt	Iron
Fluorine	Lithium
Lead	Molybdenum
Manganese	Nitrogen
Mercury	Oxygen
Nickel	Phosphorus
Polonium ‡	Potassium
Radium ‡	Silicon
Radon ‡	Sodium
Selenium	Sulfur
Thorium	Titanium
Uranium	Vanadium
	Zinc

* Regulated by Public Law 101-549, 1990

‡ Radioactive isotopes of these elements were calculated from the analytical concentrations of Th and U.

Table 2. Relative precision and methods for minor and trace elements

Element	Relative Precision %	Average detection limit	Method*						
			WDXRF	AAS	INAA	OEP	EDX	PyroIC	
MINOR oxides									
Al ₂ O ₃	ash	3	0.1 %	X					
CaO	ash	3	0.02 %	X					
Fe ₂ O ₃	ash	3	0.01 %	X					
HgO	ash	5	0.1 %	X					
MnO	ash	5	0.01 %	X					

MnO	coal	7	3 ppm			X			
P ₂ O ₅	ash	5	0.02 %	X					
K ₂ O	ash	2	0.01 %	X					
SiO ₂	ash	1	0.1 %	X					
Na ₂ O	ash	5	0.05 %	X					
TiO ₂	ash	3	0.01 %	X					

TRACE elements									
As	coal	7	1 ppm			X			
B	ash	15	10 ppm				X		
Be	ash	5	0.5 ppm					X	
Cd	ash	10	2.5 ppm		X				
Co	coal	5	0.3 ppm			X			

Cr	coal	10	7 ppm			X			
Cu	ash	5	2.5 ppm		X				
F	coal	10	20 ppm						X
Hg	coal	15	0.01 ppm		X**				
Li	ash	12	5 ppm		X				

Mo	ash	25	10 ppm						X
Mo	ash	25	10 ppm					X	
Mo	coal	20	10 ppm			X			
Ni	ash	10	15 ppm		X				
Pb	ash	20	25 ppm		X				

Pb	ash	20	10 ppm					X	
Sb	coal	10	0.2 ppm			X			
Se	coal	10	2 ppm			X			
Th	coal	5	0.4 ppm			X			
U	coal	15	3 ppm			X			

V	ash	3	8 ppm					X	
Zn	ash	7	1.5 ppm		X				

* WDXRF - wave length-dispersive x-ray fluorescence spectrometry

AAS - atomic absorption spectrometry

INAA - instrumental neutron activation analysis

OEP - optical emission (photographic) spectrometry

PyroIC- pyrohydrolysis and ion chromatography

** Hg by cold vapor atomic absorption spectrometry

Table 3. Summary of sample types and seams in the USGS database on trace elements in coal. Samples from Illinois: Other Station Total No. Samples

SAMPLE TYPE	Other Station	Total No. Samples
Channel & equivalent	222	289
Bench (partial seams)	158	169
Float-sink fractions	77	97
Run-of-mine	20	37
As-shipped	47	55
Shales & coal associated rock	240	253
All types	764	900
SEAMS		
Herrin seam		
(111 no. 6)	473	477
Springfield seam		
(111 no. 5)	166	186
Colchester seam		
(111 no. 2)	50	55
Other seams & rocks	75	182

Table 4. Ash content (dry, wt%), heating value (dry, BTU/lb), and trace element concentrations (dry, million per million, BTU (mg/BTU)) in channel samples and in as-shipped coals from Illinois.

Sample type	Region	Ash	BTU/lb	As	B	Be	Ca	Co	Cr	Cu	F	Hg	Mn	Mo	Ni	Pb	Sb	Se	Th	U	V	Zn	
Channel	all	mean	12.4	12532	506	3778	63	132	227	651	481	2320	6	565	2419	389	702	1426	44	90	78	71	1037
		stddev	3.4	646	814	1810	37	339	147	365	338	1458	5	610	2014	301	422	1561	45	49	40	54	707
		cases	186	195	201	190	199	90	198	198	200	167	161	112	193	170	194	191	201	197	142	111	200
	all (excluding NE)	mean	12.4	12535	497	3777	63	115	229	658	484	2420	6	518	2150	410	678	1464	43	90	78	73	1097
		stddev	3.4	660	732	1900	39	330	148	377	344	1541	4	560	1715	313	337	1591	44	48	39	56	728
		cases	159	159	167	175	166	171	81	172	172	141	136	92	166	148	168	167	175	171	121	99	172
	NE	mean	12.8	12511	552	3781	66	286	211	605	464	1779	8	781	1025	252	848	1167	51	92	79	84	670
		stddev	3.5	1244	1264	1924	49	254	143	271	475	1725	7	480	2074	395	818	1278	62	52	50	75	1117
		cases	12	12	12	12	12	12	12	12	12	12	12	12	12	12	12	12	12	12	12	12	12
	NW	mean	12.8	12278	469	5147	66	334	283	468	412	1928	7	480	2670	376	435	2530	67	58	48	42	633
		stddev	3.0	590	1021	1515	54	621	216	413	397	794	4	372	1606	274	335	2530	67	58	48	42	633
		cases	12	12	12	12	12	12	12	12	12	12	12	12	12	12	12	12	12	12	12	12	12
SC	mean	12.0	12706	450	3237	52	42	247	608	473	2079	6	744	2061	289	664	1115	35	76	76	47	945	
	stddev	4.4	722	514	1050	27	45	111	408	492	620	4	1019	1365	294	277	738	22	33	48	33	546	
	cases	11	11	11	11	11	11	11	11	11	11	11	11	11	11	11	11	11	11	11	11	11	
SE	mean	11.8	12858	605	2260	63	55	224	610	445	2870	6	439	1891	515	623	1761	43	92	75	35	85	
	stddev	3.3	627	721	1181	35	55	129	331	217	2455	5	224	2039	384	294	1402	34	55	30	79	998	
	cases	13	13	13	13	13	13	13	13	13	13	13	13	13	13	13	13	13	13	13	13	13	
SW	mean	13.3	12210	214	5653	46	29	185	737	408	2699	5	434	2159	382	182	512	27	96	89	73	993	
	stddev	2.5	412	376	1494	13	22	95	360	132	892	3	297	1518	182	274	383	32	35	29	40	563	
	cases	10	10	10	10	10	10	10	10	10	10	10	10	10	10	10	10	10	10	10	10	10	
As-shipped	mean	10.1	12952	263	3222	50	39	126	64	325	3336	3	334	1336	387	509	996	31	69	52	81	1088	
	stddev	2.4	470	292	1649	11	44	29	247	1435	2	253	1138	154	197	916	25	34	34	34	34	34	
	cases	34	34	34	34	34	34	34	34	34	34	34	34	34	34	34	34	34	34	34	34	34	
NW	mean	9.7	12860	209	4918	64	53	94	606	338	3095	3	147	1964	390	491	1427	32	63	41	77	722	
	stddev	2.5	435	203	1378	33	67	33	136	106	726	2	89	2116	106	270	1633	26	30	11	77	224	
	cases	9	9	9	9	9	9	9	9	9	9	9	9	9	9	9	9	9	9	9	9	9	
SC	mean	9.8	13069	330	2283	41	32	159	437	334	3169	2	579	1031	173	527	949	41	52	59	33	344	
	stddev	3.3	523	220	372	11	0	77	133	128	1092	1	445	662	0	192	704	41	12	24	8	947	
	cases	9	9	9	9	9	9	9	9	9	9	9	9	9	9	9	9	9	9	9	9	9	
SE	mean	9.6	13193	354	1788	46	26	135	440	290	2981	5	366	936	422	458	1127	30	63	52	106	1281	
	stddev	2.0	402	408	635	8	13	34	72	64	834	2	143	354	103	142	817	15	22	10	61	692	
	cases	11	11	11	11	11	11	11	11	11	11	11	11	11	11	11	11	11	11	11	11	11	
SW	mean	11.9	12473	83	4639	46	24	105	805	368	4675	2	285	1545	377	567	406	16	109	60	100	1423	
	stddev	1.8	234	17	302	9	16	21	419	92	2664	0	73	487	154	200	109	6	50	12	26	600	
	cases	17	17	17	17	17	17	17	17	17	17	17	17	17	17	17	17	17	17	17	17	17	

Table 5. Natural radioactivity in as-shipped Illinois coals

Region		Th (ppm)	Th-232 series * (Bq/kg)	U (ppm)	U-238 series ** (Bq/kg)	U-235 series*** (Bq/kg)	K (ppm)	K-40 (Bq/kg)
All	mean	1.5	6.0	2.2	27.8	0.68	2039	63.2
	stddev	0.4	1.6	1.9	24.0	0.59	792	24.6
NW	mean	1.2	4.7	2.1	25.6	0.6	1676	51.9
	stddev	0.3	1.2	2.3	28.0	0.7	427	13.2
SW	mean	1.6	6.6	2.7	33.7	0.82	2122	65.8
	stddev	0.3	1.1	0.7	8.5	0.21	1559	48.3
SC	mean	1.7	6.8	0.9	11.7	0.29	2225	69.0
	stddev	0.6	2.4	0.2	2.7	0.07	650	20.2
SE	mean	1.5	6.1	2.9	40.0	0.90	2163	67.0
	stddev	0.2	1.0	2.4	29.2	0.72	515	16.0

* Th232, Ra228, Ac228, Th228, Ta224, Rn220, Po216, Pb212, Bi212, Po212, Tl208

** U238, Th234, U234, Th230, Ta226, Rn222, Po218, Pb214, Bi214, Po214, Pb210, Bi210, Po210

*** U235, Th231, Pa231, Ac227, Th227, Ra223, Pb211, Bi211

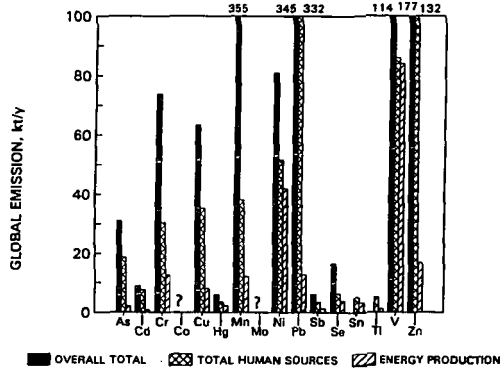


Figure 1. Global emissions of trace elements into atmosphere (after Nriagu, 1990).

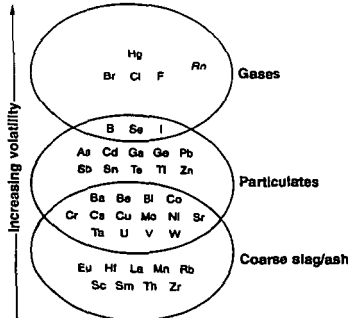


Figure 2. Behavior of trace elements during coal combustion and gasification (after Clarke and Sloss, 1992).

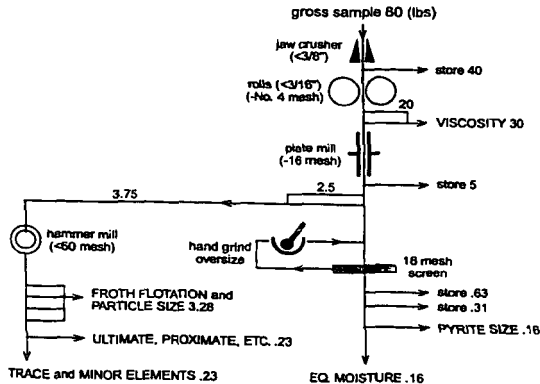


Figure 3. Flow chart for sample preparation. The weight (lbs) of the laboratory sample is given after the indicated test.

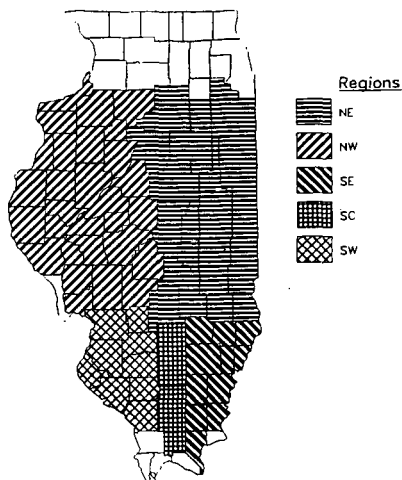


Figure 4. Sample regions of Illinois coal field.

H																	He																																
Li	Be											B	C	N	O	F	Ne																																
Na	Mg											Al	Si	P	S	Cl	Ar																																
K	Ca	Sc	Ti	V	Cr	Mn	Fe	Co	Ni	Cu	Zn	Ga	Ge	As	Se	Br	Kr																																
Rb	Sr	Y	Zr	Nb	Mo	Tc	Ru	Rh	Pd	Ag	Cd	In	Sn	Sb	Te	I	Xe																																
Cs	Ba	L	Hf	Ta	W	Re	Os	Ir	Pt	Au	Hg	Tl	Pb	Bi	Po	At	Rn																																
Fr	Ra	A																																															
<table border="1"> <tr> <td>L</td> <td>La</td> <td>Ce</td> <td>Pr</td> <td>Nd</td> <td>Pm</td> <td>Sm</td> <td>Eu</td> <td>Gd</td> <td>Tb</td> <td>Dy</td> <td>Ho</td> <td>Er</td> <td>Tm</td> <td>Yb</td> <td>Lu</td> </tr> <tr> <td>A</td> <td>Ac</td> <td>Th</td> <td>Pa</td> <td>U</td> <td>Np</td> <td>Pu</td> <td>Am</td> <td>Cm</td> <td>Bk</td> <td>Cf</td> <td>Es</td> <td>Fm</td> <td>Md</td> <td>No</td> <td>Lr</td> </tr> </table>																		L	La	Ce	Pr	Nd	Pm	Sm	Eu	Gd	Tb	Dy	Ho	Er	Tm	Yb	Lu	A	Ac	Th	Pa	U	Np	Pu	Am	Cm	Bk	Cf	Es	Fm	Md	No	Lr
L	La	Ce	Pr	Nd	Pm	Sm	Eu	Gd	Tb	Dy	Ho	Er	Tm	Yb	Lu																																		
A	Ac	Th	Pa	U	Np	Pu	Am	Cm	Bk	Cf	Es	Fm	Md	No	Lr																																		

Figure 5. Analytical results on these 60 elements (shaded) are available for many sample-records in the IGS database of trace elements in coal.

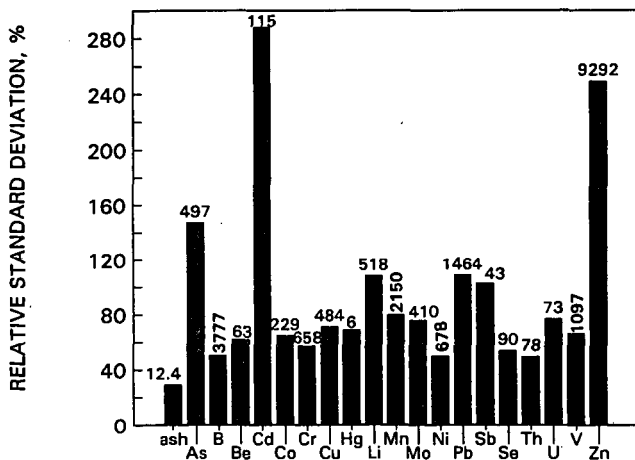


Figure 6. Variability of trace element concentrations in channel samples of Illinois coals, all regions (excluding NE region). Relative standard deviation was obtained by dividing standard deviation by mean and multiplying the result by 100. Numbers over bar indicate average concentrations of ash (wt%) or trace elements (mg/MBTU).

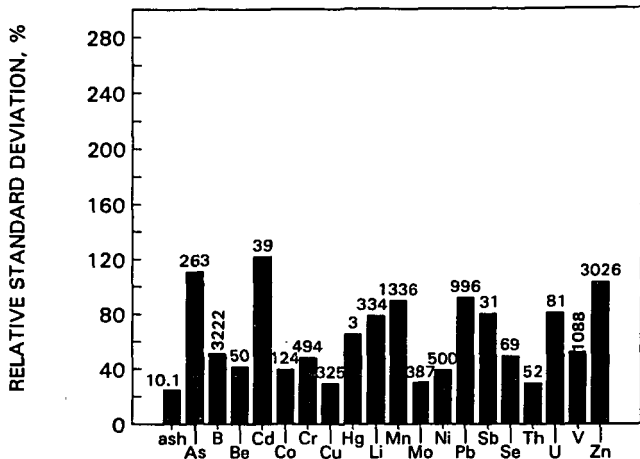


Figure 7. Variability of trace element concentrations in the 34 as-shipped coals, all regions (excluding NE region). Relative standard deviation was obtained by dividing standard deviation by mean and multiplying the result by 100. Numbers over bar indicate average concentrations of ash (wt%) or trace elements (mg/MBTU).

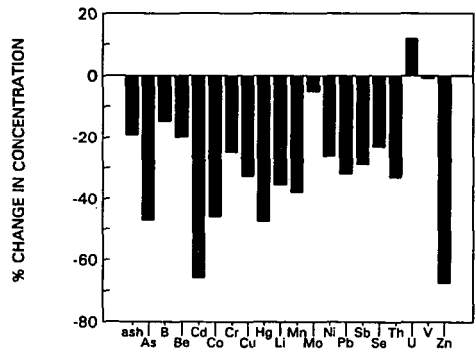


Figure 8. Reduction of trace element concentrations in as-shipped coals relative to those in the database channel samples, mean of state, excluding samples from NE region.

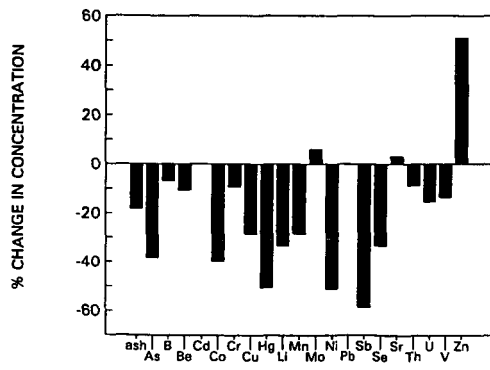


Figure 9. Reduction of trace element concentrations in the as-shipped coal relative to those in channel samples from a mine in the NW region. Data for Cd and Pb was not sufficient to compute the reduction for these two elements.

Surface Composition and Chemical State of Fe and Mo Impregnated Subbituminous Coal

Hengfei Ni, Richard K. Anderson, Edwin N. Givens, John M. Stencil
University of Kentucky Center for Applied Energy Research
3572 Iron Works Pike, Lexington, KY 40511-8433

Keywords: X-ray Photoelectron Spectroscopy, Coal Liquefaction, Catalyst, Iron, Molybdenum

ABSTRACT

The surface composition and chemical states of elements in samples of Wyodak subbituminous coal impregnated with Fe and Mo were investigated. The concentrations of Fe, Mo, S, Al, Si, Ca, C, O, and N were determined by x-ray photoelectron spectroscopy (XPS) in samples impregnated with 0.7-2.0 wt% Fe and 500-1000 ppm Mo. The metals were deposited on the samples by an incipient wetness technique using solutions of ferric nitrate, ferric sulfate, ferrous sulfate and ammonium molybdate. The effect of the metal precursor, the relative amounts of Fe and Mo loading, the effect of base-treatment with NH_4OH and the chemical states of the elements are discussed. Deconvolution of the overlapped S_{2s} and Mo_{3d} peaks is described along with a brief overview of the liquefaction performance of these coals.

INTRODUCTION

Highly dispersed iron-based catalysts have been extensively studied for direct coal liquefaction during the last several years. Cugini and his workers[1,2] found that finely divided and highly dispersed FeOOH -impregnated coals prepared by an incipient wetness technique have high activity in direct liquefaction. These coals were prepared by impregnating the surface of the coal with a solution of ferric nitrate followed by precipitation of FeOOH using an excess of NH_4OH . The influence of several parameters in the preparation procedure on the surface chemistry and performance of the impregnated coals was previously reported.[3]

Considerable research has been directed toward exploiting the improved liquefaction performance of mixed Fe and Mo catalyst.[4,5] Garg, et al., found higher conversion and oil yields by simultaneously impregnating coal with 1% Fe and 0.02% Mo using solutions of 10% ferrous sulfate and 0.5% ammonium molybdate.[6] The iron sulfates are among the least expensive form of iron compounds that are available because of their abundance as a by-product from the iron and steel industry. Andres, et. al.,[7] prepared Mo-free impregnated coals using aqueous solutions of FeSO_4 and reported poor reproducibility of the impregnation technique and relatively low catalytic activity in liquefaction. Pradhan, et al.,[8] reported increased activity for direct liquefaction of subbituminous coal with sulfated α -hematites containing small amounts of added Mo.

Since Mo is expensive, its application in liquefaction will depend on maximizing activity at low concentrations while simplifying the preparation in order to minimize catalyst processing costs. In order to optimize the metal function, it is necessary to understand the surface chemistry of the catalytic components. The present study extends the investigation to coals impregnated with both ferric and ferrous sulfate and compares them with results previously reported using ferric nitrate. The effect of base precipitation and method of drying, whether in air or N_2 at atmospheric pressure or under vacuum, were determined for coals impregnated with 0.7-2.0 wt % Fe and 0.05-0.1 wt % Mo. The surface composition and chemical state of several surface elements were studied using XPS. The technique for measuring low concentrations of Mo by XPS is discussed.

EXPERIMENTAL

Materials - Reagent grade $\text{Fe}(\text{NO}_3)_3 \cdot 9\text{H}_2\text{O}$, $\text{FeSO}_4 \cdot 7\text{H}_2\text{O}$ and $\text{Fe}_2(\text{SO}_4)_3 \cdot 5\text{H}_2\text{O}$ were purchased from Aldrich Chemical Co. and Wyodak coal from the Black Thunder Mine in Wright, Wyoming was provided by CONSOL, Inc. The ultimate analysis of the coal on a dry basis was as follows: carbon, 72.2%; hydrogen, 4.3%; nitrogen, 1.2%; sulfur, 0.5%; oxygen (by difference), 16.0%; ash, 5.8%.

Preparation of Impregnated Coals - Metal impregnated coal samples were prepared as described previously[3]. To as-received coal, which contained 21 wt% moisture, was added dropwise, while stirring, 0.25 ml per gram dry coal of ammonium molybdate solution followed by 0.5 ml per gram dry coal of aqueous Fe salt solution. For those samples treated with base, 1.54 M NH_4OH solution was added at an $\text{NH}_4\text{OH}/\text{Fe}$ mole ratio of 139 and filtered. In some cases samples were further washed with water. All were dried to a final moisture content of 3-10%.

XPS Analysis - XPS analyses were performed on a LHS-10 Leybold-Heraeus spectroscope

as described previously[3]. The quantification of elemental concentrations was performed using background subtraction and element sensitivity factors. Mo measurements were complicated by the overlap of the S_{2s} peak with the Mo_{3d} peaks. Reference samples containing sulfated iron oxides were used to determine the correct position and the area under the S_{2s} peak. Knowing the area of the S_{2p} peak and the S_{2s}/S_{2p} ratio, the S_{2s} peak area was calculated. Subtraction of the S_{2s} peak area from the Mo_{3d} peak area provided a measurement of the Mo concentration.

RESULTS AND DISCUSSION

The surface composition of coals impregnated with the Fe^{++} or Fe^{+++} sulfates are shown in Table 1 and compared with coal impregnated with $Fe(NO_3)_3$ and precipitated as $FeOOH$ by addition of NH_4OH (CH-31). The surface iron concentrations of the 0.77 wt% Fe-impregnated coals prepared from either Fe^{++} or Fe^{+++} sulfates were less than for the $Fe(NO_3)_3$ impregnated coal. For these same coals the sulfur concentrations on the surface are significantly less when base was used to precipitate the iron. Sulfate analysis of the NH_4OH filtrate from the base treatment of CH-51 indicated that all of the $SO_4^{=}$ ion had dissolved in the filtrate making the surface free of any sulfur and oxygen associated with the $SO_4^{=}$ ion. Although several of the NH_4OH preparations were further washed with water with the intention of removing sulfate, including CH-51, it was not necessary. The surface concentrations of Si and Al, and Ca for the 0.77 wt% Fe-impregnated coals, except for CH-502, decreased on the surface when base was used. There was no consistent bias from drying in air, nitrogen or under vacuum.

Surface concentrations of Fe-Mo impregnated coals are shown in Table 1. For those coals subjected to base precipitation (CH-6, CH-61), the Mo concentration is lower (CH-601, CH-604), presumably because part of the molybdate had partially dissolved in the NH_4OH solution. Coals impregnated with Mo at 500 (CH-61) and 1000 ppm (CH-6) had Mo concentrations on the surface of 1100 and 1400 ppm, respectively. For the non-base washed coals, to which 1000 ppm Mo was added, the final Mo levels were 3000 and 5100 ppm. The Fe concentrations of 2.3-3.0 wt% on Mo-impregnated coals were higher than for the Mo-free coals, but still tended to be lower than for the base-treated coals, of which CH-6 is at the lower end. The oxygen levels were slightly higher while the sulfur levels were significantly higher for the non-base treated samples indicating significant deposition of $SO_4^{=}$ on the surface relative to the $SO_4^{=}$ -free ferric nitrate impregnated coals. The rather narrow range of oxygen concentrations on the surface for these 0.77 wt% Fe-impregnated coals (23.1-26.6) suggest that oxygen concentration is related to the iron surface concentration. Like the Mo-free coals, the surface concentrations of Si and Al decreased for the NH_4OH treated coals. No difference in Ca concentration was observed. There didn't appear to be any significant differences in the surface compositions of the Fe^{+++} and Fe^{++} -impregnated coals, even though in the preparations the instability of the ferrous salt solution was obvious. The original blue-green color of the $FeSO_4$ solution rapidly changed to yellow upon exposure to air during the application step. A slight deposit of particles was found in the beaker.

Surface Chemistry - The binding energies of the various elements are shown in Table 2. For both the Fe- and Fe-Mo-impregnated coals treated with base, binding energies for $Fe_{2p\ 3/2}$ and Fe_{3p} were ≥ 711.1 eV and 56.0-56.6 eV, respectively. The O_{1s} binding energies for all the samples prepared with iron sulfates were ≥ 532.0 eV, except for the base-treated sample containing 2 wt% added Fe, CH-51. The $Fe(NO_3)_3$ impregnated coal had a lower O_{1s} binding energy (CH-31), which is consistent with the $FeOOH$ structure. The higher binding energies, reported previously for the raw coal and low Fe concentrations[3], indicate the dominance of the Si and Al oxide structures. The $Fe_{2p\ 3/2}$ peak for the non-base treated samples was broadened toward lower energy suggesting either more contribution from FeO , Fe_3O_4 , or Fe_2O_3 type structure. Low-intensity peaks were observed in the sulfur region at 169.0-169.7 eV, specifically for the base-treated samples, and much more intense peaks were observed between 170.9-171.5 eV for the non-base treated samples. The latter are related to the abundance of $SO_4^{=}$ species present in the samples while the lower energy peaks are related to the background mineral sulfur content of the coal.

The $Ca_{2p\ 3/2}$ and $Ca_{2p\ 1/2}$ binding energies for the base-treated samples (347.2-347.5 eV) were lower than for the non-treated samples (349.8-350.1 eV). The lower binding energy observed for the treated coals is consistent with CaO while the higher energy of the non-treated coals is related to $CaSO_4$.

Molybdenum Analysis - The dual Mo_{3d} peaks were uniform for the Mo containing coals indicating that base-treatment had little effect on the bonding of the metal. The concentration of the metal was so small that no perturbation of the oxygen binding energy was observable. Quantification and characterization of Mo in the 500-1000 ppm range is difficult because it is close to the detection limit of XPS, even though the surface concentration is typically higher than the

bulk concentration. The S_{2s} peak overlaps with the Mo_{3d} peak measurement and is especially troublesome in samples having low concentrations of Mo and high concentrations of S. Pradhan, et al.,⁸ employed a peak subtraction method to resolve this problem. Although the Mo_{3d} peak in the Fe-Mo-impregnated coals is broadened, peak deconvolution was performed based upon external standards and knowing the S_{2s} and Mo_{3d} peak positions and the relative intensities of the S_{2p} peak (169-171 eV), which is quite intense, and the S_{2s} peak. Standards were provided by Mo, Ni and W impregnated sulfated iron oxide samples. The S_{2s} and S_{2p} peak positions for SO_4^{2-} were at 169.5 eV and 232.6 eV, respectively. The relative intensity ratio of S_{2s}/S_{2p} was 0.45-0.52. The Mo_{3d} peak at 232.0 and Mo_{3d} at 235.1 agree with those observed for the Fe-Mo-impregnated coals. Subtraction of the half-height S_{2p} peak area from the measured Mo_{3d} peak area provided a reliable method for determining Mo concentration.

Liquefaction Performance - The Fe- and Fe-Mo-impregnated coals gave significantly higher THF conversion and oil yields than raw coal when reacted in tetralin at 415°C, 1 hour, and 1000 psi H_2 cold. As-received coal gave 85 wt% THF conversion and 43 wt% oil yield; Fe-impregnated coals gave THF conversions of 88-90 wt% and oil yields of 45-50 wt%; Fe-Mo-impregnated coals gave THF conversions from 88-93 wt% and oil yields from 51-52 wt%. The use of iron sulfate salts without base-treatment appears to provide increased THF conversion and oil yield compared to metal impregnation with either sulfate or nitrate salts followed by base-treatment.

- Conclusions** - 1. Fe concentrations on the surface of Mo-free coals, impregnated with either Fe^{++} or Fe^{+++} sulfates, were lower than obtained with Fe^{+++} nitrates.
2. Fe concentrations on the surface of Mo-Fe-impregnated coals, whether prepared from sulfate or nitrate salts, were intermediate between the Mo-free sulfate and nitrate preparations.
3. Fe on the surface of all of the sulfate-impregnated coals was not present as $FeOOH$, which was the dominant form for the nitrate-impregnated, base-treated coals.
4. Mo was present on the surface of the coal as MoO_3 .
5. Sulfate is removed from sulfate-treated coals during the base-treatment step.
6. Sulfur, on the surface of the non-base-treated coals that were treated with sulfates, was present as SO_4^{2-} .
7. Oxygen concentrations on the surface of all the 0.77 wt% Fe-impregnated coals fall within a narrow range.
8. Si, Al and Ca concentrations on the surface of the base-treated coals tend to be lower than for the non-base-treated samples.

ACKNOWLEDGEMENT

The authors gratefully acknowledge financial support provided by the Commonwealth of Kentucky and the U. S. Department of Energy under contract number DE-AC22-91PC91040. They also thank G. Thomas, M. Moore and W. Schram for the analysis of the coals and filtrates and T. Hager for supplying the sulfated iron oxides.

REFERENCES

- [1]. Cugini, A. V.; Utz, B. R.; Krastman, D.; Hickey, R. F. *Prep. Pap. - Amer. Chem. Soc., Div. Fuel Chem.* 1991, 36 (1), 91.
- [2]. Utz, B. R.; Cugini, A. V. U. S. Patent 5,096,570, Mar. 17, 1992.
- [3]. Ni, H. F.; Anderson, R. K.; Givens, E. N.; Stencel, J. M. *Prep. Pap. - Amer. Chem. Soc., Div. Fuel Chem.* 1993, 38 (3), 1107
- [4]. P. Courty and C. Marcilly, Preparation of Catalysts, edited by B. Delmon, P. A. Jacobs and G. Poncelet, 1976, Elsevier Scientific; New York; p 191.
- [5]. Scaroni, A. W.; Derbyshire, F. K.; Abotsi, G. M. K.; Solar, J. M. Final Technical Report, DOE/PC/60050, June, 1987.
- [6]. Garg, D.; Givens, E. N. *Fuel Processing Technology*, 1984, 8, 123.
- [7]. Andres, M.; Charcosset, H.; Chiche, P.; Djega-Mariadassou, G.; Joly, J. P.; Pregermain, S. *Preparation of Catalysts III*; Elsevier Science; New York, 1983, p 675.
- [8]. Pradhan, V. R.; Tierney, J. W.; Wender, I. *Prep. Pap. - Amer. Chem. Soc., Div. Fuel Chem.* 1992, 37 (1), 254.

Table 1. Surface Composition of Fe-Impregnated Coals^a, wt%

Number	CH-31	CH-51	CH-53	CH-503	CH-504	CH-52	CH-502	CH-501	CH-6	CH-61	CH-604	CH-601
Impregnating Salt ^b	none											
Added Fe, wt.% dry coal	0.77	2.0	0.77	0.77	0.77	0.77	0.77	0.77	0.77	0.71	0.77	0.77
	FN	Fe ⁺³	Fe ⁺³	Fe ⁺³	Fe ⁺³	Fe ⁺²	Fe ⁺²	Fe ⁺²	FN-AM	FN-AM	Fe ⁺³ -AM	Fe ⁺² -AM
Precipitated ^c	Y	Y	Y	N	N	Y	N	N	Y	Y	N	N
Washing	N	Y	Y	N	N	Y	N	N	N	N	N	N
Drying @ 40°C	Vac	Vac	Vac	N ₂	Air	Vac	N ₂	Air	Vac	Vac	Air	Air
Fe	4.2	7.9	1.5	1.6	1.9	1.2	1.9	0.8	2.5	3.0	2.3	2.5
Mg, ppm wt	-	-	-	-	-	-	-	-	0.14	0.11	0.51	0.30
Carbon	71.1	62.4	67.9	63.3	57.1	66.3	57.1	60.9	62.8	63.9	56.3	58.7
Oxygen	20.6	24.8	23.1	23.2	26.6	23.2	26.6	25.6	24.4	24.4	25.5	25.3
Nitrogen	1.3	1.2	1.1	1.0	1.0	1.3	1.0	1.0	1.5	1.4	1.5	1.2
Silicon	4.0	3.3	4.2	4.3	5.0	4.1	5.0	5.7	3.8	2.8	5.9	5.3
Aluminum	2.0	2.5	4.3	3.4	4.6	2.6	4.6	4.1	3.5	3.4	5.5	4.9
Calcium	0.5	1.0	0.9	0.8	1.2	0.8	1.5	0.8	1.3	0.9	1.0	0.8
Sulfur	0.2	0.6	0.4	0.4	2.4	0.4	2.4	1.2	0.03	0.03	1.4	1.1

a. Starting coal as "as-received" coal b. FN=Fe(NO₃)₃•9H₂O ; F⁺³=Fe₂(SO₄)₃•5H₂O ; Fe⁺²=FeSO₄•7H₂O ; AM=Ammonium Molybdate
c. Precipitated with NH₄OH solution; Y=yes, N=no.

Table 2. Binding Energies of Elements in Fe and Fe-Mo Impregnated Coals

	Salt ¹	Base	Fe eV			O _{1s} eV	N _{1s} eV	Si _{2p} eV	Al _{2p} eV	C _{2p} eV		S _{2p} eV	Mo _{3d} eV	
			Fe _{2p,3/2}	Fe _{2p,1/2}	Fe _{3p}					C _{2p,3/2}	C _{2p,1/2}		Mo _{3d,3/2}	Mo _{3d,5/2}
CH-31	FN	Y	711.1	725.1	56.6	531.7	399.1	103.8	75.0	346.2	351.0	162.1 168.4	N.D.	N.D.
CH-51	Fe ⁺³	Y	711.3	725.1	56.6	531.7	399.5	N.D.	N.D.	N.D.	N.D.	163.3 167.0	N.D.	N.D.
CH-52	Fe ⁺²	Y	711.7	725.4	56.3	532.5	399.1	N.D.	N.D.	347.4	350.6	164.0 169.7	N.D.	N.D.
CH-53	Fe ⁺³	Y	711.5	725.6	56.2	532.4	400.0	103.6	N.D.	347.2	351.0	163.6 169.6 168.4	N.D.	N.D.
CH-501 ²	Fe ⁺²	N	710.5 711.8	727.5 725.9	54.1	532.9	400.2 396.6	104.5	76.1 74.2	349.9	353.1	163.2 171.2	N.D.	N.D.
CH-502	Fe ⁺²	N	710.0 711.4		55.6	532.6	399.8	104.1	75.6	349.8	353.3	163.3 171.1	N.D.	N.D.
CH-504	Fe ⁺³	N	710.9 711.4 711.9	726.6	56.4	532.7	400.7	104.1	75.4	350.1	353.9	163.6 171.5	N.D.	N.D.
CH-6	FN-AM	Y	711.3	724.8	56.1	532.2	399.6	103.0	74.8	N.D.	N.D.	164.8 169.2	232.4	235.9
CH-61	FN-AM	Y	711.3	725.1	56.0	532.0	399.8	N.D.	74.8	347.5	351.0	163 169	232.5	235.6
CH-601	Fe ⁺² -AM	N	709.8	727.4	53.5	532.6	400.1 392.3	104.0	73.3	349.9	354.0	164.3 171.2	232.5	235.4
CH-604	Fe ⁺³ -AM	N	710.5	727.6	55.4	532.6	399.5 394.1	104.1	73.7	N.D.	N.D.	163.0 170.9	232.3	235.4

N.D. = not detected

1. FN=Fe(NO₃)₃·9H₂O ; F⁺³=Fe₂(SO₄)₃·5H₂O ; Fe⁺²=FeSO₄·7H₂O ; AM=Ammonium Molybdate 2. CH-501 Fe_{3s}=93.8 and 96.0 eV.

AN *IN SITU* EXAMINATION OF THE FE SPECIES IN THE ARGONNE PREMIUM COAL SAMPLES USING X-RAY ABSORPTION SPECTROSCOPY

Stephen R. Wasserman, Randall E. Winans, and Kathleen A. Carrado
Chemistry Division
Argonne National Laboratory
9700 S. Cass Ave.
Argonne, IL 60439

Keywords: XAS, XANES, EXAFS, iron, coals, neural networks

Introduction

The elucidation of the inorganic materials within coals is particularly important for coal processing, since these compounds may function as *in situ* catalysts for coal liquefaction. In addition, these species will have to be separated from the organic compounds prior to the use of coal as a fuel or chemical feedstock, a process that will be facilitated by detailed knowledge of the materials to be removed. In recent years, X-ray absorption spectroscopy (XAS) has been used to probe the trace transition metals which are contained within the matrix of coals,^{1,2} as well as the nitrogen³ and sulfur⁴ functionality within organic coal constituents. Here we present the results of XAS studies, both near edge (XANES) and extended fine structure (EXAFS), on the iron species present within the eight Argonne Premium Coal Samples (APCS). Our aim is to provide at least a semi-qualitative analysis of the composition of the iron moieties in these particular coals. Previously the determination of Fe species in coals has been the province of Mössbauer spectroscopy^{5,6} although the surface iron species of the Argonne coals have also been examined by XPS.⁷ Because of the availability of these alternative methods for analyzing iron, XAS has not been applied, in general, for this element. Here we compare the results from XAS with those previously found by Mössbauer spectroscopy for the Argonne premium coals.⁶

Experimental

X-ray absorption spectra were taken on fresh Argonne Premium Coals, which were removed from their containers and mounted in holders two days prior to acquisition of the spectra. The absorption spectra were acquired at beamlines X23-A2 and X19A of the National Synchrotron Light Source. The beamlines were equipped with Si[311] (X23) and Si[220] (X19) double crystal monochromators. Harmonics were rejected on X19 by detuning of the monochromator. Transmission spectra were collected using ion chambers with nitrogen fill gas. A Lytle detector with argon fill gas was utilized for the fluorescence data. The energy calibration was maintained by monitoring the maximum at 7112 eV in the derivative spectrum of Fe foil. The reported data are the average of 2 scans.

Results

For convenience we have divided the eight Argonne Premium Coals into two groups of four. The first set consists of those coals that contain significant amounts of pyrite, FeS₂. The Upper Freeport, Illinois, Pittsburgh, and Blind Canyon coals fall into this category. The absorption edges and radial structure functions for these samples are shown in Figure 1. The radial functions indicate the presence of long-range order about the iron, at least out to 8 Å.

The second set consists of the Wyodak-Anderson, Pocahontas, Lewiston-Stockton, and Beulah-Zap coals. Figure 2 presents the absorption edges and radial functions for these materials. In some of these samples, in particular the Beulah-Zap, the presence of pyrite is detected. But within this subset, both the absorption edges and the radial distributions indicate that the iron species are present in a variety of different structures. The Wyodak-Anderson and the Beulah-Zap apparently contain similar mixtures of iron species, since the absorption edges are nearly identical. The EXAFS spectra suggest that, at least qualitatively, the other iron compounds in these four coals are not as well ordered as pyrite.

The analysis of mixtures of materials by XAS is somewhat problematical. We have used a new approach based on neural networks to separate the individual iron components.⁸ The advantage of this method is that spectra of standard compounds which exactly match the components of the system are not required. There is, however, an accompanying loss in numerical precision. The network was trained with authentic spectra of FeO, Fe₂O₃, and FeS₂, as well as simulated mixtures of these materials. These standards effectively provide a method for distinguishing between ferrous, ferric, and pyritic species in the coals. The resulting network was then verified using ferrous ammonium sulfate, magnetite (Fe₃O₄), and a pyrite whose spectrum differed markedly in intensity from that which was used in the training process. Finally the network was used to analyze the near edge (XANES) spectra for each of the Argonne coals. The results of this analysis are shown in Table I. The numbers in parenthesis, when present, indicate the actual results from the neural network. Comparisons on duplicate samples indicate that these numbers are accurate to ± 10 % absolute.

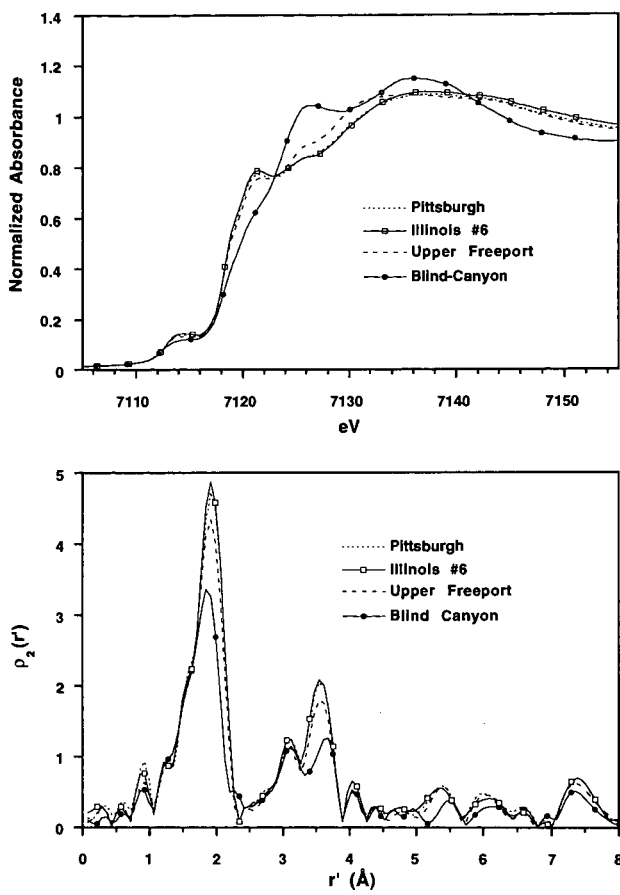


Figure 1. (top) X-ray absorption near edge spectra (XANES) and (bottom) radial structure functions for iron in Upper Freeport, Illinois #6, Pittsburgh #8, and Blind Canyon Coals

Table 1			
Iron Composition of Argonne Premium Coals			
Coal	Ferrous (%)	Ferric (%)	Pyritic (%)
Upper Freeport	10	2	88
Wyodak-Anderson	7	59	32
Illinois #6	0 (-2)	0	100 (104)
Pittsburgh #8	0	0	100 (101)
Pocahontas #3	90 (111)	10 (12)	0 (-20)
Blind Canyon	28	8	62
Lewiston-Stockton	51	43	5
Beulah-Zap	0 (-3)	52	48

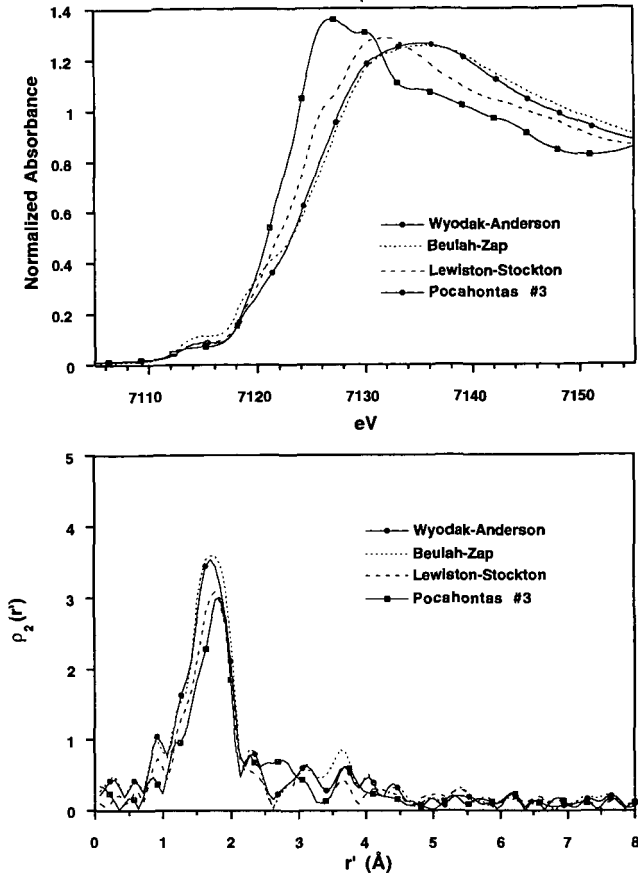


Figure 2. (top) X-ray absorption near edge spectra (XANES) and (bottom) radial structure functions for iron in Wyodak-Anderson, Beulah-Zap, Lewiston-Stockton, and Pocahontas #3 Coals

For seven of the eight coal samples, the results appear reasonable. However, in the case of Pocahontas, our analysis yields a significant negative percentage of pyrite, while the ferrous composition is over 100%. We deduce that the Pocahontas coal consists primarily of ferrous species, but that the compounds present are not well represented by FeO. The XANES and EXAFS spectra for this coal support this supposition. The edge spectrum of Pocahontas does not coincide with those of the other coals. In addition, there is an extra peak in the radial structure function at 2.6 \AA which is not found in the other premium samples. Both these observations indicate that the iron species in Pocahontas is unique among the APCS.

The iron compositions presented here are in approximate agreement with those from Mössbauer spectroscopy⁶ for the Upper Freeport, Illinois #6, Pittsburgh #8 and Blind Canyon coals. Significant discrepancies exist between the Mössbauer and XAS analyses for the remaining four samples. The question remains as to which technique results in the more reliable analysis. Fortunately, the radial structure functions provide an independent check on the pyrite content deduced from the analysis of the XANES spectra. The peak in the radial distribution at 3.6 \AA primarily results from an Fe-Fe interaction in pyrite.⁹ Figure 3 plots this feature for six of the APCS. (Pocahontas is omitted for the reasons discussed above, while the iron content of Illinois #6 is virtually identical to that in Pittsburgh #8). The intensity of this feature clearly correlates with the pyrite content as deduced from the near edge spectra.

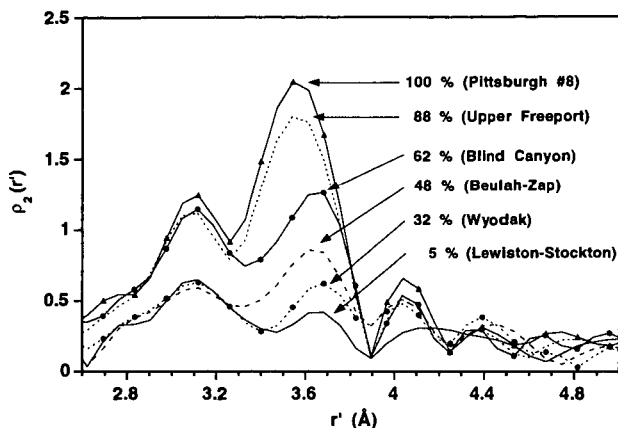


Figure 3. Intensity of Fe-Fe scattering in pyrite from EXAFS. The percentages of pyrite are those determined from XANES.

Summary

We believe that XAS can reliably assign the various iron species present in coal in terms of Fe(II), Fe(III), and pyritic constituents. A search for the best representation of the iron species in Pocahontas is underway, since it does not appear to be well represented by the standards used in this investigation.

In addition, the application of neural networks to the analysis of XANES spectra has been demonstrated for the first time. This approach appears to be a viable method for the analysis of complex mixtures.

Acknowledgment

We would like to thank F. W. Lytle for providing several of the spectral standards for the neural network and K. Pandya for aid in obtaining some of the preliminary spectra for this study. This work was performed under the auspices of the Office of Basic Energy Sciences, Division of Chemical Sciences, U. S. Department of Energy, under contract number W-31-109-ENG-38.

References

- Huggins, F. E.; Shah, N.; Zhao, J.; Lu, F.; Huffman, G. P. *Energy Fuels* **1993**, *7*, 482-489.
- Huggins, F. E.; Helble, J. J.; Shah, N.; Zhao, J.; Srinivasachar, S.; Morency, J. R.; Lu, F.; Huffman, G. P. *Prepr. Div. Fuel Chem. Am. Chem. Soc.* **1993**, *38*, 265-271.
- Mitra-Kirtley, S.; Mullins, O. C.; Branthaver, J.; van Elp, J.; Cramer, S. P. *Prepr. Div. Fuel Chem. Am. Chem. Soc.* **1993**, *38*, 762-768.
- George, G. N.; Gorbaty, M. L.; Kelemen, S. R.; Sansone, M. *Energy Fuels*, **1991**, *5*, 93-97.
- Montano, P. A. *Coal Structure, Advances in Chemistry Series, Vol. 192*; Gorbaty, M. L. and Ouchi, K., Eds., American Chemical Society: Washington, D. C., 1981, pp. 337-361.
- Shah, N.; Keogh, R. A.; Huggins, F. E.; Huffman, G. P.; Shah, A.; Ganguly, B.; Mitra, S. *Prepr. Div. Fuel Chem. Am. Chem. Soc.* **1990**, *35*, 784-792.
- Kelemen, S. R.; Gorbaty, M. L.; George, G. N.; Kwiatek, P. J. *Energy Fuels*, **1991**, *5*, 720-723.
- Freeman, J. A. *Simulating Neural Networks with Mathematica*, Addison-Wesley Publishing Company: Reading, Massachusetts, 1994.
- Brostigen, G.; Kjekshus, A. *Acta Chem. Scan.* **1969**, *23*, 2186-2188.